Interaction of a Screw Dislocation with Interfaces and Surfaces in Couple Stress Elasticity Theory

by

Alireza Gharahi

A thesis submitted in partial fulfillment of the requirements for the degree of

Master of Science

Department of Mechanical Engineering
University of Alberta

Abstract

The fundamental problem of interaction of a screw dislocation with planar surfaces and interfaces is of great theoretical and practical interest from micro/nano mechanical point of view. In the present study, we aim to capture the micro/nano mechanical effects through the continuum based model of couple stress elasticity using an analytical approach for the problem. To do so, we establish the boundary value problem corresponding to a screw dislocation near planar interfaces and surfaces in couple stress materials. We evaluate four main cases: the presence of a screw dislocation near a bi-material interface; a screw dislocation in a substrate near a thin film interface; a screw dislocation inside a thin-film lying over a substrate; a screw dislocation in an unconfined thin-film. Using classical Fourier transform techniques, we solve the corresponding boundary value problem for antiplane deformations with appropriate boundary conditions. The interfaces are assumed to be perfectly bonded and we impose continuity of displacements and tractions. For the surfaces, the traction free condition is set up for the problem. We solve the antiplane problem for the displacement field and use the resulting displacement to calculate stresses and couple stresses in the entire media. We employ the displacement and stress distributions to calculate the force induced by the boundaries on the dislocation. The interaction force is important because it determines the state of mobility of dislocations in certain configurations which is highly influential on the plastic behavior of materials. We use conservative J-integral techniques with numerical integration over a path enclosing the dislocation to obtain the interaction force. The classical elasticity solutions of a screw dislocation near interfaces and surfaces of bi-materials, thin films and substrates are well-documented in the literature. We compare the resulting solutions with the reported solutions in the literature to verify our results, accordingly. The comparison also reveals the contribution of couple stresses to

stress distributions and interaction forces. It is illustrated that, in general, couple stresses endow the structure with an extra stiffness which results in higher stress concentrations as well as higher values of interaction force.

Preface

Two journal papers were published based on the present work.

Based on Chapter 5: A. Gharahi, M. Dai, G. F. Wang and P. Schiavone, Interaction of a screw dislocation with bi-material interface in anti-plane couple stress elasticity, Mathematics and Mechanics of Solids, 2017, DOI: 10.1177/1081286516686824

Based on Chapters 6 to 8: A.Gharahi, M. Dai, P. Schiavone, Screw dislocation in a thin-film substrate in couple stress elasticity, Journal of Applied Mathematics and Physics (ZAMP), 2017 68:37.

Acknowledgements

I wish to express my highest gratitude to my supervisor Professor Schiavone who trusted me and persistently inspired me with his positive attitude and professional passion. I found him a great scholar and scientist, and a wonderful teacher. I truly think of him as my mentor and my role model both professionally and personally.

I thank my dear colleague, Dr. Ming Dai, my course instructors Professor Chong-Qing Ru, Professor Ben Jar and Dr. Mustafa Gül and my friends and officemates whom I learned a lot form during the last year.

I would like to express my special appreciation to my beloved family who always believe in me, encourage me, support me patiently and give me strength. I owe my life, my everything to them.

Contents

List of Figures

1 Introduction

Following the recognition of the importance of crystalline structure in many solid materials and observations regarding the mechanisms with which plastic deformation occurs, crystallographic defects were identified to play the leading role in the mechanisms of plastic deformation [1]. However, mathematical models describing these crystallographic defects were later established by Volterra [2], Love [3], Taylor [4], and others but only in the framework of classical elasticity. Among the defects or imperfections in the crystalline structure of solids, dislocations have proven to be of great interest and importance because of their notable influence on the properties of the materials from both microscopic and macroscopic points of view. Years of effort toward establishing a sensible theory of plasticity [5] applicable to various areas of engineering and science accounts also for the increasing number of studies on dislocations, aiming for a better understanding of the physical explanation of the plastic properties of crystalline materials.

The state of mobility of dislocations, though a microscopic feature, is a key aspect that influences the material's macroscopic properties, such as strength, hardening, ductility, plastic deformation and corrosion, which are all decisive in the design of mechanical, electrical, optical and other engineering devices. For this reason, the concepts of a dislocation's self-stress, image effects as well as the interaction of dislocations and energetic forces have long been under scrutiny by several researchers. Leibfried and Dietze [6], Peierls [7], Nabarro [8], Read [9], and Head [10][11], are few examples of pioneering work in the study of dislocations. Most of the efforts during that era were conducted in the framework of classical elasticity without considering any kind of size dependence. Head [10] [12] for example, applied the electrostatic

problem of line charges to model straight dislocations and from that calculated the image force. Smith [13] [14] used the analytical approach on an isolated screw dislocation as well as a group of screw dislocations interacting with cylindrical inhomogeneities. A collection of analyses of dislocation problems in interaction with interfaces and surfaces, up to the end of the 1960s, is presented in Dundurs [15].

In the second half of the 20th century, the application of small-scale objects, micro- and nanomaterials, thin films, and coating technology led to the expansion of investigations into the behavior of materials of micro and nano-scales. The discrepancy between results obtained from classical theories and experiments in small-scale mechanics gave rise to discussions and illustrative works such as Kroner [16], Kaloni and Ariman [17], Mindlin [18], Schijve [19] and Cowin [20]. In response to this deficiency the long abandoned Cosserats' theory [21] was revived in order to capture the effect of microstructures on the behavior of materials. Subsequently, Eringen [22] [23], Eringen and Suhubi [24] and Nowacki and Olszak [25] introduced micropolar theories of elasticity which were capable of capturing the size effects through the specification of independent local microrotations and couple stress transmission at a material point. In addition, strain-gradient theories [26] [27] [28] were proposed as higher-order continuum theories where constitutive equations are dependent on the gradient of the strain in addition to the strain itself. Eringen and Edelen [29] presented nonlocal elasticity theory allowing for the capability to describe mechanical effects at molecular scales. Tiffin and Stevenson [30], Truesdell and Toupin [31], Grioli [32], Koiter [33], Toupin [34] and Mindlin and Tiersten [35], modified the original Cosserats' continuum theory to Cosserats' media with constrained rotation and their efforts gave rise to a mathematically more elegant couple stress theory. In their theory, the kinematics of the continuum is similar to the classical model, yet the presence of couple stresses capture the essence of microstructural effects. All the aforementioned theories, introduce a new intrinsic property of matter at small scales that has the dimension of length. This property was soon after defined as the characteristic length of the material.

In addition to the profound macro scale effects in the properties of a material, dislocation in crystalline solids is by nature a micro or even nanoscale phenomenon for it is basically a defect in the atomistic arrangement. Therefore, when we study a dislocation's interaction with surfaces, interfaces or thin film structures we usually cannot simply ignore the small-scale effects. In the

early 1990s, a series of experiments on plastic behavior of metals was conducted where Fleck et al [36], Joshi et al [37], Zbib and Aifantis [38], and Ma and Clarke [39] showed plainly that the strength and hardening in the plastic state of a material is strictly dependent on the size of the specimen. Nix [40] published his experimental results on a thin film-substrate structure in the presence of dislocations, where he used this to reveal the microstructural properties of the metals. Stelmashenko et al [41] tested the indentation size effect on the plastic flow of anisotropic crystals. Experiments of this kind showed that plastic strength increases with decrease in size, hence the motto "smaller is stronger" became popular in the literature. These discoveries were sufficient motivation for researchers such as Drugan and Willis [42], and Fleck and Hutchinson [43] [44] to try to establish nonlocal constitutive equations as well as strain gradient plasticity theories founded on the concept of couple stress in Toupin-Mindlin theory [26][27].

Nonetheless, plasticity is a consequence of the action of numerous dislocations which turn out to be size-dependent. This supports the idea that a more accurate evaluation of problems of a single or a finite number of dislocations, specifically regarding their behavior around interfaces, thin films and other dislocations is possible only by taking into account the effect of size in the geometry of the problem. At the end of the last century, with the huge development in computational methods, several attempts have been made to acquire a more realistic account of dislocations in solids. For example, Kenway [45] calculated grain boundaries in Aluminum oxide through atomistic simulation. Watson et al [46] modeled the behavior of dislocations and grain boundaries to the atomistic level in Magnesium oxide and compared their results with classical elasticity theory. Devincre and Kubin [47] simulated the dynamics of dislocation in elastic media by the use of molecular dynamics schemes considering the dislocation interactions with other dislocations in a group and interacting with other obstacles. Verdier et al [48] reviewed the atomistic dynamic simulation techniques to study self-organization of dislocations at the mesoscopic scale which is the scale between macroscopic and atomistic levels. Blanckenhagen et al [49] modeled the plastic deformation of a thin film metal by using the simulation of dynamics of discrete dislocations. Espinosa et al [50] also adopted the molecular dynamic simulation to identify the size effect in the plasticity of a free standing thin film under pure tension and verified their results with previous experiments [51]. The dislocation dynamic modeling and simulation remains an active area of research found even in recent works such as Wang and Beyerlein [52] who adopted a dislocation dynamics model for body-centered cubic metals and

compared the mobility of screw and edge dislocations. Also, Shin and Carter [53] simulated the dislocation's mobility using orbital-free density functional theory at the atomic scale. Simulation techniques, though very useful, are highly dependent on special cases of materials, with certain elements, atoms and crystal formations and so far, do not lead to a general explanation for the behavior of dislocations or indeed a general theory of plasticity. In the literature, several dislocation models have been proposed, each of which refers to a special crystalline material with a certain arrangement of atoms. Nevertheless, simulation techniques are particularly advantageous for complex geometries and situations involving a large number of dislocations which often require intensive calculation. However, they do not always guarantee agreement with experimental results [54].

Rational continuum-based models with the capability of considering size effects such as those discussed earlier, despite their limitations (mainly due to their mathematical complexity), have proven to be useful in modeling single or finite numbers of dislocations in simple geometries. They also become helpful in establishing a general theory of the behavior of materials with dislocation mechanisms including plastic deformation. From the earliest advent of size-dependent theories, many researchers have applied these models to dislocation problems. For example, Cohen [55] formulated screw and edge dislocations in couple stress elasticity introduced by Mindlin and Tiersten [35]. Eringen [56] [57] [58], described screw and edge dislocations in his non-local theory [59] and removed the intrinsic singularities that appear in the classical portrayal of elastic dislocations. Lazar et al [60] [61] applied first and second strain gradient elasticity to edge and screw dislocation problems and related their results to that of Eringen's nonlocal theory [62]. Lazar and Maugin [63] [64] also combined micropolar theory with strain gradient elasticity to formulate screw and edge dislocations and wedge disclination. Lardner [65], compared the effect of second-grade materials on dislocation induced fields with that of couple stress materials and showed how stress fields have a greater deviation from classical theory in second-grade materials. The effect of couple stresses on elastic properties of edge dislocations was analyzed by Knésl and Semela [66]. Lubarda [67], studied the elastic strain energy created by screw and edge dislocations in a couple stress material. Shankar et al [68] evaluated the interaction between dislocations in a couple stress medium and showed that the mutual interaction between dislocations changes only when their distances are comparable to the characteristic material length scale. Taking advantage of a distributed dislocations solution in

couple stress elasticity, Gourgiotis and Georgiadis [69] [70] modeled crack growth mechanisms in materials with couple stresses. Their work also is an example of the application of dislocations' mobility in a mechanism other than plasticity. Despite all the aforementioned efforts, when it comes to the analysis of dislocations interacting with interfaces and surfaces using couple stress elasticity, there is a perceptible void in the literature.

In this thesis, we aim to address this deficiency. We treat the problem of a screw dislocation near inhomogeneous interfaces and planar surfaces in couple stress elasticity. Firstly, we deal with the problem of a dislocation in interaction with a bi-material interface, where each material region consists of a half-plane. Then, we determine the solution for the special case of a screw dislocation near a traction-free planar surface. Secondly, we generalize our results to the interaction of a screw dislocation near the interface of a thin film on a substrate. Next, we evaluate the case when the dislocation has occurred inside the thin film. Finally, we recover our results for the particular state of this case when the screw dislocation is located in an unsupported thin film. In each case, we compare our results to those obtained in classical elasticity which does not account for size effects. This comparison is useful for understanding the extent to which couple stresses can alter the results based on the geometrical dimensions of the problem relative to the characteristic lengths of materials.

The thesis is organized as follows. In Chapter 2, we recount the micropolar theory of elasticity as developed by Eringen [23]. Then, we unfold the assumptions based on which the Mindlin-Tiersten's [35] couple stress theory was built. In Chapter 3, we present a concise review of the elasticity theory of dislocations. We also recalculate the stress fields and interaction force in classical elasticity in order to illustrate the procedure and use the results in our extension to couple stress theory. In Chapter 4, we present the fundamental concept that we use for calculation of the interaction forces on the screw dislocation in various states. In this chapter, we explain the concept of conservation energy integrals used in determining the force. Chapter 5 is dedicated to the solution of the problem in an infinite bi-material. The stress distributions and the interaction force are presented for a variety of parameters indicating the effects of each. The problem of the interaction of a screw dislocation with a thin film on a substrate is considered in Chapter 6. We use the Fourier transform method as in the previous chapter to evaluate the stress field induced around the dislocation in a couple stress medium. In Chapter 7, we position the

dislocation in a thin film which is supported by a substrate. Again, in this case, we determine the fields induced by the dislocation for different geometries and materials and compare them to classical results. The special case of a screw dislocation in an unconfined thin film is presented in Chapter 8, where we show that the couple stress theory used in this thesis does not lead to any significant difference in the interaction force. Finally, in Chapter 9, we draw several conclusions on the contribution of couple stresses and size effects using the extensive analysis presented in the thesis.

2 Micropolar Elasticity and Couple Stress Theory

The fundamental assumption in classical elasticity is that the constitutive properties of a body are independent of the size of the body and therefore, the laws of motion and constitutive equations are valid however infinitesimal the part of the body under examination. In classical elasticity, material constitutive properties depend only on the position vector of a point in the body. In reality, however, the microstructural, granular and molecular qualities of materials play a greater role as the size of an element becomes smaller. The importance of microstructure on the accuracy of an analysis is clearer when the length scale of a body or the external physical stimuli are of the same order as the grain, microstructure, or molecular size of the material. For example, in wave propagation problems, when the wavelength is comparable to the dimensions of microstructures, the motion of every microstructural constituent (or microelement) individually affects the outcome. Also, in the analysis of cracks and notches, where the geometry of the problem is near the order of microelements, classical elasticity is incapable of reconciling theory with experiment. The situation is also common when the microelements are so large that classical models of continuum mechanics are not reliable for engineering applications. Examples of such materials include polymeric and composite materials containing macromolecules, fibers, and granular constituents. To generate mathematical models to describe such materials, researchers tried to develop enhanced continuum theories. The micropolar theory of elasticity is one remedy to the aforementioned deficiencies. In this theory, the rotation vector of every point or microelement is independent of the displacement vector. Therefore, in a micropolar continuum, every particle has a displacement $\underline{u}$ and a rotation $\underline{\phi}$ (E and F Cosserat [21]). This

extra degree of freedom necessitates the existence of an extra form of transmitted load namely couple stress. Thus the interaction of two parts of a body on a surface element dA is through a force vector $\underline{p}dA$ and a moment vector $\underline{m}dA$ (Voigt [71]), where $\underline{p}$ and $\underline{m}$ denote the force and moment per unit area, respectively.

In this chapter, we present an overview of the micropolar theory and its special case couple stress elasticity. The detailed explanation of these theories can be found in Eringen [23], Toupin [26] and Mindlin and Tiersten [35]. First, we derive balance laws for a body in the presence of couple stresses. Next, we describe deformation theory in micropolar continua. Using energy methods, we next obtain the constitutive equations for micropolar linearly elastic materials. In the last section, we define couple stress theory as a special case of micropolar elasticity and derive the corresponding governing equations.

2.1 Balance of force

Consider a material body whose point elements correspond to a Euclidean space E. A vector $\underline{X}$ denotes the position of each point of the material body relative to an origin o. We assume that the material body is subjected to external and internal mechanical forces that produce interactions on the scale of microelements. These forces include body forces, body couples, surface forces and surface couples. In the context of Newtonian mechanics, the force acting on every point in a body is a function of the position of that point, $\underline{X}$ and time, t. Thus, we can introduce forces acting in the volume V and on the surface S of the body as follows:

$\underline{f}(\underline{X},t)$: Body force per unit volume at the point $\underline{X}$ and time t.

$\underline{m}(\underline{X},t)$: Body couple (moment) per unit volume at the point $\underline{X}$ and time t.

$\underline{T}(\underline{X},t)$: Force per unit area (stress) at the point $\underline{X}$ on the surface with normal $\underline{n}$ and at time t.

$\underline{M}(\underline{X},t)$: Moment per unit area (couple stress) at the point $\underline{X}$ on the surface with normal $\underline{n}$ and at time t.

Consider a Cartesian coordinate system $\{o: X_1, X_2, X_3\}$ with the standard basis $\{\underline{e}_1, \underline{e}_2, \underline{e}_3\}$ which locates each material point by its components as $\underline{X} = X_1\underline{e}_1 + X_2\underline{e}_2 + X_3\underline{e}_3$. A general configuration of exerted forces is shown in Fig. 2-1.

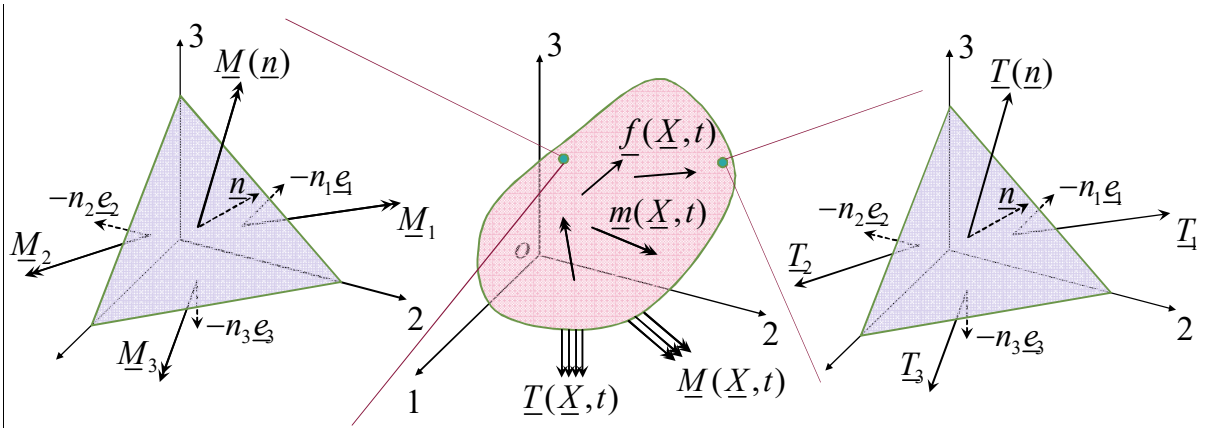

Fig. 2-1- An arbitrary configuration of a micropolar body under the influence of forces and moments

If we separate an infinitesimal tetrahedron which represents an arbitrary surface $\underline{n}$ inside or on the body, we can write equilibrium of forces and moments in the tetrahedron as

$$\begin{aligned} &\underline{T}(\underline{n})\Delta A - (\underline{T}_1\Delta A_1 + \underline{T}_2\Delta A_2 + \underline{T}_3\Delta A_3) + \underline{f}\Delta V = 0, \\ &\underline{M}(\underline{n})\Delta A - (\underline{M}_1\Delta A_1 + \underline{M}_2\Delta A_2 + \underline{M}_3\Delta A_3) + \underline{m}\Delta V = 0, \end{aligned} \tag{2.1}$$

where ΔA is area of the diagonal surface with normal $\underline{n}$, ΔV is volume of the tetrahedron and the stress and couple stress $\underline{T}(\underline{n})$ and $\underline{M}(\underline{n})$, respectively, are functions of the corresponding surface normals. $\underline{T}_i$ and $\underline{M}_i$ $(i = 1,2,3)$ denote the stress and the couple stress acting on the surface with normal $\underline{e}_i$ whose area is ΔA_i. Dividing both sides of (2.1) by ΔA and letting the dimensions be sufficiently small, we can deduce that $\Delta V / \Delta A \to 0$. Therefore, we can write in differential form,

$$\begin{aligned} &\underline{T}(\underline{n})dA = \underline{T}_1 dA_1 + \underline{T}_2 dA_2 + \underline{T}_3 dA_3 = \underline{T}_i dA_i, \\ &\underline{M}(\underline{n})dA = \underline{M}_1 dA_1 + \underline{M}_2 dA_2 + \underline{M}_3 dA_3 = \underline{M}_i dA_i. \end{aligned} \tag{2.2}$$

We assume that Latin indices (i, j, k,…) take the values 1,2,3, and that the convention of summation over repeated indices is adopted. For the closed surface of the tetrahedrons in Fig.

2-1, the area of the diagonal surface ΔA can be expressed in terms of the areas of faces perpendicular to the Cartesian coordinates' axes as

$$dA_i \underline{e}_i = \underline{n} dA = n_i \underline{e}_i dA \Rightarrow dA_i = n_i dA. \tag{2.3}$$

Therefore, (2.2) can be written as

$$\begin{aligned} \underline{T}(\underline{n}) &= \underline{T}_i n_i, \\ \underline{M}(\underline{n}) &= \underline{M}_i n_i, \end{aligned} \tag{2.4}$$

Decomposing $\underline{T}_i$ and $\underline{M}_i$ into their rectangular components according to $\{\underline{e}_1, \underline{e}_2, \underline{e}_3\}$, we get

$$\begin{aligned} \underline{T}_i &= \sigma_{ij} \underline{e}_j, \\ \underline{M}_i &= \mu_{ij} \underline{e}_j. \end{aligned} \tag{2.5}$$

Now, σ_{ij} and μ_{ij} denote stress and couple stress tensor components, respectively. Thus, inserting (2.5) into (2.4), for an arbitrary surface in the material body

$$\begin{aligned} \underline{T}(\underline{n}) &= \sigma_{ij} n_i \underline{e}_j, \\ \underline{M}(\underline{n}) &= \mu_{ij} n_i \underline{e}_j. \end{aligned} \tag{2.6}$$

With these preliminary concepts in mind, we may establish balance of forces and couples in the whole system of a material body in a form of integrals over the surface and volume of the body:

$$\oint_A \underline{T}(\underline{n}) dA + \int_V \underline{f} dV = \int_V \rho \underline{a} dV, \tag{2.7}$$

$$\oint_A \left(\underline{X} \times \underline{T}(\underline{n}) + \underline{M}(\underline{n}) \right) dA + \int_V \left(\underline{m} + \underline{X} \times \underline{f} \right) dV = \int_V \left(\underline{X} \times (\rho \underline{a}) + \rho \underline{\alpha} \right) dV. \tag{2.8}$$

In the above expressions, A and V stand for the total surface area and total volume of the body, respectively, dA and dV are the surface and volume elements of A and V over which the integration is performed, $\times$ indicates cross-product, ρ is the mass density at the point $\underline{X}$, $\underline{a}$ is the acceleration vector at $\underline{X}$ and $\underline{\alpha}$ is a vector representing the outcome of the product of the moment of inertia tensor and angular momentum. Substituting stress and couple stress from (2.4) into (2.7) and (2.8) the two set of equations can be written as

$$\oint_A \underline{T}_i n_i dA + \int_V \underline{f} dV = \int_V \rho \underline{a} dV, \tag{2.9}$$

$$\oint_A \left(\underline{X} \times \underline{T}_i n_i + \underline{M}_i n_i \right) dA + \int_V \left(\underline{m} + \underline{X} \times \underline{f} \right) dV = \int_V \left(\underline{X} \times \underline{a} + \underline{\alpha} \right) \rho dV. \tag{2.10}$$

Using the Divergence Theorem, the surface integrals can be converted into volume integrals. Then, by incorporating the Cartesian coordinates through (2.6), we have

$$\int_V (\sigma_{ij,i} \underline{e}_j + f_j \underline{e}_j - \rho a_j \underline{e}_j) dV = 0, \tag{2.11}$$

$$\begin{aligned} &\int_V \Big(\varepsilon_{njk} \delta_{ij} \sigma_{ki} \underline{e}_n + \varepsilon_{njk} X_j \sigma_{ki,i} \underline{e}_n + \mu_{in,i} \underline{e}_n + m_n \underline{e}_n \\ &+ \varepsilon_{nkj} X_k f_j \underline{e}_n - \varepsilon_{nkj} X_k (\rho a_j) \underline{e}_n - \rho \alpha_n \underline{e}_n \Big) dV = 0, \end{aligned} \tag{2.12}$$

where ε_{ijk} are the components of the alternating tensor defined by

$$\varepsilon_{ijk} = \begin{cases} +1 & \text{if } (i,j,k) \text{ is } (1,2,3), (3,1,2) \text{ or } (2,3,1) \\ -1 & \text{if } (i,j,k) \text{ is } (1,3,2), (2,1,3) \text{ or } (3,2,1) \\ 0 & \text{otherwise} \end{cases} \tag{2.13}$$

the subscript "$,i$" denotes $\partial / \partial X_i$. The foregoing equations of motion must be satisfied at each part of the body. As a result, the integrands in (2.11) and (2.12) must be equal to zero and for every point in the body we write:

$$\sigma_{ij,i} + f_j - \rho a_j = 0, \tag{2.14}$$

$$\varepsilon_{jnk} \sigma_{nk} + \mu_{ij,i} + m_j - \rho \alpha_j = 0. \tag{2.15}$$

These are the local equations of motion for a micropolar material.

2.2 Deformation theory

Consider a material point (P) of a body in its undeformed state. A vector $\underline{X}$ indicates the position of (P) with respect to a Cartesian reference system via its components X_1, X_2 and X_3. After deformation, the point P moves to a new position which in the same reference frame will be denoted by $\underline{x}$ with components x_1, x_2 and x_3. It is assumed that during the deformation

every point undergoes a bijective mapping. Therefore, the position of a point in the undeformed state can be related to a unique position in the deformed configuration and conversely, every point in the deformed configuration can be traced back to a unique point in the undeformed configuration. In either case, we express the position vector of a deformed point as a function of its location before deformation or the position of an undeformed point as a function of its deformed state. That is,

$$\underline{x} = \underline{x}(\underline{X}, t) \Rightarrow x_i = x_i(X_1, X_2, X_3, t), \tag{2.16}$$

$$\underline{X} = \underline{X}(\underline{x}, t) \Rightarrow X_i = X_i(x_1, x_2, x_3, t). \tag{2.17}$$

Also, we note that for the one-to-one mapping to be valid, the following Jacobian determinant must be nonzero:

$$J = \begin{vmatrix} \frac{\partial x_1}{\partial X_1} & \frac{\partial x_2}{\partial X_1} & \frac{\partial x_3}{\partial X_1} \\ \frac{\partial x_1}{\partial X_2} & \frac{\partial x_2}{\partial X_2} & \frac{\partial x_3}{\partial X_2} \\ \frac{\partial x_1}{\partial X_3} & \frac{\partial x_2}{\partial X_3} & \frac{\partial x_3}{\partial X_3} \end{vmatrix} \neq 0. \tag{2.18}$$

To take into account the granular properties of the material body, we assume that every element of the body contains sub-elements called “microelements”. Consequently, for an undeformed body, $\underline{X}$ indicates the position vector of the center of mass for each element hereafter referred to as macro-element. In addition, each material point corresponding to a microelement can be located by its position relative to the center of mass of the macro-element containing that point. Therefore, the position of each material point in this continuum can be expressed by the location of its macro-element relative to a reference origin o, and the position of its microelement relative to the center of mass of that macro-element (see Fig. 2-2). In vectorial form

$$\underline{X}^{(mi)} = \underline{X} + \underline{\Xi}^{(mi)}, \tag{2.19}$$

where $\underline{X}^{(mi)}$ is the position of general microelements with respect to the origin o and $\underline{\Xi}^{(mi)}$ is the position of the same microelement with respect to the center of mass of the macro element $\underline{X}$. Accordingly, we may also express the position vector of a microelement in a deformed state as

$$\underline{x}^{(mi)} = \underline{x} + \underline{\xi}^{(mi)}. \tag{2.20}$$

Similarly, $\underline{x}^{(mi)}$ and $\underline{\xi}^{(mi)}$ have the same definitions as $\underline{X}^{(mi)}$ and $\underline{\Xi}^{(mi)}$ in the deformed state of the body.

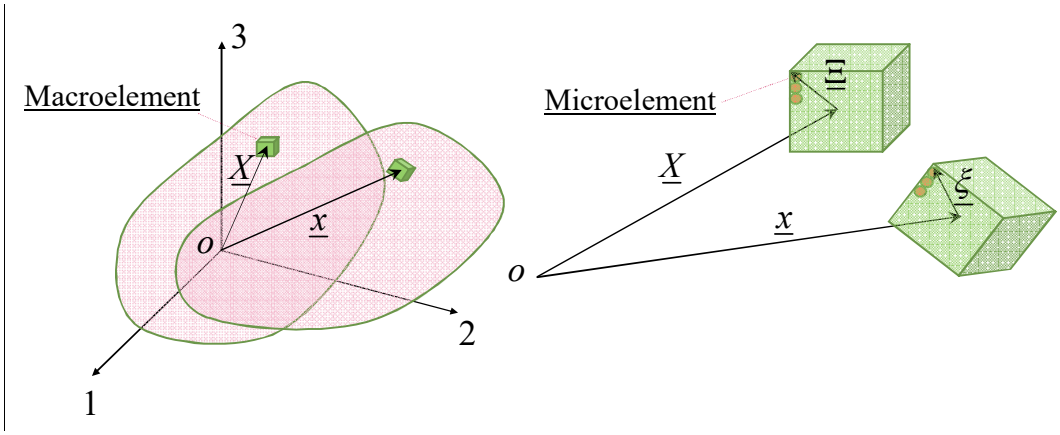

Fig. 2-2- Macro-elements and microelements

Again, we relate the position of a microelement point in a deformed and undeformed configuration by defining functions,

$$\underline{X}^{(mi)} = \underline{X}^{(mi)}(\underline{x}^{(mi)}, t), \tag{2.21}$$

$$\underline{x}^{(mi)} = \underline{x}^{(mi)}(\underline{X}^{(mi)}, t). \tag{2.22}$$

Using (2.20) and (2.19), the position of a microelement relative to the center of mass of its containing macro-element in a deformed body will be restated as

$$\underline{\xi}^{(mi)} = \underline{x}^{(mi)}(\underline{X} + \underline{\Xi}^{(mi)}, t) - \underline{x}(\underline{X}, t). \tag{2.23}$$

As a result, $\underline{\xi}^{(mi)}(\underline{X}, \underline{\Xi}^{(mi)}, t)$ is a function of $\underline{X}$, $\underline{\Xi}^{(mi)}$ and t. One can write the Mclaurin series of this function in terms of $\underline{\Xi}^{(mi)}$ as

$$\underline{\xi}^{(mi)} = \underline{\xi}^{(mi)}(\underline{X}, 0, t) + \frac{\partial \underline{\xi}^{(mi)}}{\partial \underline{\Xi}^{(mi)}} \underline{\Xi}^{(mi)} + \ldots. \tag{2.24}$$

Since the center of mass of the macro-element does not change during the deformation the term $\underline{\xi}^{(mi)}(\underline{X}, 0, t)$ vanishes. On the assumption of homogeneous motion [72], we neglect the second

and higher order terms in (2.24) so that the only meaningful term in the expansion generates a linear relation between $\underline{\xi}^{(mi)}$ and $\underline{\Xi}^{(mi)}$. Thus, it is true that,

$$\underline{\xi}^{(mi)} = \frac{\partial \underline{\xi}^{(mi)}}{\partial \underline{\Xi}^{(mi)}} \underline{\Xi}^{(mi)}, \text{ or } \underline{\xi}^{(mi)} = \underline{\chi}_i(\underline{X},t)\Xi_i^{(mi)}, \text{ or } \xi_j^{(mi)} = \chi_{ji}(\underline{X},t)\Xi_i^{(mi)}, \tag{2.25}$$

where χ_{ij} denote the Cartesian components of a second order tensor ($i, j = 1,2,3$). The relation (2.25) formulates the motion of a microelement point relative to the center of mass of the macro-element or "micromotion" of the point. Conversely, the undeformed $\Xi_i^{(mi)}$, can be written as

$$\Xi_j^{(mi)} = \alpha_{ji}(\underline{X},t)\xi_i^{(mi)}, \tag{2.26}$$

which represents the inverse micromotion. As an inverse micromotion necessarily nullifies the corresponding micromotion, we can infer that for a micromotion and inverse micromotion $\chi_{ij}\alpha_{jk} = \delta_{ik}$, where δ_{ik} is Kronecker delta defined by

$$\delta_{ik} = \begin{cases} 1 & i = k \\ 0 & i \neq k \end{cases} \tag{2.27}$$

Therefore, the motion of a point in micropolar theory can be expressed in terms of its components as

$$x_i^{(mi)}(\underline{X},t) = x_i(\underline{X},t) + \chi_{ij}(\underline{X},t)\Xi_j^{(mi)}, \tag{2.28}$$

and an inverse motion as

$$X_i^{(mi)}(\underline{x},t) = X_i(\underline{x},t) + \alpha_{ij}(\underline{x},t)\xi_j^{(mi)}. \tag{2.29}$$

By total differentiation rule, (2.28) becomes

$$dx_i^{(mi)} = (x_{i,k} + \chi_{ij,k}\Xi_j^{(mi)})dX_k + \chi_{ik}d\Xi_k^{(mi)}. \tag{2.30}$$

In order to evaluate the magnitude of infinitesimal changes in the position vector after deformation ($dx_i^{(mi)}$), we determine the inner product,

$$dx_i^{(mi)} \cdot dx_k^{(mi)} = \left(x_{i,k} x_{i,m} + 2x_{i,k} \chi_{in,m} \Xi_n^{(mi)} + \chi_{ij,k} \chi_{in,m} \Xi_j^{(mi)} \Xi_n^{(mi)} \right) dX_m dX_k$$
$$+ \left(2x_{i,k} \chi_{im} + 2\chi_{im} \chi_{ij,k} \Xi_j^{(mi)} \right) d\Xi_m^{(mi)} dX_k \qquad (2.31)$$
$$+ \chi_{ik} \chi_{im} d\Xi_k^{(mi)} d\Xi_m^{(mi)}.$$

This expression equals the square of the differential arc length in the body after deformation. One can see that except $x_{i,k} x_{i,m}$ in (2.31) which is Green's deformation tensor in classical elasticity, the remainder of the expression emerges from micropolar theory. From (2.31), the deformation tensors in micropolar theory can be defined as

$$G_{km} = x_{i,k} x_{i,m}, \quad \Gamma_{knm} = x_{i,k} \chi_{in,m}, \quad \Psi_{km} = x_{i,k} \chi_{im}. \qquad (2.32)$$

Now, we may define the displacement vector of a point as a vector extended from the undeformed to the deformed position of that point. The definition of displacement is clarified in Fig. 2-3. This can be expressed as

$$\underline{u}^{(mi)} = \underline{x}^{(mi)} - \underline{X}^{(mi)}. \qquad (2.33)$$

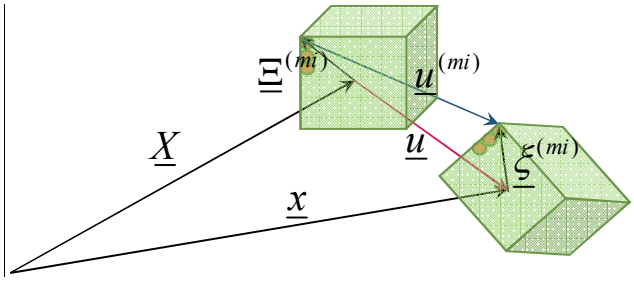

Fig. 2-3-Definition of displacement vector

The relation (2.33) can be written in terms of displacement of the center of mass of a macro-element, $\underline{u}$, as

$$\underline{u}^{(mi)} = \underline{u} + \underline{\xi}^{(mi)} - \underline{\Xi}^{(mi)}. \qquad (2.34)$$

From (2.34), we find in deformed and undeformed configurations that,

$$u_i^{(mi)} = u_i + (\chi_{ij} - \delta_{ij}) \Xi_j,$$
$$u_i^{(mi)} = u_i + (\delta_{ij} - \alpha_{ij}) \xi_j, \qquad (2.35)$$

and we define

$$\begin{aligned}\phi_{ij} &= \chi_{ij} - \delta_{ij},\\ \varphi_{ij} &= \delta_{ij} - \alpha_{ij},\end{aligned} \tag{2.36}$$

as the components of micro-displacement tensors. Also, the displacement gradient of a macro-element will have components:

$$u_{i,j} = x_{i,j} - \delta_{ij}. \tag{2.37}$$

Using (2.37) deformation tensors introduced in (2.32) can be rephrased in terms of displacement as

$$\begin{aligned}G_{km} &= x_{i,k}x_{i,m} = (u_{i,k} + \delta_{ik})(u_{i,m} + \delta_{im}) = \underline{u_{i,k}u_{i,m}} + u_{m,k} + u_{k,m} + \delta_{mk},\\ \Gamma_{knm} &= x_{i,k}\chi_{in,m} = (u_{i,k} + \delta_{ik})(\phi_{in,m}) = \underline{u_{i,k}\phi_{in,m}} + \phi_{kn,m},\\ \Psi_{km} &= x_{i,k}\chi_{im} = (u_{i,k} + \delta_{ik})(\phi_{im} + \delta_{im}) = \underline{u_{i,k}\phi_{im}} + u_{m,k} + \phi_{km} + \delta_{mk},\end{aligned} \tag{2.38}$$

and from the invertibility condition for micromotion ($\chi_{ij}\alpha_{jk} = \delta_{ik}$), we relate micro-displacement tensors ϕ_{ij} and φ_{ij} by

$$\phi_{ik} = \varphi_{ik} + \underline{\varphi_{ij}\phi_{jk}}. \tag{2.39}$$

In expressions (2.38) and (2.39), the underline identifies the nonlinear parts of deformation tensors. In the framework of small deformations, however, we can neglect the nonlinear parts so as to express deformation tensors in the following form,

$$\begin{aligned}G_{km}^{(L)} &= u_{m,k} + u_{k,m} + \delta_{mk},\\ \Gamma_{knm}^{(L)} &= \phi_{kn,m},\\ \Psi_{km}^{(L)} &= u_{m,k} + \phi_{km} + \delta_{mk},\end{aligned} \tag{2.40}$$

and also

$$\phi_{ik} = \varphi_{ik}, \tag{2.41}$$

which shows that with the assumption of small deformations in micropolar theory, as in classical theory, the expressions in terms of deformed and undeformed coordinates will be the same. In

accordance with (2.40), the strain tensor components ε_{ij} and the microstrain tensors components, γ_{ijk} and $\varepsilon_{ij}^{(mi)}$ are defined as

$$\begin{aligned}
&\varepsilon_{ij} = \frac{1}{2}\left(u_{i,j} + u_{j,i}\right), \\
&\gamma_{ijk} = \phi_{ij,k}, \\
&\varepsilon_{ij}^{(mi)} = \Psi_{ij}^{(L)} - \delta_{ij} = \phi_{ij} + u_{j,i}.
\end{aligned} \tag{2.42}$$

Now, in terms of newly defined parameters, we may write the square of differential arc length before (dS) and after (ds) deformation as

$$\begin{aligned}
&ds^2 = dx_i^{(mi)} \cdot dx_k^{(mi)} \\
&= 2\left(\varepsilon_{km} + \gamma_{knm}\Xi_n^{(mi)}\right)dX_m dX_k + dX_k dX_k \\
&+2\left(\varepsilon_{km}^{(mi)} + \gamma_{mjk}\Xi_j^{(mi)}\right)d\Xi_m^{(mi)}dX_k + 2d\Xi_k^{(mi)}dX_k \\
&+\left(\varepsilon_{mk}^{(mi)} + \varepsilon_{km}^{(mi)} - 2\varepsilon_{mk}\right)d\Xi_k^{(mi)}d\Xi_m^{(mi)} + d\Xi_k^{(mi)}d\Xi_k^{(mi)},
\end{aligned} \tag{2.43}$$

$$dS^2 = (dX_k + d\Xi_k^{(mi)})(dX_k + d\Xi_k^{(mi)}). \tag{2.44}$$

The difference between the square differential arc length before and after deformation will be

$$\begin{aligned}
&ds^2 - dS^2 = 2\left(\varepsilon_{km} + \gamma_{knm}\Xi_n^{(mi)}\right)dX_m dX_k \\
&+2\left(\varepsilon_{km}^{(mi)} + \gamma_{mjk}\Xi_j^{(mi)}\right)d\Xi_m^{(mi)}dX_k \\
&+\left(\varepsilon_{mk}^{(mi)} + \varepsilon_{km}^{(mi)} - 2\varepsilon_{mk}\right)d\Xi_k^{(mi)}d\Xi_m^{(mi)}.
\end{aligned} \tag{2.45}$$

Upon eliminating the microelement factors, $\Xi_j^{(mi)}$, the relation (2.45) can be reduced to the classical definition of strain,

$$ds^2 - dS^2 = 2\varepsilon_{km}dX_m dX_k \tag{2.46}$$

A special assumption made in micropolar theory entails rigid local motion of microelements comprising a macro-element. Based on this assumption, micro-displacement tensors are antisymmetric and can be regarded as micro-rotations. That is

$$\phi_{km} = -\phi_{mk}. \tag{2.47}$$

We can write the antisymmetric micro-rotation tensor (2.47) in an axial vectorial form as

$$\phi_k = \tfrac{1}{2}\varepsilon_{kmn}\phi_{nm}. \tag{2.48}$$

The relation (2.48) means that $\phi_1 = \phi_{32}$, $\phi_2 = \phi_{13}$ and $\phi_3 = \phi_{21}$.

Multiplying both sides of (2.48) by the alternating tensor ε_{klt}, the result will be,

$$\phi_{lt} = -\varepsilon_{klt}\phi_k. \tag{2.49}$$

Using the definition of rotation in classical theory, we can also introduce a familiar form of rotation, namely macro-rotation tensor. That is

$$\omega_{ij} = -\omega_{ji} = \tfrac{1}{2}(u_{i,j} - u_{j,i}), \tag{2.50}$$

or in axial vectorial form,

$$\omega_i = \tfrac{1}{2}\varepsilon_{ijk}\omega_{kj} = \tfrac{1}{2}\varepsilon_{ijk}u_{k,j}. \tag{2.51}$$

Similar to (2.49), we obtain

$$\omega_{lt} = -\varepsilon_{klt}\omega_k. \tag{2.52}$$

As in the classical theory, macro-rotation and strain tensors are related to displacement gradient by the following:

$$u_{i,j} = \varepsilon_{ij} + \omega_{ij} = \varepsilon_{ij} - \varepsilon_{ijk}\omega_k. \tag{2.53}$$

We also express microstrain tensors (2.42) in terms of axial vectors ϕ_k and ω_k:

$$\begin{aligned} \varepsilon_{ij}^{(mi)} &= \varepsilon_{ij} + \varepsilon_{jik}(\phi_k - \omega_k), \\ \gamma_{ijn} &= -\varepsilon_{kij}\phi_{k,n}. \end{aligned} \tag{2.54}$$

It is obvious that micro-rotations ϕ_k are independent of macro-rotations ω_k and hence, independent of macro-displacement u_k. As a result, one finds that the degrees of freedom in a micropolar continuum are $u_i(\underline{X},t)$ and $\phi_i(\underline{X},t)$. Going back to the deformed position vector

$\underline{x}^{(mi)}$, if we write this vector in terms of the foregoing deformation parameters, from the definition of displacements (2.33), we find that

$$\underline{x}^{(mi)} = \underline{X} + \underline{\Xi}^{(mi)} + \underline{\xi}^{(mi)} + \underline{u} - \underline{\Xi}^{(mi)}, \tag{2.55}$$

which with the aid of (2.25), becomes

$$\underline{x}^{(mi)} = \underline{X} + \underline{\Xi}^{(mi)} + \underline{u} + (\chi_{ij} - \delta_{ij})\Xi_j^{(mi)}\underline{e}_i. \tag{2.56}$$

Taking (2.36) into consideration, and upon substituting (2.49) into (2.56), we find

$$\underline{x}^{(mi)} = \underline{X} + \underline{\Xi}^{(mi)} + \underline{u} - \underline{\Xi}^{(mi)} \times \underline{\phi}, \tag{2.57}$$

in vectorial form. This represents the deformation of a micropolar body as the summation of displacement of a macro-element (center of mass of a macro element) and angular rigid rotation of a microelement about the center of mass of the macro-element. In differential form (2.57) gives

$$d\underline{x}^{(mi)} = d\underline{X} + d\underline{\Xi}^{(mi)} + d\underline{u} - d\underline{\Xi}^{(mi)} \times \underline{\phi} - \underline{\Xi}^{(mi)} \times d\underline{\phi}. \tag{2.58}$$

Using total differential definitions for $d\underline{u}$ and $d\underline{\phi}$, and incorporating the second equation in (2.54), after some simplifications, (2.58) can be expressed by

$$\begin{aligned} d\underline{x}^{(mi)} = & \underbrace{d\underline{X} + d\underline{\Xi}^{(mi)}}_{1} \\ & \underbrace{-\left(d\underline{X} \times \underline{\omega} + d\underline{\Xi}^{(mi)} \times \underline{\phi} - \tfrac{1}{2}(\gamma_{ikj} - \gamma_{jki})\Xi_k^{(mi)} dX_j \underline{e}_i\right)}_{2} \\ & \underbrace{+\left[\varepsilon_{ij} + \tfrac{1}{2}(\gamma_{ikj} + \gamma_{jki})\Xi_k^{(mi)}\right] dX_j \underline{e}_i}_{3}. \end{aligned} \tag{2.59}$$

In (2.59) the 1st underlined part refers to the rigid translation, the 2nd underlined part specifies the rigid rotation of macro and microelement, and the 3rd underline can be interpreted as the stretch in a micropolar body. If one puts $\underline{\Xi}^{(mi)} = 0$, then (2.59) will be reduced to its classical form,

$$d\underline{x} = d\underline{X} - d\underline{X} \times \underline{\omega} + \varepsilon_{ij} dX_j \underline{e}_i. \tag{2.60}$$

In the equation (2.59), Eringen [23] defines a second order tensor $\gamma_{ij}^{\ *} = \gamma_{ikj}\Xi_k^{\ (mi)}$. Thus, the symmetric part of $\gamma_{ij}^{\ *}$ appears in the 3rd underline in (2.59) and the antisymmetric part in the 2nd underline. Eringen [23] transforms the antisymmetric part $\gamma_{ij}^{\ *(A)} = \frac{1}{2}(\gamma_{ikj} - \gamma_{jki})\Xi_k^{\ (mi)}$ into an axial vector and names it mini-rotation,

$$\gamma_m = \tfrac{1}{2}\varepsilon_{mji}\gamma_{ij}^{\ *(A)}. \tag{2.61}$$

Consequently, linear deformation of a body in micropolar theory can be characterized by macrostrain tensor (or briefly strain tensor),

$$\varepsilon_{ij} = \tfrac{1}{2}\left(u_{i,j} + u_{j,i}\right), \tag{2.62}$$

microstrain tensor,

$$\varepsilon_{ij}^{\ (mi)} = \phi_{ij} + u_{j,i} = u_{j,i} - \varepsilon_{kij}\phi_k, \tag{2.63}$$

micropolar 3rd order strain tensor,

$$\gamma_{ijk} = \phi_{ij,k} = -\varepsilon_{nij}\phi_{n,k}, \tag{2.64}$$

macro-rotation vector,

$$\omega_i = \tfrac{1}{2}\varepsilon_{ijk}u_{k,j}, \tag{2.65}$$

and mini-rotation vector,

$$\gamma_m = \tfrac{1}{2}(\phi_{i,m} - \phi_{i,i})\Xi_m^{\ (mi)}. \tag{2.66}$$

The foregoing parameters make up the components of deformation in micropolar elasticity theory.

2.3 Constitutive equations

In mechanical problems, constitutive equations specify ideal material properties which model the real behavior of an actual material body. In fact, these relations connect kinematics to mechanical fields, such as a force field, and in turn, yield a foundation for governing field equations. These constitutive equations can be derived using the energy balance law and its

resultant minimum total potential energy principle. According to this principle, among all the admissible deformations of a body, only the one that minimizes the total potential energy represents the body in its equilibrium state. Consider the material body shown in Fig. 2-1. The total potential energy of such a system, Π, is defined as the sum of internal energy U and work of external forces on the system W.

$$\Pi = U - W. \tag{2.67}$$

Now, we assume that the internal energy per unit volume at each point or the internal energy density u is a function of independent degrees of freedom. i.e. $u(\varepsilon_{ij}^{(mi)}, \phi_{n,k})$. Thus, the internal energy of the system will be

$$U = \int_V u(\varepsilon_{ij}^{(mi)}, \phi_{n,k}) dV. \tag{2.68}$$

From variational principles and using total differentiation techniques, we may show that the variation of energy density is

$$\delta u = \frac{\partial u}{\partial \varepsilon_{ij}^{(mi)}} \delta \varepsilon_{ij}^{(mi)} + \frac{\partial u}{\partial \phi_{n,k}} \delta \phi_{n,k}. \tag{2.69}$$

On the other hand, one can calculate the work of external forces on the body as the work of surface forces and surface couples plus the work of body forces and body couples. It follows that

$$W = \oint_A \left(\sigma_{ij} u_j + \mu_{ij} \phi_j \right) n_i dA + \int_V \left(f_j u_j + m_j \phi_j \right) dV. \tag{2.70}$$

Using the Divergence Theorem, (2.70) becomes

$$W = \int_V \left(\sigma_{ij,i} u_j + \sigma_{ij} u_{j,i} + \mu_{ij,i} \phi_j + \mu_{ij} \phi_{j,i} + f_j u_j + m_j \phi_j \right) dV. \tag{2.71}$$

Therefore, we define work density as

$$w = \sigma_{ij,i} u_j + \sigma_{ij} u_{j,i} + \mu_{ij,i} \phi_j + \mu_{ij} \phi_{j,i} + f_j u_j + m_j \phi_j. \tag{2.72}$$

Since the total potential energy is under consideration, the equations of motion (2.14) and (2.15), in static form are incorporated into (2.72). Then, the work density is expressed by

$$\mathsf{w} = \sigma_{ij}\varepsilon_{ij}^{(mi)} + \mu_{ij}\phi_{j,i}. \tag{2.73}$$

As for the internal energy density, we regard work density as a function of $\varepsilon_{ij}^{(mi)}$ and $\phi_{n,k}$. Therefore, the variation of work density will be

$$\delta\mathsf{w} = \sigma_{ij}\delta\varepsilon_{ij}^{(mi)} + \mu_{ij}\delta\phi_{j,i}. \tag{2.74}$$

For the total potential energy to be minimized, the variation of the total potential energy $\delta\Pi$ should vanish. As a result, we write

$$\delta\Pi = \delta\mathsf{U} - \delta\mathsf{W} = 0. \tag{2.75}$$

Based on the fact that the relation (2.75) holds for every arbitrary part of the body, we eliminate volume dependence from both sides to show that variations of work density and internal energy density (2.69) and (2.74) are equal. By comparison, we deduce that

$$\sigma_{ij} = \frac{\partial\mathsf{u}}{\partial\varepsilon_{ij}^{(mi)}}, \quad \mu_{ij} = \frac{\partial\mathsf{u}}{\partial\phi_{j,i}}. \tag{2.76}$$

The relations (2.76) are true for all micropolar elastic material bodies. Based on experimental studies however, for several elastic mechanical systems, especially when the deformations are small the stress-strain relation may be considered linear. Also, depending on the application of micropolar theory, in the simplest form the material may be considered as isotropic. Therefore, giving attention to (2.76), we can impose the linear condition by taking u as a quadratic function of $\varepsilon_{ij}^{(mi)}$ and $\phi_{j,i}$. This means that in the micropolar theory of linear elasticity for an isotropic material body, in the absence of residual stresses, the internal energy density can be expressed as

$$\begin{aligned}\mathsf{u} = &\left(\frac{\mu+\alpha}{2}\right)\varepsilon_{ij}^{(mi)}\varepsilon_{ij}^{(mi)} + \left(\frac{\mu-\alpha}{2}\right)\varepsilon_{ij}^{(mi)}\varepsilon_{ji}^{(mi)} + \frac{\lambda}{2}\varepsilon_{kk}^{(mi)}\varepsilon_{nn}^{(mi)} \\ &+\left(\frac{\gamma+e}{2}\right)\phi_{j,i}\phi_{j,i} + \left(\frac{\gamma-e}{2}\right)\phi_{i,j}\phi_{j,i} + \frac{\beta}{2}\phi_{k,k}\phi_{n,n}.\end{aligned} \tag{2.77}$$

Now, referring to (2.76), stresses and couple stresses are related to microstrains and micro-rotation gradients as

$$\sigma_{ij} = (\mu+\alpha)\varepsilon_{ij}^{(mi)} + (\mu-\alpha)\varepsilon_{ji}^{(mi)} + \lambda\delta_{ij}\varepsilon_{nn}^{(mi)}, \tag{2.78}$$

$$\mu_{ij} = (\gamma + e)\phi_{j,i} + (\gamma - e)\phi_{i,j} + \beta\delta_{ij}\phi_{n,n}. \tag{2.79}$$

In relations (2.77), (2.78) and (2.79), μ, α, λ, γ, e and β are elastic moduli for a micropolar isotropic or micro-isotropic material. In classical elasticity of an isotropic material, only μ and λ, known as Lamé coefficients, are involved in the constitutive equations.

2.4 Field equations in micropolar elasticity

To obtain the general governing field equations in terms of displacements and micro-rotations, we substitute (2.78) into the equations of motion (2.14) and (2.15). The result gives us the two equations,

$$(\mu + \alpha)u_{j,ii} + (\mu + \lambda - \alpha)u_{i,ji} - 2\alpha\varepsilon_{kij}\phi_{k,i} + f_j - \rho\ddot{u}_j = 0, \tag{2.80}$$

$$(\gamma + e)\phi_{j,ii} + (\gamma + \beta - e)\phi_{i,ji} - 2\alpha\varepsilon_{jkn}u_{k,n} - 4\alpha\phi_j + m_j - \rho I\ddot{\phi}_j = 0, \tag{2.81}$$

where dot and double dot on parameters refer to the first and second total derivatives of the parameters with respect to time t. Note that on the assumption of micro-isotropy for material, in deriving (2.80) and (2.81) from (2.14) and (2.15), the inertial terms in the equations of motion are converted to

$$\rho\underline{a} = \rho\underline{\ddot{u}}, \quad \rho\underline{\alpha} = \rho I\underline{\ddot{\phi}}, \tag{2.82}$$

where, $\underline{\ddot{u}}$ and $\underline{\ddot{\phi}}$ are respectively, the second total derivatives of displacement and rotation vectors $\underline{u}$ and $\underline{\phi}$ with respect to time t. I is the micro-inertia coefficient and is derived from a general micro-inertia tensor I_{ij} which in the case of isotropy reduces to $I_{ij} = I\delta_{ij}$. One can also convert the field equations (2.80) and (2.81) into vectorial form as

$$(\mu + \alpha)\nabla^2\underline{u} + (\mu + \lambda - \alpha)\nabla(\nabla \cdot \underline{u}) + 2\alpha\nabla \times \underline{\phi} + \underline{f} - \rho\underline{\ddot{u}} = \underline{0}, \tag{2.83}$$

$$(\gamma + e)\nabla^2\underline{\phi} + (\gamma + \beta - e)\nabla(\nabla \cdot \underline{\phi}) + 2\alpha\nabla \times \underline{u} - 4\alpha\underline{\phi} + \underline{m} - \rho I\underline{\ddot{\phi}} = \underline{0}, \tag{2.84}$$

where "$\cdot$" indicates inner product, ∇ is the gradient operator defined by $(\partial / \partial X_i)\underline{e}_i$ in Cartesian coordinates and ∇^2 is the Laplacian operator defined by $\nabla^2 = \nabla \cdot \nabla$. The equations (2.83) and (2.84) along with boundary and initial conditions make up a boundary value problem whose solution specifies the state of a micro-isotropic body under the given conditions. It is clear that

the foregoing system of equations is not easy to solve in general. Thus, many researchers have tried to simplify the theory further in order to make it more applicable to solid mechanics problems.

2.5 Couple stress theory of elasticity

Couple stress theory stems from the micropolar theory if certain further simplifying assumptions are made. Truesdell and Toupin [31], Grioli [32], Toupin [26] and Mindlin and Thiersten [35] were the first researchers to develop the theory around half a century ago. Couple stress theory can be derived as a special case of micropolar elasticity when the independent micro-rotations are omitted from the degrees of freedom. Consequently, the displacement field remains only to characterize kinematics of the continuous material body and rotations retain their classical definition as

$$\underline{\phi} = \underline{\omega} = \frac{1}{2}\nabla \times \underline{u}, \tag{2.85}$$

or in terms of the vector components,

$$\phi_i = \omega_i = \frac{1}{2}\varepsilon_{ijk} u_{k,j}. \tag{2.86}$$

Following this assumption, the micro-strain tensor (2.54), becomes

$$\varepsilon_{ij}^{(mi)} = \varepsilon_{ij} = \frac{1}{2}\left(u_{j,i} + u_{i,j}\right), \tag{2.87}$$

which is a symmetric tensor as in classical elasticity. It follows that by substituting (2.87) into the constitutive equation (2.78), we obtain a symmetric stress tensor as

$$\sigma_{ij}^{S} = 2\mu\varepsilon_{ij} + \lambda\delta_{ij}\varepsilon_{nn}, \tag{2.88}$$

which can be translated in terms of displacement as

$$\sigma_{ij}^{S} = \mu\left(u_{i,j} + u_{j,i}\right) + \lambda\delta_{ij}u_{k,k}. \tag{2.89}$$

From the second set of equations of motion, (2.15) multiplied by ε_{jtl}, an antisymmetric stress tensor will result in,

$$\sigma_{tl}{}^{A} = \frac{1}{2}(\sigma_{tl} - \sigma_{lt}) = -\frac{1}{2}(\varepsilon_{jtl}\mu_{ij,i} + \varepsilon_{jtl}m_j - \varepsilon_{jtl}\rho I\ddot{\phi}_j). \tag{2.90}$$

Thus, the total stress tensor in couple stress theory is the summation of the symmetric and antisymmetric parts as

$$\sigma_{ij} = \sigma_{ij}{}^{S} + \sigma_{ij}{}^{A}. \tag{2.91}$$

Moreover, by imposing the rotation constraint (2.85) on the constitutive equation (2.79), we deduce that

$$\mu_{ij} = \frac{(\gamma + e)}{2}\varepsilon_{nmj}u_{m,ni} + \frac{(\gamma - e)}{2}\varepsilon_{nmi}u_{m,nj}, \tag{2.92}$$

which considering (2.86) and since $\omega_{i,i} = 0$, turns out to be a deviatoric tensor. Then, by inserting (2.92) into the antisymmetric part of the stress tensor (2.90), the expression in terms of displacement becomes

$$\sigma_{tl}^{A} = -\frac{(\gamma + e)}{2}u_{l,tii}^{A} - \frac{1}{2}\varepsilon_{jtl}m_j + \frac{1}{2}\rho I\ddot{u}_{l,t}{}^{A}, \tag{2.93}$$

where $u_{l,t}^{A}$ is the antisymmetric part of displacement gradient tensor described by its components as

$$u_{l,t}^{A} = \frac{1}{2}\left(u_{l,t} - u_{t,l}\right). \tag{2.94}$$

From (2.93), it is obvious that the antisymmetric part of the stress tensor depends not only on the properties of a material medium but also on the applied body moments and the inertia. On the other hand, since the rotation $\underline{\phi}$ is not independent, then the couple stresses determined by the constitutive equation (2.79) which originate from $(2.76)_2$ will no longer be independent. For these reasons, the theory is usually referred to as "indeterminate" couple stress theory.

We may also show the symmetric part of the displacement gradient tensor to be

$$u_{l,t}^{S} = \frac{1}{2}\left(u_{l,t} + u_{t,l}\right). \tag{2.95}$$

Hence, using (2.93) and (2.89), the total stress tensor (2.91), can be written as

$$\sigma_{tl} = 2\mu u_{l,t}^{S} + \lambda\delta_{tl}u_{k,k} - \frac{(\gamma+e)}{2}u_{l,tii}{}^{A} - \frac{1}{2}\varepsilon_{jtl}m_j + \frac{1}{2}\rho I\ddot{u}_{l,t}{}^{A} \tag{2.96}$$

Thus far, the second set of equations of motion and constitutive equations have been used to determine the stress tensor components. Now, if we carry the stress tensor (2.96) into the first set of equations of motion (2.14), the governing field equation in couple stress theory can be found as

$$\left(\mu - \frac{\gamma+e}{4}\nabla^2\right)u_{l,tt} + \left(\mu + \lambda + \frac{\gamma+e}{4}\nabla^2\right)u_{t,lt} - \frac{1}{2}\varepsilon_{jtl}m_{j,t} + f_l = \rho\ddot{u}_l - \frac{I}{4}\nabla^2\ddot{u}_l + \frac{I}{4}\ddot{u}_{t,lt} \tag{2.97}$$

The component expressions in (2.97) may be transformed into vectorial forms by multiplying both sides by $\underline{e}_l$ and using the identities $u_{i,ji}\underline{e}_j = \nabla(\nabla\cdot\underline{u})$ and $u_{j,ii}\underline{e}_j = \nabla(\nabla\cdot\underline{u}) - \nabla\times(\nabla\times\underline{u})$. Therefore, we write:

$$(2\mu+\lambda)\nabla(\nabla\cdot\underline{u}) - \left(\mu - \frac{\gamma+e}{4}\nabla^2\right)\nabla\times(\nabla\times\underline{u}) + \frac{1}{2}\nabla\times\underline{m} + \underline{f} = \rho\ddot{\underline{u}} + \frac{I}{4}\nabla\times(\nabla\times\ddot{\underline{u}}) \tag{2.98}$$

In the special case where the body is in a state of static equilibrium, the inertial factors vanish from (2.98). Then, we obtain

$$(2\mu+\lambda)\nabla(\nabla\cdot\underline{u}) - \left(\mu - \frac{\gamma+e}{4}\nabla^2\right)\nabla\times(\nabla\times\underline{u}) + \frac{1}{2}\nabla\times\underline{m} + \underline{f} = \underline{0} \tag{2.99}$$

Further, in the absence of body forces and body moments the field equation reduces to

$$(2\mu+\lambda)\nabla(\nabla\cdot\underline{u}) - \left(\mu - \frac{\gamma+e}{4}\nabla^2\right)\nabla\times(\nabla\times\underline{u}) = \underline{0}. \tag{2.100}$$

Now, consider the couple stress formulations in the static case. If we use the first equation of equilibrium (2.14), and exert a virtual displacement $\triangle u_i$ on the balanced system, the virtual work equals zero. Formally,

$$\int_V (\sigma_{ji,j} + f_i)\triangle u_i dV = 0. \tag{2.101}$$

Also we know that

$$\sigma_{ji,j}\triangle u_i = (\sigma_{ji}\triangle u_i)_{,j} - \sigma_{ji}\triangle u_{i,j}. \tag{2.102}$$

Using (2.102) into (2.101), we have

$$\int_V [(\sigma_{ji}\triangle u_i)_{,j} - \sigma_{ji}\triangle u_{i,j} + f_i\triangle u_i]dV = 0. \tag{2.103}$$

Applying the Divergence Theorem on the first term, we relate the internal force stresses to the force tractions on the body surface S, as

$$\int_V \sigma_{ji}\triangle u_{i,j}dV = \int_S \sigma_{ji}n_j\triangle u_i dS + \int_V f_i\triangle u_i dV. \tag{2.104}$$

We decompose the stress in terms of its symmetric and antisymmetric parts as

$$\int_V (\sigma_{ji}^S + \sigma_{ji}^A)\triangle u_{i,j}dV = \int_S \sigma_{ji}n_j\triangle u_i dS + \int_V f_i\triangle u_i dV. \tag{2.105}$$

Incorporating the second equation of equilibrium (2.15) in terms of the antisymmetric part of stress, we have

$$\int_V \sigma_{ji}^S\triangle u_{i,j}dV - \int_V \frac{1}{2}(\varepsilon_{jik}\mu_{nk,n} + \varepsilon_{jik}m_k)\triangle u_{i,j}dV = \int_S \sigma_{ji}n_j\triangle u_i dS + \int_V f_i\triangle u_i dV. \tag{2.106}$$

Then, it is easy to show that $\sigma_{ji}^S\triangle u_{i,j} = \sigma_{ji}^S\triangle\varepsilon_{ji}$. Again, using the relation,

$$\varepsilon_{jik}\mu_{nk,n}\triangle u_{i,j} = (\varepsilon_{jik}\mu_{nk}\triangle u_{i,j})_{,n} - \varepsilon_{jik}\mu_{nk}\triangle u_{i,jn}, \tag{2.107}$$

and the divergence theorem, we can relate the internal couple stresses to the couple tractions on the surface as

$$\begin{aligned}&\int_V (\sigma_{ji}^S\triangle\varepsilon_{ji} + \frac{1}{2}\varepsilon_{jik}\mu_{nk}\triangle u_{i,jn})dV \\ &= \int_S (\frac{1}{2}\varepsilon_{jik}\mu_{nk}\triangle u_{i,j}n_n)dS + \int_S \sigma_{ji}n_j\triangle u_i dS + \int_V (\frac{1}{2}\varepsilon_{jik}m_k\triangle u_{i,j})dV + \int_V f_i\triangle u_i dV.\end{aligned} \tag{2.108}$$

Using the condition (2.86), we may write

$$\int_V (\sigma_{ji}^S \triangle\varepsilon_{ji} + \mu_{nk} \triangle\omega_{k,n}) dV$$
$$= \int_S (\mu_{ji} n_j \triangle\omega_i) dS + \int_S \sigma_{ji} n_j \triangle u_i dS + \int_V (m_i \triangle\omega_i) dV + \int_V f_i \triangle u_i dV. \tag{2.109}$$

The left-hand side of the equation (2.109) represents the internal elastic energy of the system $E^{(\triangle)}$, while the right-hand side shows the work of external loads including surface tractions and body forces and couples, all produced by an arbitrary virtual displacement. Now we focus on the couple stress tractions on the surface $\mu_{ji} n_j \triangle\omega_i$ and decompose it to the normal and tangential components through

$$\mu_{ji} n_j \triangle\omega_i = \mu_{ji} n_j \delta_{ik} \triangle\omega_k = \mu_{ji} n_j \triangle\omega_k (\delta_{ik} - n_i n_k) + \underline{\mu_{ji} n_j n_i} n_k \triangle\omega_k, \tag{2.110}$$

where the underlined part in (2.110) is the normal component of the couple stress vector on S, denoted by $\mu^{(\text{nor})} = \mu_{ji} n_j n_i$. Inserting the decomposition (2.110) into (2.109) and using (2.86), we obtain:

$$E^{(\triangle)} = \int_S [\mu_{ji} n_j (\delta_{ik} - n_i n_k) \triangle\omega_k + \mu^{(\text{nor})} n_k (\tfrac{1}{2} \varepsilon_{mnk} \triangle u_{n,m})] dS$$
$$+ \int_S \sigma_{ji} n_j \triangle u_i dS + \int_V (m_i \triangle\omega_i) dV + \int_V f_i \triangle u_i dV. \tag{2.111}$$

Additionally, we can alter (2.111) to the form

$$E^{(\triangle)} = \int_S [\mu_{ji} n_j (\delta_{ik} - n_i n_k) \triangle\omega_k] dS$$
$$+ \int_S [\underline{\tfrac{1}{2} \varepsilon_{mnk} n_k (\mu^{(\text{nor})} \triangle u_n)_{,m}} - \tfrac{1}{2} \varepsilon_{mnk} n_k \triangle u_n (\mu^{(\text{nor})})_{,m}] dS \tag{2.112}$$
$$+ \int_S \sigma_{ji} n_j \triangle u_i dS + \int_V (m_i \triangle\omega_i) dV + \int_V f_i \triangle u_i dV.$$

We apply Stokes' theorem to the underlined part and since S is assumed to be a smooth closed surface this part will be eliminated. Therefore,

$$E^{(\triangle)} = \int_S [\mu_{ji} n_j (\delta_{ik} - n_i n_k) \triangle\omega_k] dS$$
$$+ \int_S (\sigma_{ji} n_j - \tfrac{1}{2} \varepsilon_{mik} n_k (\mu^{(\text{nor})})_{,m}) \triangle u_i dS + \int_V (m_i \triangle\omega_i) dV + \int_V f_i \triangle u_i dV. \tag{2.113}$$

Thus, on the surface S, the normal component of the couple stress vector remains only in combination with the stress vector as the coefficient of displacement $\triangle u_i$. Additionally, a uniform distribution of normal component of the couple stress vector on S, does not contribute to the virtual work. Based on this, Mindlin and Tiersten [35] and later Koiter [33] argue that specification of stresses and couple stresses on the surface yields five boundary conditions. Also, if we prescribe the displacement vector as a boundary condition, the normal component of the rotation vector or the normal component of the couple stress vector at the boundary cannot be specified independently. This fact is particularly useful in establishing boundary conditions for the problem of a screw dislocation interacting with interfaces. We will use the equations derived in this chapter in Chapters 5 to 8, to deal with the problem of the interaction of a screw dislocation near interfaces and surfaces in couple stress theory.

3 Interaction of a Screw Dislocation with a Bi-material Interface in Classical Elasticity

A perfect lattice region in a crystalline solid is where the crystal particles are arranged in a regular pattern. This pattern is broken when an imperfection or defect occurs. Imperfections in a crystal lattice are very common and they account for several mechanical properties of a solid material. For instance, imperfections describe the structural state of materials and deformation processes. Furthermore, an imperfection can reduce the strength of a material by orders of magnitude. A certain type of imperfection takes place when two adjacent planes of a lattice displace relatively so that the particles make bonds with their new neighbors in such a way that the lattice formation remains perfect. The plane over which the particles have slipped relative to one another is referred to as "slip plane". The slip usually happens only on a part of the slip plane and the boundary which differentiates between the slipped and unslipped region is defined as "dislocation" (Read [9], Hirth and Lothe [73]-see Fig. 3-1).

Dislocations can move through the crystal lattice. The presence and mobility of dislocations have a great deal of influence on the mechanical properties of materials. In fact, the mobility of dislocations explains the plastic deformation for crystalline solids such as metals. Work hardening property in metals is also related to the increase in the concentration of dislocations and strong interaction between them which makes a metastable configuration [9]. The motion of a dislocation can occur in two forms. First, the lattice particles continue slipping over the slip plane in which case the slipped region expands or shrinks and the boundary line, or namely the "dislocation line", moves through the lattice. This kind of movement is called conservative since

the number of particles remains constant during the process. The second kind of movement is known as climb of a dislocation which normally occurs at high temperatures. As a non-conservative motion of a dislocation, climb involves an out-of-slip-plane movement of the dislocation line and requires particles to be added to the material.

The description of dislocation behavior begins by introducing a unit vector $\underline{\zeta}$ tangent to the dislocation line whose direction determines the positive sense [73]. A dislocation vector $\underline{b}$, or the Burgers vector, is defined to determine the strength of a dislocation. Roughly speaking, the Burgers vector $\underline{b}$ determines the magnitude of slippage and the direction in which the plane particles have slipped over each other. In general form, $\underline{b}$ can be interpreted as the total displacement caused by a dislocation on a path C which lies totally in the perfect lattice, encloses the dislocation line, and whose direction is determined by the positive sense of $\underline{\zeta}$ and the right-hand rule. In mathematical form, this means,

$$\underline{b} = \oint_C d\underline{u} = \oint_C \frac{\partial \underline{u}}{\partial s} ds \tag{3.1}$$

Geometrically, dislocations are categorized into "edge" and "screw" dislocations. For an edge dislocation, the dislocation line unit vector $\underline{\zeta}$ is perpendicular to the Burger's vector $\underline{b}$, or $\underline{\zeta} \cdot \underline{b} = 0$. For a screw dislocation, on the other hand, $\underline{\zeta}$ and $\underline{b}$ are parallel to each other, or $\underline{\zeta} \cdot \underline{b} = b$, b being the magnitude of the Burger's vector (see Fig. 3-1). The present dissertation focuses on the interaction of a screw dislocation with interfaces and free surfaces in couple stress theory.

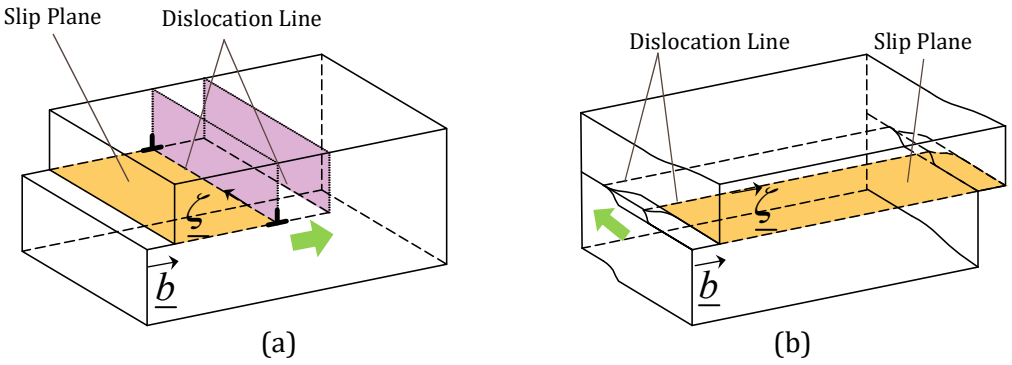

Fig. 3-1- (a) Edge dislocation and (b) screw dislocation and slippage configuration.

3.1 Screw dislocation

A dislocation can be identified by its prescribed displacement field in a surrounding infinite medium (in the Cartesian coordinates $\{o: X_1, X_2, X_3\}$, for example, $\underline{u}(X_1, X_2, X_3) = u_i(X_1, X_2, X_3)\underline{e}_i$ denotes the displacement field components). For a screw dislocation at the origin of a Cartesian coordinate system (Fig. 3-2) whose dislocation line and unit vector $\underline{\zeta}$ coincide with the X_3 - axis direction, the only non-vanishing displacement field is u_3 which can be regarded as the out-of-plane or anti-plane component. In addition, since $\underline{b}$ and $\underline{\zeta}$ are aligned, the slip plane for a screw dislocation is not unique. In order to quantify the screw dislocation in an infinite medium, from all possible choices, the $X_1 - X_3$ plane is taken as the slip plane. Therefore, one can relate the magnitude of Burger's vector b to the anti-plane displacement by

$$b = \left[u_3(X_1, 0^-) - u_3(X_1, 0^+) \right], \quad X_1 > 0. \tag{3.2}$$

Here, the superscripts "$+$" and "$-$" refer to the right and left limits as X_2 approaches zero. Also, with reference to the polar coordinates shown in Fig. 3-2, it is assumed that the displacement component u_3 increases uniformly with θ. Then, we may write:

$$u_3(r, \theta) = b\frac{\theta}{2\pi}, \tag{3.3}$$

or in the defined Cartesian coordinates,

$$u_3(X_1, X_2) = \frac{b}{2\pi}\tan^{-1}\left(\frac{X_2}{X_1}\right) \tag{3.4}$$

From the classical theory of elasticity, for a screw dislocation in an infinite medium, the prescribed displacement field induces a stress field known as self-stress of the screw dislocation. This shear stress field is derived from the displacement field by

$$\sigma_{13} = \sigma_{31} = \frac{\mu}{2}u_{3,1}, \quad \sigma_{23} = \sigma_{32} = \frac{\mu}{2}u_{3,2}, \tag{3.5}$$

where μ is the shear modulus of the material occupying the medium.

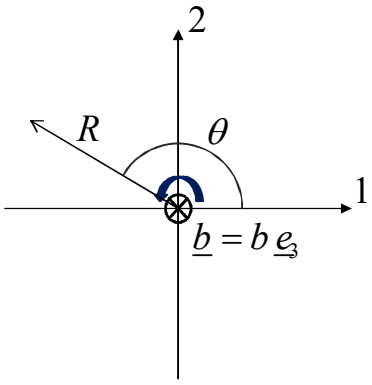

Fig. 3-2- Model of a screw dislocation in an infinite plane.

Hence, we can write:

$$\sigma_{13}=\sigma_{31}=\frac{\mu b}{2\pi}\left(\frac{-X_2}{X_1^{\,2}+X_2^{\,2}}\right),\quad \sigma_{23}=\sigma_{32}=\frac{\mu b}{2\pi}\left(\frac{X_1}{X_1^{\,2}+X_2^{\,2}}\right), \tag{3.6}$$

for the stress field components.

3.2 Screw dislocation near a free surface

Consider a screw dislocation which is located at the point $(a,0)$ in the plane Cartesian coordinate system and a free surface which lies on the X_2-axis. In this case, the traction free surface condition ($\sigma_{13}=0$) must be satisfied. Using the stress field relations (3.6), for a screw dislocation in an infinite plane at the point $(a,0)$ the stress component σ_{13} on the X_2 axis will be

$$\sigma_{13}=\frac{\mu b}{2\pi}\left(\frac{-X_2}{a^2+X_2^{\,2}}\right). \tag{3.7}$$

In order to satisfy the traction free condition on the surface, the stress component (3.7) must be nullified with another equal and opposite stress field. Hence, we superpose an imaginary screw dislocation ($-\vec{b}$) at the mirror position $(-a,0)$. Then, the displacement field in the half-plane is

$$u_3=\frac{b}{2\pi}\left[\tan^{-1}\left(\frac{X_2}{X_1-a}\right)-\tan^{-1}\left(\frac{X_2}{X_1+a}\right)\right]. \tag{3.8}$$

From (3.8), using stress-displacement relations (3.5), we find that

$$\sigma_{13} = \sigma_{31} = \frac{\mu b}{2\pi}\left(\frac{-X_2}{(X_1 - a)^2 + X_2{}^2} + \frac{X_2}{(X_1 + a)^2 + X_2{}^2} \right),$$
$$\sigma_{23} = \sigma_{32} = \frac{\mu b}{2\pi}\left(\frac{X_1 - a}{(X_1 - a)^2 + X_2{}^2} + \frac{-(X_1 + a)}{(X_1 + a)^2 + X_2{}^2} \right), \tag{3.9}$$

in the half-plane ($X_1 \geq 0$).

3.3 Screw dislocation near a bi-material interface

The solution for the more general case of a screw dislocation near a bi-material interface is given in Head [12] and his approach is restated here in detail. Let μ_1 and μ_2 be respectively, the shear moduli of phase 1 and 2 of a bi-material infinite plane medium, namely material 1 and 2. The configuration of the problem is given in Fig. 3-3(a). Again, the dislocation $\underline{b} = b\underline{e}_3$ is located at $(a, 0)$. For a perfectly bonded interface between materials 1 and 2, the continuity of displacement and traction should be enforced. In this regard, we consider materials 1 and 2 separately with boundary conditions,

$$\sigma_{13}^{(1)}(0, X_2) = \sigma_{13}^{(2)}(0, X_2), \quad u_3^{(1)}(0, X_2) = u_3^{(2)}(0, X_2). \tag{3.10}$$

Here, the superscripts "(l)" and "(2)" indicate that the respective quantities belong to materials 1 and 2. If we consider material 1 only, we may assume that an image dislocation of strength b_I at $(-a, 0)$ is superposed with the real dislocation $\underline{b}$ as in Fig. 3-3(b). The resulting displacement and stress components are

$$u_3^{(1)} = \frac{b}{2\pi}\theta_1 + \frac{b_I}{2\pi}\theta_2, \quad \sigma_{13}^{(1)} = \frac{\mu_1 b}{2\pi}\left(\frac{-X_2}{(X_1 - a)^2 + X_2{}^2} \right) + \frac{\mu_1 b_I}{2\pi}\left(\frac{-X_2}{(X_1 + a)^2 + X_2{}^2} \right). \tag{3.11}$$

Next, considering material 2 (Fig. 3-3(c)), the real dislocation outside the material at $(a, 0)$ is added to an image dislocation of strength $-b_I$ at the same location to form

$$u_3^{(2)} = \frac{(b - b_I)}{2\pi}\theta_1 + \alpha, \quad \sigma_{13}^{(2)} = \frac{\mu_2 b_I}{2\pi}\left(\frac{X_2}{(X_1 - a)^2 + X_2{}^2} \right) + \frac{\mu_2 b}{2\pi}\left(\frac{-X_2}{(X_1 - a)^2 + X_2{}^2} \right). \tag{3.12}$$

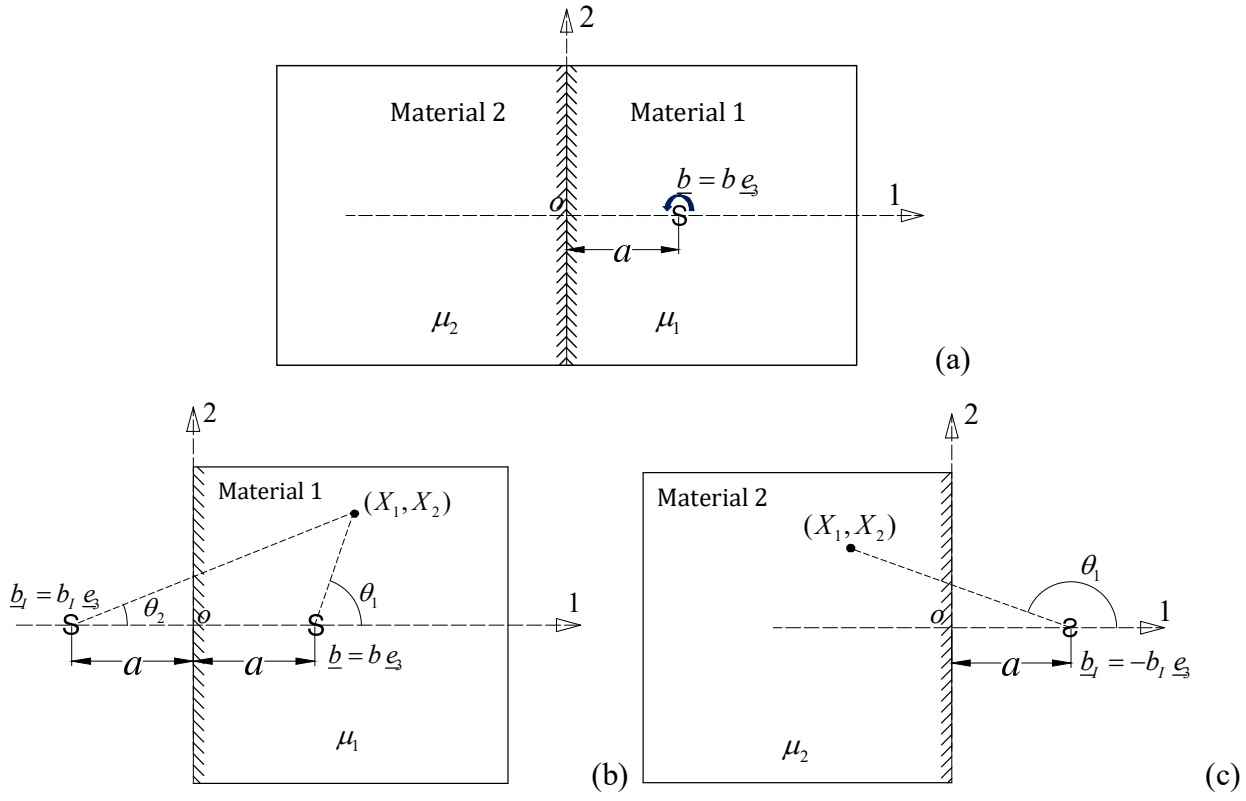

Fig. 3-3- Details of the decomposition made in solving the problem of a screw dislocation near a planar interface

In (3.12), α is an unknown coefficient which along with b_I must be found from the boundary conditions (3.10). From the first equation in (3.10) we obtain:

$$\frac{b_I}{b} = \frac{\mu_2 - \mu_1}{\mu_1 + \mu_2} = K, \tag{3.13}$$

and by applying (3.13) to the second equation,

$$\alpha = \frac{bK}{2}. \tag{3.14}$$

Therefore, using the theory classical elasticity we find the anti-plane displacement component for the boundary value problem of a screw dislocation near the interface of two adjoining half-plane materials as

$$u_3^{(1)} = \frac{b}{2\pi}\left(\theta_1 + K\theta_2\right), \quad u_3^{(2)} = \frac{b}{2\pi}\left((1-K)\theta_1 + K\pi\right), \tag{3.15}$$

where

$$\theta_1 = \tan^{-1}\left(\frac{X_2}{X_1 - a}\right), \quad \theta_2 = \tan^{-1}\left(\frac{X_2}{X_1 + a}\right). \tag{3.16}$$

For convenience, from this point forward, the following mismatch coefficient

$$\Gamma = \frac{\mu_2}{\mu_1}, \tag{3.17}$$

is adopted. Then,

$$K = \frac{\Gamma - 1}{\Gamma + 1}. \tag{3.18}$$

Thus, using (3.5) the stress field components can be expressed as

$$\sigma_{13}^{(1)} = \sigma_{31}^{(1)} = \frac{\mu_1 b}{2\pi}\left[\frac{-X_2}{(X_1 - a)^2 + X_2{}^2} + K\frac{-X_2}{(X_1 + a)^2 + X_2{}^2}\right], \tag{3.19}$$

$$\sigma_{13}^{(2)} = \sigma_{31}^{(2)} = \frac{\mu_2 b}{2\pi}(1 - K)\left(\frac{-X_2}{(X_1 - a)^2 + X_2{}^2}\right), \tag{3.20}$$

$$\sigma_{32}^{(1)} = \sigma_{23}^{(1)} = \frac{\mu_1 b}{2\pi}\left(\frac{(X_1 - a)}{(X_1 - a)^2 + X_2{}^2} + K\frac{(X_1 + a)}{(X_1 + a)^2 + X_2{}^2}\right), \tag{3.21}$$

$$\sigma_{32}^{(2)} = \sigma_{23}^{(2)} = \frac{\mu_2 b}{2\pi}(1 - K)\left(\frac{(X_1 - a)}{(X_1 - a)^2 + X_2{}^2}\right). \tag{3.22}$$

3.4 Interaction force between dislocation and interface

The force on a dislocation is defined as the negative change of total potential energy with the change of position of the dislocation. In general, the force can be written as

$$\underline{F} = -\nabla\Pi, \tag{3.23}$$

where Π indicates the total potential energy in the elastic body. In the absence of external stimuli, the potential energy equals the internal strain energy E. The defined force is a fictitious parameter that determines the state of mobility of a dislocation. Eshelby [74] [75] [76] [77] proposed a general model for the calculation of the interaction force on dislocations and other elastic defects in material bodies. As will be discussed further in the next chapter, we adopt

Eshelby's general idea to determine the force on a dislocation in couple stress elasticity. However, to compute the interaction force in classical elasticity, the Peach-Koehler model [78] is probably the most convenient. The Peach-Koehler model uses a straightforward formula based on the work done by the stress field without "self-stress" of the dislocation when the dislocation moves. Self-stress is defined as the stress field caused by the dislocation in a virtual infinite medium. Consider $\underline{\sigma}_I$ as the non-self-stress tensor field caused by the image effects of surfaces, interfaces and external loadings, and $d\underline{S}$ the element of direction in which the dislocation moves. For an element $d\underline{\zeta}$ of the dislocation line, the work done during the moving process will be the inner product of the force on the movement surface $d\underline{S}\times d\underline{\zeta}$ and the displacement of the lattice $\underline{b}$, generating the movement of the dislocation. Thus, when $d\underline{\zeta}$ moves as much as a $d\underline{S}$, the work done can be expressed as

$$dW_{d\underline{\zeta}} = \underline{b}.\left(\underline{\sigma}_I(d\underline{\zeta}\times d\underline{S})\right). \tag{3.24}$$

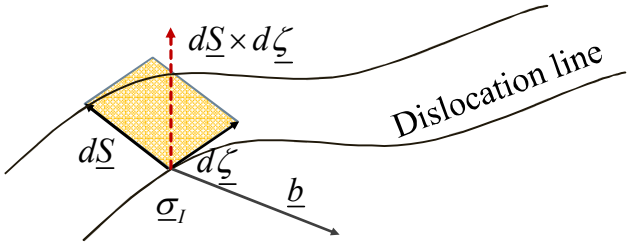

Fig. 3-4- Schematic interpretation of the Peach-Koehler model for calculation of the force

The total work on the dislocation line dW can be computed through integration over $\underline{\zeta}$ as

$$dW = \int_{\underline{\zeta}} \underline{b}.\left(\underline{\sigma}_I(d\underline{\zeta}\times d\underline{S})\right). \tag{3.25}$$

Consequently, the force, by definition, can be written as the negative of the work done during a unit movement of the dislocation $\underline{s}$:

$$\underline{F} = -\int_{\underline{\zeta}} \underline{b}.\left(\underline{\sigma}_I(d\underline{\zeta}\times \underline{s})\right) = -\int_{\underline{\zeta}} \underline{b}.\left(\underline{\sigma}_I(\underline{\zeta}\times \underline{s})\right)d\zeta. \tag{3.26}$$

Clearly, for a screw dislocation near an infinite interface the energy does not change when it moves in the direction parallel to the interface since the configuration is unchanged. Therefore,

with reference to Fig. 3-2 we regard $X_2 = 0$ as the slip plane on which the movement occurs. Using the Peach-Koehler formula (3.26) and the stress components (3.19) to (3.22), we express the interaction force on a unit line of the dislocation near the interface as

$$\underline{F} = -\underline{b}.\left(\underline{\sigma}_I(-\underline{e}_3)\right), \tag{3.27}$$

which leads to

$$\underline{F} = F_1\underline{e}_1 = \frac{\mu_1 b^2}{4\pi a} K\underline{e}_1, \tag{3.28}$$

where F_1 is the force component in the X_1-direction. From (3.28) it is apparent that when $K > 0$, the force repels the dislocation from the interface, while for $K < 0$ the nature of the force between dislocation and interface is attractive.

The classical formulation presented above will serve as a foundation for developing the problem in the case of couple stress theory. In the following chapters, we introduce couple stress effects as a perturbation to this classical solution. As well, we compare the solutions obtained from couple stress theory to the classical solutions presented in this chapter.

4 Calculation of Interaction Forces on Dislocations

The force acting on a dislocation was defined in Section 3.4. As mentioned, the interaction force can be calculated using a straightforward Peach-Koehler method in classical elasticity. This method has also proved useful in problems dealing with anisotropic materials (Ma and Lu [79]) as well as non-local approaches (Eringen, [56] [57], Kroner, [80]). In couple stress theory, however, the aforementioned approach must take into account the couple stress effects on the changes of energy as the dislocation moves. One remedy is to calculate the total elastic energy in the whole system and take the derivative in terms of the dislocation's distance to the interface. Particularly, when the numerical evaluation is needed in the problem this procedure requires a high amount of sampling points and calculations. The use of energy-momentum tensor expressions leading to J-type integrals is another approach which requires less numerical effort since the number of integral variables is less than the previous case. Therefore, for an anti-plane problem such as the screw dislocation problem the two-dimensional integration over an infinite medium is replaced with a finite path integral over an arbitrary line enclosing the dislocation. In this chapter, we outline the concept of conservative energy integrals in elastic materials which is adopted by Eshelby [74][75] in order to determine the configurational forces on material defects. Numerous researchers developed the conservation integral concept to tackle crack (Rice [81], Budiansky and Rice [82]), inclusion [83], phase boundaries [84], and dislocation problems [85]. The idea is expanded to couple stress theory in Atkinson and Leppington [86] [87], and later Lubarda and. Markenscoff [88].

4.1 Conservation law

We consider a phenomenon that is represented mathematically in the form of a partial differential equation. The system which models the phenomenon is assumed to include dependent variables f_j ($j = 1, 2, ..., n$) that are functions of the independent variables X_i ($i = 1, 2, ..., m$). We write the governing PDE for this system in the following form:

$$\mathsf{H}(X_i, f_j, f_{j,i}, ...) = 0, \tag{4.1}$$

where H denotes the differential operator. For a solution f_j of the equation (4.1), if we can find a set of functions $F_k(X_i, f_j, f_{j,i}, ...)$, ($k = 1, 2, ..., m$) associated with independent variables, satisfying,

$$\frac{\partial F_1}{\partial X_1} + \frac{\partial F_2}{\partial X_2} + ... + \frac{\partial F_m}{\partial X_m} = 0 \quad \text{or} \quad \nabla' \cdot \underline{F} = 0, \tag{4.2}$$

then we call (4.2) a conservation law (Herrmann, and Kienzle [89]). For example, if we consider the components of a position vector in Cartesian coordinates (X_1, X_2, X_3) and time t as the independent variables and define F_1, F_2 and F_3 as the flux of energy density in each direction of the coordinates and F_t the energy density at time t , then for a given point in this system, the rate of change of energy density is equal to the flux of energy density at that point. This is the law of conservation of energy which can be expressed by

$$\frac{dF_1}{dX_1} + \frac{dF_2}{dX_2} + \frac{dF_3}{dX_3} + \frac{dF_t}{dt} = 0. \tag{4.3}$$

We generalize the conservation law in an integral form over a domain of volume V . In this case, if we consider the components of a position vector in Cartesian coordinates (X_1, X_2, X_3) as independent variables and remove the time dependence, then for a conserved system of volume V , devoid of sources and sinks, we may write

$$\int_V \frac{\partial F_j}{\partial X_j} dV = 0, \tag{4.4}$$

which by the Divergence Theorem, gives

$$\int_A F_j n_j dA = 0, \tag{4.5}$$

over the boundary of the domain, A. The expression (4.5) states that in the absence of a source or sink of F_j inside the domain, the summation of a flux quantity with components F_j over the boundary of the domain is zero.

4.2 Noether's model for conservation law in couple stress theory

As implied in chapter 2, the strain energy density in couple stress theory is a function of displacement and rotation gradients $u_{i,j}$ and $\omega_{i,j}$, respectively. Here, we assume that the strain energy density in a couple stress homogeneous material in its static state is a Lagrangian function,

$$L = w(u_{i,j}, \omega_{i,j}). \tag{4.6},$$

Then, the strain energy for the whole body of volume V and surface area A can be written as

$$E = \int_V L(u_{i,j}, \omega_{i,j}) dV = \int_V w(u_{i,j}, \omega_{i,j}) dV. \tag{4.7}$$

We consider E as a functional and apply Hamilton's principle of stationary action. According to this principle, a system changes through a path on which the action (in the present case E) is stationary (unchanged of the first order). Consequently, the functions $u_{i,j}$ and $\omega_{i,j}$ that provide the stationary action condition for the functional E are the solutions to the system. Formally, the functions $u_{i,j}$ and $\omega_{i,j}$ will be the solutions to the equation

$$\delta E = 0, \tag{4.8}$$

where δ indicates the first variation of the functional E. In order to apply the condition (4.8) on (4.7), we make an infinitesimal transform in displacement, rotation, and position of the system. The transformed parameters can be expressed as

$$X_i^* = X_i + \boldsymbol{\varepsilon}\xi_i(X_j, u_m, \omega_n), \quad u_i^* = u_i + \boldsymbol{\varepsilon}\varphi_i(X_j, u_m, \omega_n), \quad \omega_i^* = \omega_i + \boldsymbol{\varepsilon}\psi_i(X_j, u_m, \omega_n), \tag{4.9}$$

where $\boldsymbol{\varepsilon}$ is an infinitesimally small scalar and ξ_i, φ_i and ψ_i are arbitrary functions. The starred

parameters indicate the transformed state of the un-starred parameters. Hence, the energy expression after the infinitesimal transformation can be written as

$$E^* = \int_{V^*} w(\frac{\partial u_i^*}{\partial X_j^*}, \frac{\partial \omega_i^*}{\partial X_j^*}) dV^*. \tag{4.10}$$

Now, we rewrite E^* in terms of untransformed state parameters u_i, ω_i and X_i. Thus, for the differential variable of integration we have

$$dV^* = |J| dV = \begin{vmatrix} \frac{\partial X_1^*}{\partial X_1} & \frac{\partial X_2^*}{\partial X_1} & \frac{\partial X_3^*}{\partial X_1} \\ \frac{\partial X_1^*}{\partial X_2} & \frac{\partial X_2^*}{\partial X_2} & \frac{\partial X_3^*}{\partial X_2} \\ \frac{\partial X_1^*}{\partial X_3} & \frac{\partial X_2^*}{\partial X_3} & \frac{\partial X_3^*}{\partial X_3} \end{vmatrix} dV, \tag{4.11}$$

which with reference to the first equation in (4.9), and elimination of the higher order terms of the small parameter $\boldsymbol{\varepsilon}$, becomes

$$dV^* = \begin{vmatrix} 1+\boldsymbol{\varepsilon}\xi_{1,1} & \boldsymbol{\varepsilon}\xi_{2,1} & \boldsymbol{\varepsilon}\xi_{3,1} \\ \boldsymbol{\varepsilon}\xi_{1,2} & 1+\boldsymbol{\varepsilon}\xi_{2,2} & \boldsymbol{\varepsilon}\xi_{3,2} \\ \boldsymbol{\varepsilon}\xi_{1,3} & \boldsymbol{\varepsilon}\xi_{2,3} & 1+\boldsymbol{\varepsilon}\xi_{3,3} \end{vmatrix} dV \simeq (1+\boldsymbol{\varepsilon}\xi_{i,i}) dV. \tag{4.12}$$

Using the chain rule, we can state that

$$\frac{\partial u_i^*}{\partial X_j^*} = \frac{\partial u_i^*}{\partial X_k} \frac{\partial X_k}{\partial X_j^*} = \left(u_{i,k} + \boldsymbol{\varepsilon}\varphi_{i,k}\right)\left(\delta_{jk} + \boldsymbol{\varepsilon}\xi_{k,j}\right) = u_{i,j} + \boldsymbol{\varepsilon}\left(\varphi_{i,j} - u_{i,k}\xi_{k,j}\right), \tag{4.13}$$

and

$$\frac{\partial \omega_i^*}{\partial X_j^*} = \frac{\partial \omega_i^*}{\partial X_k} \frac{\partial X_k}{\partial X_j^*} = \left(\omega_{i,k} + \boldsymbol{\varepsilon}\psi_{i,k}\right)\left(\delta_{jk} + \boldsymbol{\varepsilon}\xi_{k,j}\right) = \omega_{i,j} + \boldsymbol{\varepsilon}\left(\psi_{i,j} - \omega_{i,k}\xi_{k,j}\right). \tag{4.14}$$

Substituting (4.12), (4.13) and (4.14), into (4.10), we have

$$E^* = \int_V w\left(u_{i,j} + \boldsymbol{\varepsilon}\left(\varphi_{i,j} - u_{i,k}\xi_{k,j}\right), \omega_{i,j} + \boldsymbol{\varepsilon}\left(\psi_{i,j} - \omega_{i,k}\xi_{k,j}\right)\right)(1+\boldsymbol{\varepsilon}\xi_{i,i}) dV. \tag{4.15}$$

We expand the function w in Taylor series about its value at $(u_{i,j}, \omega_{i,j})$. Considering terms of first order and ignoring higher order terms, the result will be

$$E^* = \int_V \left\{ w\left(u_{i,j}, \omega_{i,j}\right) + \boldsymbol{\varepsilon}\left(\varphi_{i,j} - u_{i,k}\xi_{k,j}\right)\frac{\partial w}{\partial u_{i,j}} + \boldsymbol{\varepsilon}\left(\psi_{i,j} - \omega_{i,k}\xi_{k,j}\right)\frac{\partial w}{\partial \omega_{i,j}} \right\}(1 + \boldsymbol{\varepsilon}\xi_{k,k})dV. \quad (4.16)$$

Next, we extract the initial energy expression (before the transformation) from the relation(4.16). That is

$$E^* = \int_V w dV + \boldsymbol{\varepsilon}\int_V \left(\left(\varphi_{i,j} - u_{i,k}\xi_{k,j}\right)\frac{\partial w}{\partial u_{i,j}} + \left(\psi_{i,j} - \omega_{i,k}\xi_{k,j}\right)\frac{\partial w}{\partial \omega_{i,j}} + w\xi_{k,k} \right) dV. \quad (4.17)$$

Since we have (4.7), the variation of energy due to the transformation of the system can be written as

$$E^* - E = \boldsymbol{\varepsilon}\int_V \left(\left(\varphi_{i,j}\frac{\partial w}{\partial u_{i,j}} + \psi_{i,j}\frac{\partial w}{\partial \omega_{i,j}} \right) - \xi_{k,j}\left(u_{i,k}\frac{\partial w}{\partial u_{i,j}} + \omega_{i,k}\frac{\partial w}{\partial \omega_{i,j}} \right) + w\xi_{k,k} \right) dV. \quad (4.18)$$

We use the relation:

$$w\xi_{k,k} = \left(w\xi_k\right)_{,k} - \xi_k\left(\frac{\partial w}{\partial u_{i,j}}u_{i,jk} + \frac{\partial w}{\partial \omega_{i,j}}\omega_{i,jk} \right), \quad (4.19)$$

in (4.18), to obtain

$$\begin{aligned} E^* - E = \boldsymbol{\varepsilon}\int_V \Bigg[& \left(\varphi_{i,j}\frac{\partial w}{\partial u_{i,j}} + \psi_{i,j}\frac{\partial w}{\partial \omega_{i,j}} \right) - \xi_{k,j}\left(\frac{\partial w}{\partial u_{i,j}}u_{i,k} + \frac{\partial w}{\partial \omega_{i,j}}\omega_{i,k} \right) \\ & + \left(w\xi_k\right)_{,k} - \xi_k\left(\frac{\partial w}{\partial u_{i,j}}u_{i,jk} + \frac{\partial w}{\partial \omega_{i,j}}\omega_{i,jk} \right) \Bigg] dV. \end{aligned} \quad (4.20)$$

The above relation can be rearranged to the form,

$$E^* - E = \boldsymbol{\varepsilon}\int_V \left(\left(\varphi_i - \xi_k u_{i,k}\right)_{,j}\frac{\partial w}{\partial u_{i,j}} + \left(\psi_i - \xi_k\omega_{i,k}\right)_{,j}\frac{\partial w}{\partial \omega_{i,j}} + \left(w\xi_j\right)_{,j} \right) dV. \quad (4.21)$$

The equation (4.21) can also be expressed as

$$E^* - E = \varepsilon \int_V \left[\left(\left(\varphi_i - \xi_k u_{i,k} \right) \frac{\partial w}{\partial u_{i,j}} \right)_{,j} + \left(\left(\psi_i - \xi_k \omega_{i,k} \right) \frac{\partial w}{\partial \omega_{i,j}} \right)_{,j} + \left(w \xi_j \right)_{,j} \right.$$
$$\left. - \left(\varphi_i - \xi_k u_{i,k} \right) \frac{\partial}{\partial X_j} \left(\frac{\partial w}{\partial u_{i,j}} \right) - \left(\psi_i - \xi_k \omega_{i,k} \right) \frac{\partial}{\partial X_j} \left(\frac{\partial w}{\partial \omega_{i,j}} \right) \right] dV. \tag{4.22}$$

Using the constitutive equations obtained in Section 2.5 for couple stress theory we deduce that

$$\frac{\partial w}{\partial u_{i,j}} = \sigma_{ji}^S = \sigma_{ji} - \sigma_{ji}^A, \quad \frac{\partial w}{\partial \omega_{i,j}} = \mu_{ji}. \tag{4.23}$$

Thus (4.22) gives

$$E^* - E = \varepsilon \int_V \left[\left(\left(\varphi_i - \xi_k u_{i,k} \right) \left(\sigma_{ji} - \sigma_{ji}^A \right) + \left(\psi_i - \xi_k \omega_{i,k} \right) \mu_{ji} + w \xi_j \right)_{,j} \right.$$
$$\left. - \left(\varphi_i - \xi_k u_{i,k} \right) \left(\sigma_{ji,j} - \sigma_{ji,j}^A \right) - \left(\psi_i - \xi_k \omega_{i,k} \right) \left(-\varepsilon_{inm} \sigma_{nm}^A \right) \right] dV. \tag{4.24}$$

After taking out the antisymmetric stress from the first term and imposing the equation of equilibrium (2.14) in the absence of body forces, we apply the stationary condition to the variation of energy. We may write:

$$\frac{E^* - E}{\varepsilon} = \int_V \left[\left(\left(\varphi_i - \xi_k u_{i,k} \right) \sigma_{ji} + \left(\psi_i - \xi_k \omega_{i,k} \right) \mu_{ji} + w \xi_j \right)_{,j} \right.$$
$$\left. + \left(\varphi_i - \xi_k u_{i,k} \right)_{,j} \sigma_{ji}^A + \left(\psi_i - \xi_k \omega_{i,k} \right) \varepsilon_{inm} \sigma_{nm}^A \right] dV = 0. \tag{4.25}$$

From (4.25) we extract the conditions under which the strain energy is conserved during the transformations defined in (4.9). The conditions are:

$$\frac{\partial}{\partial X_j} \left(\left(\varphi_i - \xi_k u_{i,k} \right) \sigma_{ji} + \left(\psi_i - \xi_k \omega_{i,k} \right) \mu_{ji} + w \xi_j \right) = 0,$$
$$\left(\varphi_i - \xi_k u_{i,k} \right)_{,j} \sigma_{ij}^A = \left(\psi_i - \xi_k \omega_{i,k} \right) \varepsilon_{inm} \sigma_{nm}^A. \tag{4.26}$$

Therefore, energy is stationary under the transforms that are made by the functions ξ_i, φ_i and ψ_i satisfying the conditions (4.26). In other words, every composition of functions ξ_i, φ_i and

ψ_i that satisfy (4.26) is a conserved transform and equations (4.26) incorporating those functions are considered as conservation laws in couple stress elasticity.

For application to the present discussion, we consider a special case where

$$\varphi_i = 0, \quad \psi_i = 0, \quad \xi_i = \delta_{ij}. \tag{4.27}$$

Note that if we consider $\{\underline{e}_1, \underline{e}_2, \underline{e}_3\}$ as a standard basis for the Cartesian coordinates $\{X_1, X_2, X_3\}$, then the third relation in (4.27) becomes $\xi_i \underline{e}_i = \delta_{ij} \underline{e}_i = \underline{e}_j$, meaning that the transform applied to the system is a unit translation of configuration in the X_j-direction. One can easily verify that the set of functions defined in (4.27) satisfy the second equation in (4.26). Thus, we introduce (4.27) into the equation (4.25) to obtain:

$$\frac{E^* - E}{\boldsymbol{\varepsilon}} = \int_V \left(\left(\varphi_i - \delta_{kn} u_{i,k} \right) \sigma_{ji} + \left(\psi_i - \delta_{kn} \omega_{i,k} \right) \mu_{ji} + w \delta_{jn} \right)_{,j} dV. \tag{4.28}$$

Using the Divergence Theorem, the foregoing integral can be converted to an integral over the closed surface S of the body,

$$\frac{\delta E}{\boldsymbol{\varepsilon}} = \oint_S \left(\left(\varphi_i - \delta_{kn} u_{i,k} \right) \sigma_{ji} + \left(\psi_i - \delta_{kn} \omega_{i,k} \right) \mu_{ji} + w \delta_{jn} \right) n_j dS, \tag{4.29}$$

or in the well-known form of a J-integral,

$$J_n = \frac{\delta E}{\boldsymbol{\varepsilon}} = \oint_S \left(\delta_{nj} w - \mu_{ji} \omega_{i,n} - \sigma_{ji} u_{i,n} \right) n_j dS. \tag{4.30}$$

If there is no source of stress including inhomogeneities, dislocations or crack tips inside the enclosed surface S, then obviously, the translation of the configuration in the X_n-direction leads to a zero change of energy. This indicates the conservation law,

$$J_n = \oint_S \left(\delta_{nj} w - \mu_{ji} \omega_{i,n} - \sigma_{ji} u_{i,n} \right) n_j dS = 0, \tag{4.31}$$

and yet, accounts for path independence of the J-integral. However, in general, when a source of stress, such as a dislocation, is present within the enclosed surface of a body while the configuration undergoes a translation, the change of energy is not zero and the situation is

equivalent to a translation of the source of energy inside the body. As a result, the change of energy during a unit translation of a source of stress equals the J-integral over an arbitrary surface which is completely located in a homogeneous part of the material and encloses the source of stress. This quantity is defined in the literature as the nth component of the virtual force acting on the stress source (in our case a dislocation) and can be written as

$$F_n = \oint_S \left(\delta_{nj} w - \mu_{ji} \omega_{i,n} - \sigma_{ji} u_{i,n} \right) n_j dS, \tag{4.32}$$

where the tensor with components

$$P_{nj} = \delta_{nj} w - \mu_{ji} \omega_{i,n} - \sigma_{ji} u_{i,n} \tag{4.33}$$

is defined by Eshelby [75] as the energy-momentum tensor in an elastic field.

4.3 Intuitive explanation of forces on a dislocation

Eshelby [74] [75] expounds the idea of forces on material defects in a more straightforward manner. He divides moving of a stress source into two stages: (1) change of elastic energy due to the translation of the stress source (2) adjustment of the quantities so that they conform again with the boundary conditions. To provide a better understanding, here we develop his approach to couple stress elasticity.

Consider a body of couple stress elastic material containing a dislocation shown in Fig. 4-1. The boundary conditions on the surface S of this body include displacement and rotations u_j and ω_j as well as force and couple tractions $\sigma_{ij} n_i$ and $\mu_{ij} n_i$, respectively. The objective is to evaluate the change of total potential energy in the material as the dislocation translates by a corresponding vector with components ξ_k. In stage (1), we assume that the dislocation is fixed and the surrounding body along with all its quantities (stress and couple stress fields) moves by a vector with components $-\xi_k$ (Fig. 4-1). Consequently, in the new position, the stress field induces new boundary conditions, $u_j - \xi_k u_{j,k}$, $\omega_j - \xi_k \omega_{j,k}$, $\left(\sigma_{ij} - \xi_k \sigma_{ij,k} \right) n_i$ and $\left(\mu_{ij} - \xi_k \mu_{ij,k} \right) n_i$, for displacement, rotation, force stress, and couple stress tractions, respectively. The change of stain energy in stage (1) can be written as

$$\delta E^{(\mathrm{I})}_{elastic} = \int_V w_{,i}\xi_i dV = \xi_i \int_V w_{,i} dV = \xi_i \oint_S w_i n_i dS \tag{4.34}$$

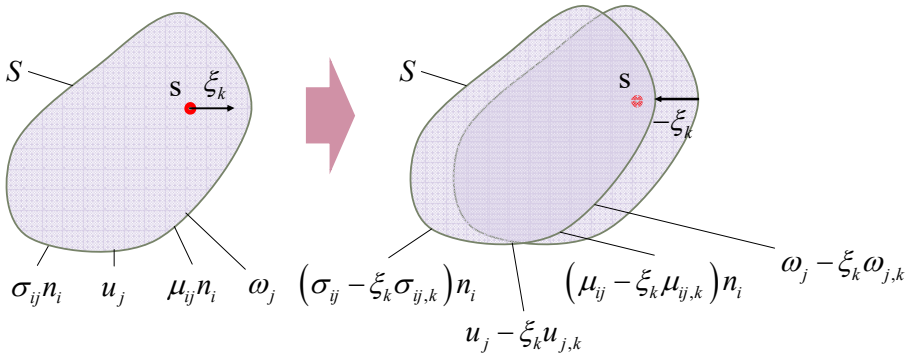

Fig. 4-1- Stage 1: Translation of a dislocation inside a body

In stage (2), we adjust the boundary conditions to the final values for displacement and rotations u_j^f and ω_j^f, so that we regain $\sigma_{ij}n_i$ and $\mu_{ij}n_i$, for stress and couple stress tractions. During the adjustment stage shown in Fig. 4-2, we neglect changes in traction since those changes are of the order of ξ_k, and we express the change of elastic energy due to the tractions $\sigma_{ij}n_i$ and $\mu_{ij}n_i$ on the surface S of the body at the stage (2) as

$$\delta E^{(\mathrm{II})}_{elastic} = \oint_S \left[\sigma_{ij}(u_j^f - u_j + \xi_k u_{j,k}) + \mu_{ij}(\omega_j^f - \omega_j + \xi_k \omega_{j,k})\right] n_i dS. \tag{4.35}$$

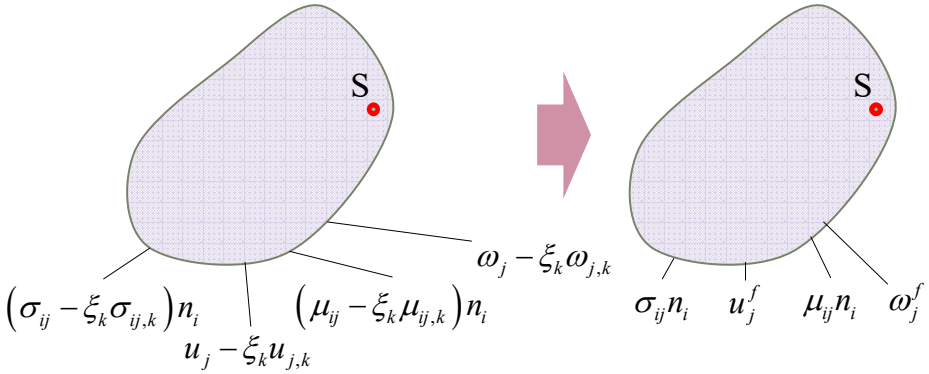

Fig. 4-2-Stage 2: Adjustment of boundary conditions

Now, we consider the work done during the total process. A dislocation is displaced inside an elastic body so that the final values of displacements and rotations on the surface become u_j^f and

ω_j^f, respectively. The work done by the surface tractions $\sigma_{ij}n_i$ and $\mu_{ij}n_i$ as external factors, during this process can be formulated as

$$\delta W_{External}^{(\mathrm{I\&II})} = \oint_S \left[\sigma_{ij}(u_j^f - u_j) + \mu_{ij}(\omega_j^f - \omega_j) \right] n_i dS. \tag{4.36}$$

With the aid of (4.34), (4.35) and (4.36) we may establish the variation of total potential energy as

$$\delta E_{elastic}^{(\mathrm{I})} + \delta E_{elastic}^{(\mathrm{II})} - \delta W_{External}^{(\mathrm{I\&II})} = \delta\Pi = \oint_S w\xi_i n_i - \sigma_{ij}n_i\xi_k u_{j,k} - \mu_{ij}n_i\xi_k\omega_{j,k} dS. \tag{4.37}$$

Therefore, the change of total energy for a unit translation of the dislocation can be written as

$$\frac{\delta E}{\xi_k} = J_k = \oint_S (w\delta_{ik} - \sigma_{ij}u_{j,k} - \mu_{ij}\omega_{j,k})n_i dS \tag{4.38}$$

which is equivalent to the force acting on the dislocation in the X_k-direction of the reference Cartesian coordinates. Again, the condition stated in Eshelby [75] for the use of the J-integral must be satisfied. Accordingly, the closed surface S must not cross any singularity or inhomogeneity. In addition, the integral (4.38) is path independent as long as the surface we choose is placed entirely in the homogeneous material and encompasses the same singularities.

We use this concept to calculate the force on a screw dislocation with a high degree of certainty for different configurations. To do so, considering the aforementioned conditions, we choose an arbitrary surface which for the anti-plane problem at hand reduces to a path enclosing the screw dislocation. Consequently, we use (4.38) for the special case of an anti-plane problem and we choose an arbitrary rectangular path to incorporate the quantities obtained in the rectangular Cartesian coordinates assigned to the problem. In the next chapters, we represent the obtained results for the force on screw dislocations induced by nearby bi-material interfaces, substrate-film interfaces, and free surfaces. We also present illustrative examples and discussions regarding the influence of different parameters on the force.

5 Screw Dislocation Near an Interface in Couple Stress Theory

The fundamentals of couple stress theory have been discussed in Chapter 2. The main purpose of this chapter is to employ couple stress theory to solve the problem of a screw dislocation near a bi-material interface. As mentioned in Chapter 3, a screw dislocation induces anti-plane shear deformations on the surrounding medium. Therefore, first, we derive the governing equation for an anti-plane problem in the couple stress theory. Next, we use Fourier integral transforms to derive the solution to the boundary value problem. Then, using the results from stress and couple stress fields we determine the interaction force between the dislocation and the interface. Finally, numerical results are presented to illustrate the influence of couple stresses on the solution and compare them to the existing classical results.

5.1 Couple stress theory for anti-plane problems

The general governing field equation in couple stress theory in the absence of body forces has been obtained in Section 2.5. If we adopt Cartesian coordinates as in Chapter 3, then for the anti-plane problem of a screw dislocation, the non-vanishing displacement component acts in the X_3-direction. Thus, the displacement field is a function of X_1 and X_2. We can write:

$$\underline{u} = u_3(X_1, X_2)\underline{e}_3, \tag{5.1}$$

and from (2.87) we can deduce that the non-vanishing components of stress and strain tensors are

$$\varepsilon_{ij}=\begin{bmatrix}0 & 0 & \varepsilon_{13}\\ 0 & 0 & \varepsilon_{23}\\ \varepsilon_{31} & \varepsilon_{32} & 0\end{bmatrix},\quad \sigma_{ij}=\begin{bmatrix}0 & 0 & \sigma_{13}\\ 0 & 0 & \sigma_{23}\\ \sigma_{31} & \sigma_{32} & 0\end{bmatrix}, \tag{5.2}$$

where,

$$\varepsilon_{13}=\varepsilon_{31}=\frac{1}{2}u_{3,1},\quad \varepsilon_{23}=\varepsilon_{32}=\frac{1}{2}u_{3,2}. \tag{5.3}$$

Using the expression (2.96) for the static case, in the absence of body forces and body couples,

$$\sigma_{tl}=\mu\left(u_{t,l}+u_{l,t}\right)+\lambda\delta_{tl}u_{k,k}-\frac{(\gamma+e)}{2}u_{l,tii}{}^{A}, \tag{5.4}$$

we may translate the stress components in terms of displacement component u_3 as

$$\sigma_{ij}=\begin{bmatrix}0 & 0 & \sigma_{13}=\mu u_{3,1}-\dfrac{\gamma+e}{4}\nabla^2u_{3,1}\\ 0 & 0 & \sigma_{23}=\mu u_{3,2}-\dfrac{\gamma+e}{4}\nabla^2u_{3,2}\\ \sigma_{31}=\mu u_{3,1}+\dfrac{\gamma+e}{4}\nabla^2u_{3,1} & \sigma_{32}=\mu u_{3,2}+\dfrac{\gamma+e}{4}\nabla^2u_{3,2} & 0\end{bmatrix}. \tag{5.5}$$

Pursuing the same procedure, from (2.92) we find the following for the couple stress components:

$$\mu_{ij}=\begin{bmatrix}\mu_{11}=\gamma u_{3,21} & \mu_{12}=-\left(\dfrac{\gamma+e}{2}\right)u_{3,11}+\left(\dfrac{\gamma-e}{2}\right)u_{3,22} & 0\\ \mu_{21}=\left(\dfrac{\gamma+e}{2}\right)u_{3,22}-\left(\dfrac{\gamma-e}{2}\right)u_{3,11} & \mu_{22}=-\gamma u_{3,21} & 0\\ 0 & 0 & 0\end{bmatrix} \tag{5.6}$$

The governing field equation in terms of displacement components is given in (2.97) This equation for the static case, in the absence of body forces and body couples can be rewritten as

$$\left(\mu-\frac{\gamma+e}{4}\nabla^2\right)u_{l,tt}+\left(\mu+\lambda+\frac{\gamma+e}{4}\nabla^2\right)u_{t,lt}=0. \tag{5.7}$$

Since u_3 is the only displacement component and a function of X_1 and X_2, then the second term in (5.7) vanishes, so that (5.7) becomes

$$\left(\mu - \frac{\gamma + e}{4}\nabla^2\right)u_{3,tt} = 0, \tag{5.8}$$

which can be written in the form

$$\left(\nabla^2 - \frac{\gamma + e}{4\mu}\nabla^4\right)u_3 = 0, \tag{5.9}$$

or

$$\left(\nabla^2 - l^2\nabla^4\right)u_3 = 0, \tag{5.10}$$

where $\nabla^4 = \nabla^2\nabla^2$. The parameter $l = \sqrt{(\gamma + e)/4\mu}$ in (5.9) has the dimension of length and it is known as the characteristic length of material in the literature (Mindlin and Tiersten [35], Mindlin [18]). The characteristic length is believed to be the range of atomic forces [16], the size of the grains or size of other microstructural features of a material (Yang and Lakes [90]). Both for the purpose of simplicity, and because of its justification through Grioli's [32] representation of constitutive equations on the grounds that the rigid rotation has no contribution to the elastic energy, we can assume that the $\gamma = e$. A detailed explanation of Grioli's approach is given in Mindlin and Tiersten [35]. Taking $\gamma = e$ is equivalent to taking $\eta' = 0$ in the representation by Mindlin and Tiersten [35], since in their notation $\eta' = (\gamma - e)/4$. Note that $(\gamma - e)/4$ does not appear in the displacement field equation (5.9) and affects the solution only through the boundary conditions. Accordingly, the stress components become

$$\sigma_{ij} = \begin{bmatrix} 0 & 0 & \mu u_{3,1} - \frac{\gamma}{2}\nabla^2 u_{3,1} \\ 0 & 0 & \mu u_{3,2} - \frac{\gamma}{2}\nabla^2 u_{3,2} \\ \mu u_{3,1} + \frac{\gamma}{2}\nabla^2 u_{3,1} & \mu u_{3,2} + \frac{\gamma}{2}\nabla^2 u_{3,2} & 0 \end{bmatrix}, \tag{5.11}$$

and the couple stress components,

$$\mu_{ij} = \begin{bmatrix} \gamma u_{3,21} & -\gamma u_{3,11} & 0 \\ \gamma u_{3,22} & -\gamma u_{3,21} & 0 \\ 0 & 0 & 0 \end{bmatrix}. \tag{5.12}$$

The characteristic length is also converted to

$$l = \sqrt{\frac{\gamma}{2\mu}} \tag{5.13}$$

5.2 Solution to the boundary value problem of a screw dislocation near a bi-material interface

Fig. 5-1, illustrates the configuration of the boundary value problem of a screw dislocation near a bi-material interface. As shown in the figure, we consider two semi-infinite adjoining linear elastic isotropic material phases referred to as "Phase (Material) 1" and "Phase (Material) 2". We assign shear moduli μ_1 and μ_2, and bending-twisting moduli γ_1 and γ_2 to Phase 1 and Phase 2 respectively. Similar to the previous chapter, we place the rectangular Cartesian coordinates system $\{o : X_1, X_2, X_3\}$ described by the standard basis $\{\underline{e}_1, \underline{e}_2, \underline{e}_3\}$ in a way that the interface coincides with the X_2-axis and a right-handed screw dislocation is located at the point $(X_1 = a, X_2 = 0)$. Again, we consider $X_1 - X_3$ as the slip plane and as in Section 3.1, we formulate the dislocation by

$$b = \left[u_3(X_1, 0^-) - u_3(X_1, 0^+) \right], \quad X_1 > a \tag{5.14}$$

We assume that the two material phases are perfectly bonded ensuring continuity of displacements, rotations, and tractions at the interface.

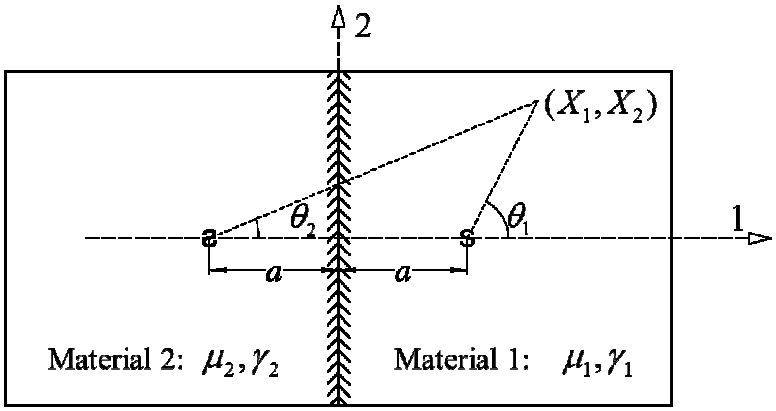

Fig. 5-1- Configuration of the problem.

The solution of the boundary value problem using classical elasticity has been obtained in section 3.3 in the form,

$$u_3'^{(1)} = \frac{b}{2\pi}\left(\theta_1 + K\theta_2\right), \quad u_3'^{(2)} = \frac{b}{2\pi}\left((1-K)\theta_1 + K\pi\right), \tag{5.15}$$

where,

$$\theta_1 = \tan^{-1}\left(\frac{X_2}{X_1 - a}\right), \quad \theta_2 = \tan^{-1}\left(\frac{X_2}{X_1 + a}\right), \quad \Gamma = \frac{\mu_2}{\mu_1}, \quad K = \frac{\Gamma - 1}{\Gamma + 1}. \tag{5.16}$$

Using superposition, we introduce the effects of couple stress theory on the solution as perturbations added to (5.15). Thus, the displacement solution can be expressed as

$$u_3^{(1)} = u_3'^{(1)} + \hat{u}_3^{(1)}, \quad u_3^{(2)} = u_3'^{(2)} + \hat{u}_3^{(2)}. \tag{5.17}$$

The defined displacement field must satisfy the governing equation (5.10) in each one of the material phases. Then,

$$\begin{aligned} &\left(\nabla^2 - l_1^2\nabla^4\right)u_3^{(1)} = 0, \quad X_1 \geq 0 \\ &\left(\nabla^2 - l_2^2\nabla^4\right)u_3^{(2)} = 0, \quad X_1 < 0. \end{aligned} \tag{5.18}$$

where, $l_1^2 = \gamma_1 / 2\mu_1$ and $l_2^2 = \gamma_2 / 2\mu_2$. Inserting (5.17) into (5.18), we find that the classical part already satisfies the governing equation. Therefore, we have:

$$\left(\nabla^2 - l_1^2\nabla^4\right)\hat{u}_3^{(1)} = 0, \quad \left(\nabla^2 - l_2^2\nabla^4\right)\hat{u}_3^{(2)} = 0. \tag{5.19}$$

Considering the discussion on boundary conditions in couple stress theory made in Section 2.5, the perfectly bonded boundary conditions at the interface can be written as

$$\begin{aligned} &\sigma_{13}^{(1)}(0,X_2)=\sigma_{13}^{(2)}(0,X_2), \quad \mu_{12}^{(1)}(0,X_2)=\mu_{12}^{(2)}(0,X_2), \\ &u_3^{(1)}(0,X_2)=u_3^{(2)}(0,X_2), \quad u_{3,1}^{(1)}(0,X_2)=u_{3,1}^{(2)}(0,X_2). \end{aligned} \tag{5.20}$$

Also, with reference to the results available for an infinite medium by Lubarda [67] and the earlier work of Cohen [55], we posit that the parts of the solution induced by the couple stress effects, $\hat{u}_3^{(1)}$ and $\hat{u}_3^{(2)}$, vanish as $X_1 \to \pm\infty$ or $X_2 \to \pm\infty$.

Using the equations (5.11), (5.12), (5.15) and (5.17), the boundary conditions (5.20) can be expanded to

$$\begin{aligned} &\sigma_{13}^{(1)}(0,X_2)=\sigma_{13}^{(2)}(0,X_2) \Rightarrow \\ &\left(\mu_1\hat{u}_{3,1}^{(1)}(0,X_2)-\mu_2\hat{u}_{3,1}^{(2)}(0,X_2)\right)-\left(\frac{\gamma_1}{2}\nabla^2\hat{u}_{3,1}^{(1)}(0,X_2)-\frac{\gamma_2}{2}\nabla^2\hat{u}_{3,1}^{(2)}(0,X_2)\right)=0, \end{aligned} \tag{5.21}$$

$$\begin{aligned} &\mu_{12}^{(1)}(0,X_2)=\mu_{12}^{(2)}(0,X_2) \Rightarrow \\ &\frac{b}{2\pi}\left(\left[(\gamma_1-\gamma_2)(1-K)\right]\frac{2X_2a}{\left[a^2+X_2^{\,2}\right]^2}\right)-\left(\gamma_1\hat{u}_{3,11}^{(1)}(0,X_2)-\gamma_2\hat{u}_{3,11}^{(2)}(0,X_2)\right)=0, \end{aligned} \tag{5.22}$$

$$u_3^{(1)}(0,X_2)=u_3^{(2)}(0,X_2) \Rightarrow \hat{u}_3^{(1)}(0,X_2)-\hat{u}_3^{(2)}(0,X_2)=0, \tag{5.23}$$

$$\begin{aligned} &u_{3,1}^{(1)}(0,X_2)=u_{3,1}^{(2)}(0,X_2) \Rightarrow \\ &\frac{b}{2\pi}\left(\frac{-2KX_2}{a^2+X_2^{\,2}}\right)+\hat{u}_{3,1}^{(1)}(0,X_2)-\hat{u}_{3,1}^{(2)}(0,X_2)=0. \end{aligned} \tag{5.24}$$

We apply the Fourier integral transform in the form,

$$\tilde{U}(s)=\frac{1}{\sqrt{2\pi}}\int_{-\infty}^{\infty}u(X_2)e^{-isX_2}dX_2, \tag{5.25}$$

and the inverse transform,

$$u(X_2) = \frac{1}{\sqrt{2\pi}} \int_{-\infty}^{\infty} \tilde{U}(s) e^{is X_2} ds, \tag{5.26}$$

to the governing field equations (5.19). Consequently, we obtain

$$\left(\frac{\partial^2}{\partial X_1^{\,2}} - s^2 \right) \left(-l_1^{\,2} \frac{\partial^2}{\partial X_1^{\,2}} + 1 + s^2 l_1^{\,2} \right) \tilde{U}_3^{(1)}(X_1, s) = 0, \tag{5.27}$$

and

$$\left(\frac{\partial^2}{\partial X_1^{\,2}} - s^2 \right) \left(-l_2^{\,2} \frac{\partial^2}{\partial X_1^{\,2}} + 1 + s^2 l_2^{\,2} \right) \tilde{U}_3^{(2)}(X_1, s) = 0, \tag{5.28}$$

for Phases 1 and 2, respectively. The two resultant ordinary differential equations yield the following general solutions:

$$\tilde{U}_3^{(1)} = A_1(s) e^{|s| X_1} + B_1(s) e^{-|s| X_1} + C_1(s) e^{\sqrt{\frac{1}{l_1^{\,2}} + s^2} X_1} + D_1(s) e^{-\sqrt{\frac{1}{l_1^{\,2}} + s^2} X_1}, \tag{5.29}$$

$$\tilde{U}_3^{(2)} = A_2(s) e^{|s| X_1} + B_2(s) e^{-|s| X_1} + C_2(s) e^{\sqrt{\frac{1}{l_2^{\,2}} + s^2} X_1} + D_2(s) e^{-\sqrt{\frac{1}{l_2^{\,2}} + s^2} X_1}, \tag{5.30}$$

for the Phase 1 and 2, respectively. With the application of vanishing response at infinity to (5.29) and (5.30), we can write the solution as

$$\frac{\tilde{U}_3^{(1)}}{b} = B_1'(s) e^{-|s|(X_1 - a)} + D_1'(s) e^{-\sqrt{\frac{1}{l_1^{\,2}} + s^2}(X_1 - a)}, \tag{5.31}$$

$$\frac{\tilde{U}_3^{(2)}}{b} = A_2'(s) e^{|s|(X_1 + a)} + C_2'(s) e^{\sqrt{\frac{1}{l_2^{\,2}} + s^2}(X_1 + a)}. \tag{5.32}$$

We also transform the boundary conditions (5.21) to (5.24) by (5.25) to obtain

$$\left(\mu_1 B_1'(s) + \mu_2 A_2'(s) \right) |s| e^{|s| a} = 0, \tag{5.33}$$

$$\begin{aligned} &+ \left(\gamma_1 B_1'(s) - \gamma_2 A_2'(s) \right) s^2 e^{a|s|} + \gamma_1 D_1'(s) \left(\frac{1}{l_1^{\,2}} + s^2 \right) e^{a\sqrt{\frac{1}{l_1^{\,2}} + s^2}} \\ &- \gamma_2 C_2'(s) \left(\frac{1}{l_2^{\,2}} + s^2 \right) e^{a\sqrt{\frac{1}{l_2^{\,2}} + s^2}} + \frac{\left[(\gamma_1 - \gamma_2)(1 - K) \right]}{2\sqrt{2\pi}} i s e^{-a|s|} = 0, \end{aligned} \tag{5.34}$$

$$\left(B_1'(s)-A_2'(s)\right)e^{a|s|}+\left(D_1'(s)e^{a\sqrt{\frac{1}{l_1^2}+s^2}}-C_2'(s)e^{a\sqrt{\frac{1}{l_2^2}+s^2}}\right)=0, \tag{5.35}$$

$$\begin{aligned}&\left(B_1'(s)+A_2'(s)\right)|s|e^{a|s|}+D_1'(s)\sqrt{\frac{1}{l_1^2}+s^2}\,e^{a\sqrt{\frac{1}{l_1^2}+s^2}}+C_2'(s)\sqrt{\frac{1}{l_2^2}+s^2}\,e^{a\sqrt{\frac{1}{l_2^2}+s^2}}\\&-\frac{K}{\sqrt{2\pi}}i\,\mathrm{sgn}(s)e^{-a|s|}=0,\end{aligned} \tag{5.36}$$

respectively. Equations (5.33) to (5.36) comprise a system of four linear algebraic equations whose solution in terms of $B_1'(s)$, $A_2'(s)$, $D_1'(s)$ and $C_2'(s)$, can be found as

$$A_2'(s)=\frac{\left[-\left[\left(1-N\right)\left(1-K\right)\right](\beta_1+\beta_2)s-2K(\beta_1^{\,2}-N\beta_2^{\,2})\,\mathrm{sgn}(s)\right]i\,e^{-2a|s|}}{2\sqrt{2\pi}\left[-(\Gamma+N)(\beta_1+\beta_2)s^2+\left((1+\Gamma)\beta_2-(1-\Gamma)|s|\right)\beta_1^{\,2}+N\left((1+\Gamma)\beta_1+(1-\Gamma)|s|\right)\beta_2^{\,2}\right]}, \tag{5.37}$$

$$B_1'(s)=\frac{\left[\Gamma\left[\left(1-N\right)\left(1-K\right)\right](\beta_1+\beta_2)s+2K\Gamma(\beta_1^{\,2}-N\beta_2^{\,2})\,\mathrm{sgn}(s)\right]i\,e^{-2a|s|}}{2\sqrt{2\pi}\left[-(\Gamma+N)(\beta_1+\beta_2)s^2+\left((1+\Gamma)\beta_2-(1-\Gamma)|s|\right)\beta_1^{\,2}+N\left((1+\Gamma)\beta_1+(1-\Gamma)|s|\right)\beta_2^{\,2}\right]} \tag{5.38}$$

$$D_1'(s)=\frac{\left\{-2K\,\mathrm{sgn}(s)\left[(\Gamma+N)s^2-N(1+\Gamma)\beta_2^{\,2}\right]-\left[\left(1-N\right)\left(1-K\right)\right]\left[(1+\Gamma)\beta_2-(1-\Gamma)|s|\right]s\right\}i\,e^{-2a|s|}}{2\sqrt{2\pi}\left[-(\Gamma+N)(\beta_1+\beta_2)s^2+\left((1+\Gamma)\beta_2-(1-\Gamma)|s|\right)\beta_1^{\,2}+N\left((1+\Gamma)\beta_1+(1-\Gamma)|s|\right)\beta_2^{\,2}\right]}e^{a(|s|-\beta_1)}, \tag{5.39}$$

$$C_2'(s)=\frac{\left\{-2K\,\mathrm{sgn}(s)\left[(\Gamma+N)s^2-(1+\Gamma)\beta_1^{\,2}\right]+\left[\left(1-N\right)\left(1-K\right)\right]\left[(1+\Gamma)\beta_1+(1-\Gamma)|s|\right]s\right\}i\,e^{-2a|s|}}{2\sqrt{2\pi}\left[-(\Gamma+N)(\beta_1+\beta_2)s^2+\left((1+\Gamma)\beta_2-(1-\Gamma)|s|\right)\beta_1^{\,2}+N\left((1+\Gamma)\beta_1+(1-\Gamma)|s|\right)\beta_2^{\,2}\right]}e^{a(|s|-\beta_2)}, \tag{5.40}$$

where,

$$\beta_1=\sqrt{\frac{1}{l_1^2}+s^2},\quad \beta_2=\sqrt{\frac{1}{l_2^2}+s^2},\quad N=\frac{\gamma_2}{\gamma_1},\quad i=\sqrt{-1},\quad \mathrm{sgn}(s)=\begin{cases}1 & s>0\\0 & s=0\\-1 & s<0\end{cases}. \tag{5.41}$$

With these coefficients known and using the inverse transform (5.26), the perturbed parts of the displacement solution can be expressed in the form of improper integrals,

$$\hat{u}_3^{(1)}=\frac{b}{\sqrt{2\pi}}\int_{-\infty}^{\infty}\left(B_1'(s)e^{-|s|(X_1-a)}+D_1'(s)e^{-\sqrt{\frac{1}{l_1^2}+s^2}(X_1-a)}\right)e^{isX_2}ds, \tag{5.42}$$

$$\hat{u}_3^{(2)} = \frac{b}{\sqrt{2\pi}} \int_{-\infty}^{\infty} \left(A_2'(s) e^{|s|(X_1+a)} + C_2'(s) e^{\sqrt{\frac{1}{l_2^2}+s^2}(X_1+a)} \right) e^{isX_2} ds. \tag{5.43}$$

Therefore, the anti-plane displacement induced by the presence of the screw dislocation in Phases 1 and 2 of the bi-material medium is determined as

$$\begin{aligned} u_3^{(1)} &= \frac{b}{2\pi} \left(\tan^{-1}\left(\frac{X_2}{X_1 - a} \right) + K \tan^{-1}\left(\frac{X_2}{X_1 + a} \right) \right) \\ &+ \frac{b}{\sqrt{2\pi}} \int_{-\infty}^{\infty} \left(B_1'(s) e^{-|s|(X_1-a)} + D_1'(s) e^{-\sqrt{\frac{1}{l_1^2}+s^2}(X_1-a)} \right) e^{isX_2} ds, \end{aligned} \tag{5.44}$$

$$\begin{aligned} u_3^{(2)} &= \frac{b}{2\pi} \left((1-K) \tan^{-1}\left(\frac{X_2}{X_1 - a} \right) + K\pi \right) \\ &+ \frac{b}{\sqrt{2\pi}} \int_{-\infty}^{\infty} \left(A_2'(s) e^{|s|(X_1+a)} + C_2'(s) e^{\sqrt{\frac{1}{l_2^2}+s^2}(X_1+a)} \right) e^{isX_2} ds \end{aligned} \tag{5.45}.$$

In order to facilitate comparison of the results, as well as evaluation of the influence of each parameter on various components of the solution, we normalize the displacement (5.45) in terms of the distance of the dislocation to the interface. The normalized parameters are defined here:

$$x_1 = \frac{X_1}{a}, \quad x_2 = \frac{X_2}{a}, \quad \bar{l}_1 = \frac{l_1}{a}, \quad \bar{l}_2 = \frac{l_2}{a}, \tag{5.46}$$

Subsequently, we translate the parameters,

$$\bar{\beta}_1 = a\beta_1 \Rightarrow \bar{\beta}_1 = \sqrt{\bar{s}^2 + \frac{1}{\bar{l}_1^2}}, \quad \bar{\beta}_2 = a\beta_2 \Rightarrow \bar{\beta}_2 = \sqrt{\bar{s}^2 + \frac{1}{\bar{l}_2^2}}, \tag{5.47}$$

where $\bar{s} = as$. Also,

$$\begin{aligned} A_2'(s) &= \frac{A_2''(s)}{\sqrt{2\pi}} e^{-2a|s|}, \quad C_2'(s) = \frac{C_2''(s)}{\sqrt{2\pi}} e^{-a(|s|+\beta_2)}, \\ B_1'(s) &= \frac{B_1''(s)}{\sqrt{2\pi}} e^{-2a|s|}, \quad D_1'(s) = \frac{D_1''(s)}{\sqrt{2\pi}} e^{-a(|s|+\beta_1)}. \end{aligned} \tag{5.48}$$

Hence, the displacement solution in normalized form is

$$u_3^{(1)} = \frac{b}{2\pi}\left(\begin{array}{l} \tan^{-1}\left(\dfrac{x_2}{x_1-1}\right) + K\tan^{-1}\left(\dfrac{x_2}{x_1+1}\right) \\ + \displaystyle\int_{-\infty}^{\infty}\left(\bar{B}_1''(\bar{s})e^{-|\bar{s}|(x_1+1)} + \bar{D}_1''(\bar{s})e^{-(|\bar{s}|+\bar{\beta}_1 x_1)}\right)e^{i\bar{s}x_2}d\bar{s} \end{array}\right), \tag{5.49}$$

$$u_3^{(2)} = \frac{b}{2\pi}\left((1-K)\tan^{-1}\left(\frac{x_2}{x_1-1}\right) + K\pi + \int_{-\infty}^{\infty}\left(\bar{A}_2''(\bar{s})e^{|\bar{s}|(x_1-1)} + \bar{C}_2''(\bar{s})e^{\bar{\beta}_2 x_1-|\bar{s}|}\right)e^{i\bar{s}x_2}d\bar{s}\right). \tag{5.50}$$

Using (5.49) and (5.50), we can determine stresses and couple stresses through (5.11) and (5.12). The stress components corresponding to each material phase are

$$\sigma_{13}^{(1)} = \frac{\mu_1 b}{2\pi a}\left(\frac{-x_2}{(x_1-1)^2+x_2^{\,2}} + K\frac{-x_2}{(x_1+1)^2+x_2^{\,2}} + \int_{-\infty}^{\infty}\left(-|\bar{s}|\,\bar{B}_1''(\bar{s})e^{-|\bar{s}|(x_1+1)}\right)e^{i\bar{s}x_2}d\bar{s}\right), \tag{5.51}$$

$$\begin{aligned}\sigma_{31}^{(1)} = \frac{\mu_1 b}{2\pi a}\Bigg(&\frac{-x_2}{(x_1-1)^2+x_2^{\,2}} + K\frac{-x_2}{(x_1+1)^2+x_2^{\,2}} \\ &+ \int_{-\infty}^{\infty}\left(-|\bar{s}|\,\bar{B}_1''(\bar{s})e^{-|\bar{s}|(x_1+1)} - 2\bar{\beta}_1\bar{D}_1''(\bar{s})e^{-(|\bar{s}|+\bar{\beta}_1 x_1)}\right)e^{i\bar{s}x_2}d\bar{s}\Bigg),\end{aligned} \tag{5.52}$$

$$\sigma_{23}^{(1)} = \frac{\mu_1 b}{2\pi a}\left(\frac{(x_1-1)}{(x_1-1)^2+x_2^{\,2}} + K\frac{(x_1+1)}{(x_1+1)^2+x_2^{\,2}} + \int_{-\infty}^{\infty}\left(i\bar{s}B_1''(\bar{s})e^{-|\bar{s}|(x_1+1)}\right)e^{i\bar{s}x_2}d\bar{s}\right), \tag{5.53}$$

$$\begin{aligned}\sigma_{32}^{(1)} = \frac{\mu_1 b}{2\pi a}\Bigg(&\frac{(x_1-1)}{(x_1-1)^2+x_2^{\,2}} + K\frac{(x_1+1)}{(x_1+1)^2+x_2^{\,2}} \\ &+ \int_{-\infty}^{\infty}\left(i\bar{s}\left(\bar{B}_1''(\bar{s})e^{-|\bar{s}|(x_1+1)} + 2\bar{D}_1''(\bar{s})e^{-(|\bar{s}|+\bar{\beta}_1 x_1)}\right)\right)e^{i\bar{s}x_2}d\bar{s}\Bigg),\end{aligned} \tag{5.54}$$

$$\sigma_{13}^{(2)} = \frac{\mu_2 b}{2\pi a}\left((1-K)\frac{-x_2}{(x_1-1)^2+x_2^{\,2}} + \int_{-\infty}^{\infty}\left(|\bar{s}|\,\bar{A}_2''(\bar{s})e^{|\bar{s}|(x_1-1)}\right)e^{i\bar{s}x_2}d\bar{s}\right), \tag{5.55}$$

$$\sigma_{31}^{(2)} = \frac{\mu_2 b}{2\pi a}\left((1-K)\frac{-x_2}{(x_1-1)^2+x_2^{\,2}} + \int_{-\infty}^{\infty}\left(|\bar{s}|\,\bar{A}_2''(\bar{s})e^{|\bar{s}|(x_1-1)} + 2\bar{\beta}_2\bar{C}_2''(\bar{s})e^{-|\bar{s}|+\bar{\beta}_2 x_1}\right)e^{i\bar{s}x_2}d\bar{s}\right), \tag{5.56}$$

$$\sigma_{23}^{(2)} = \frac{\mu_2 b}{2\pi a}\left((1-K)\frac{(x_1-1)}{(x_1-1)^2+x_2^{\,2}} + \int_{-\infty}^{\infty}\left(i\bar{s}\bar{A}_2'(\bar{s})e^{|\bar{s}|(x_1-1)}\right)e^{i\bar{s}x_2}d\bar{s}\right), \tag{5.57}$$

$$\sigma_{32}^{(2)}=\frac{\mu_2 b}{2\pi a}\left((1-K)\frac{(x_1-1)}{(x_1-1)^2+{x_2}^2}+\int_{-\infty}^{\infty}\left(i\bar{s}\left(\bar{A}_2''(\bar{s})e^{|\bar{s}|(x_1-1)}+2\bar{C}_2''(\bar{s})e^{-|\bar{s}|+\bar{\beta}_2 x_1}\right)\right)e^{i\bar{s}x_2}d\bar{s}\right), \quad (5.58)$$

and the couple stresses are

$$\mu_{11}^{(1)}=\frac{\gamma_1 b}{2\pi a^2}\left(\frac{{x_2}^2-(x_1-1)^2}{\left[(x_1-1)^2+{x_2}^2\right]^2}+K\frac{{x_2}^2-(x_1+1)^2}{\left[(x_1+1)^2+{x_2}^2\right]^2}+\int_{-\infty}^{\infty}\left(-i\bar{s}\left(|\bar{s}|\,\bar{B}_1''(\bar{s})e^{-|\bar{s}|(x_1+1)}+\bar{\beta}_1\bar{D}_1''(\bar{s})e^{-(|\bar{s}|+\bar{\beta}_1 x_1)}\right)\right)e^{i\bar{s}x_2}d\bar{s}\right) \quad (5.59)$$

$$\mu_{22}^{(1)}=\frac{\gamma_1 b}{2\pi a^2}\left(\frac{(x_1-1)^2-{x_2}^2}{\left[(x_1-1)^2+{x_2}^2\right]^2}+K\frac{(x_1+1)^2-{x_2}^2}{\left[(x_1+1)^2+{x_2}^2\right]^2}-\int_{-\infty}^{\infty}\left(-i\bar{s}\left(|\bar{s}|\,\bar{B}_1''(\bar{s})e^{-|\bar{s}|(x_1+1)}+\bar{\beta}_1\bar{D}_1''(\bar{s})e^{-(|\bar{s}|+\bar{\beta}_1 x_1)}\right)\right)e^{i\bar{s}x_2}d\bar{s}\right) \quad (5.60)$$

$$\mu_{21}^{(1)}=-\frac{\gamma_1 b}{2\pi a^2}\left(\frac{2x_2(x_1-1)}{\left[(x_1-1)^2+{x_2}^2\right]^2}+K\frac{2x_2(x_1+1)}{\left[(x_1+1)^2+{x_2}^2\right]^2}-\int_{-\infty}^{\infty}\left(-\bar{s}^2\left(\bar{B}_1''(\bar{s})e^{-|\bar{s}|(x_1+1)}+\bar{D}_1''(\bar{s})e^{-(|\bar{s}|+\bar{\beta}_1 x_1)}\right)\right)e^{i\bar{s}x_2}d\bar{s}\right) \quad (5.61)$$

$$\mu_{12}^{(1)}=-\frac{\gamma_1 b}{2\pi a^2}\left(\frac{2x_2(x_1-1)}{\left[(x_1-1)^2+{x_2}^2\right]^2}+K\frac{2x_2(x_1+1)}{\left[(x_1+1)^2+{x_2}^2\right]^2}+\int_{-\infty}^{\infty}\left(\bar{s}^2\bar{B}_1''(\bar{s})e^{-|s|(x_1+1)}+\bar{\beta}_1^2\bar{D}_1''(\bar{s})e^{-(|s|+\bar{\beta}_1 x_1)}\right)e^{i\bar{s}x_2}d\bar{s}\right) \quad (5.62)$$

5.3 Special case: A screw dislocation near a free surface

In Section 3.2, we presented the idea of using an image dislocation to satisfy the traction free boundary conditions in classical elasticity. In couple stress theory, however, an image screw is not sufficient to cancel out the couple stress component μ_{12} on the expected traction-free

surface. However, we may use the approach presented in Section 5.2 to solve the problem in couple stress theory. Also, if we let $\Gamma, N \to 0$ in the general case of the bi-material interface problem, we can obtain the same results for a free surface as a special case. In this case, the usual arrangement of coordinates is used for consistency so that the X_2-axis lies on the planar free surface and the screw dislocation is located at $(a,0)$. The material properties including shear and bending-twisting moduli are denoted by μ and γ, respectively. Again, we decompose the displacement in the semi-infinite medium to the sum of the classical solution and couple stress effects such that,

$$u_3(X_1,X_2) = u_3'(X_1,X_2) + \hat{u}_3(X_1,X_2), \quad X_1 \geq 0. \tag{5.63}$$

Note that the classical solution u_3' is given in Section 3.2 as

$$u_3' = \frac{b}{2\pi}\left[\tan^{-1}\left(\frac{X_2}{X_1-a}\right) - \tan^{-1}\left(\frac{X_2}{X_1+a}\right)\right] \tag{5.64}$$

Using the Fourier transform approach we find that the governing equation,

$$\left(\nabla^2 - l^2\nabla^4\right)\hat{u}_3 = 0, \quad X_1 \geq 0. \tag{5.65}$$

in transformed form becomes

$$\tilde{U}_{3,11} - \left(s^2 + \frac{1}{l^2}\right)\tilde{U}_3 = 0, \tag{5.66}$$

which yields the solution in the form,

$$\tilde{U}_3 = Be^{-|s|X_1} + De^{-\sqrt{s^2+\frac{1}{l^2}}X_1} \tag{5.67}$$

with regard to the vanishing response at infinity. The boundary conditions for a free surface case can be written as

$$\mu_{12}(0,X_2) = 0, \quad \sigma_{13}(0,X_2) = 0. \tag{5.68}$$

Using the expressions (5.11) and (5.12), and applying the Fourier transform to (5.68) we have

$$\begin{aligned}&\frac{b}{\sqrt{2\pi}}\left(-ise^{-a|s|}\right)=\tilde{U}_{3,11}(0,s),\\&\tilde{U}_{3,1}(0,s)-l^2\tilde{U}_{3,111}(0,s)+s^2l^2\tilde{U}_{3,1}(0,s)=0.\end{aligned}\tag{5.69}$$

which with the aid of (5.67), can be expressed as a set of linear equations,

$$\begin{cases}\dfrac{b}{\sqrt{2\pi}}ise^{-a|s|}+s^2B+\left(s^2+\dfrac{1}{l^2}\right)D=0\\-|s|\left(s^2+\dfrac{1}{l^2}\right)B+s^2|s|B=0\end{cases}\tag{5.70}$$

whose solution will be

$$D=\frac{-bis}{\sqrt{2\pi}\left(s^2+\dfrac{1}{l^2}\right)}e^{-a|s|},\quad B=0.\tag{5.71}$$

Using the inverse transform (5.26), along with the coefficients D and B, the anti-plane displacement can be expressed as

$$u_3(X_1,X_2)=\frac{b}{2\pi}\left[\tan^{-1}\left(\frac{X_2}{X_1-a}\right)-\tan^{-1}\left(\frac{X_2}{X_1+a}\right)+\int_{-\infty}^{\infty}\frac{-is}{\left(s^2+\dfrac{1}{l^2}\right)}e^{-\left(a|s|+\sqrt{s^2+\frac{1}{l^2}}X_1\right)}e^{isX_2}ds\right]\tag{5.72}$$

With u_3 determined, the stress and couple stress fields can be obtained through (5.11) and (5.12). The stress components are

$$\sigma_{31}=\frac{\mu b}{2\pi}\left(\frac{-X_2}{(X_1-a)^2+{X_2}^2}+\frac{X_2}{(X_1+a)^2+{X_2}^2}+\int_{-\infty}^{\infty}\frac{2is}{\sqrt{s^2+\dfrac{1}{l^2}}}e^{-\left(a|s|+\sqrt{s^2+\frac{1}{l^2}}X_1\right)}e^{isX_2}ds\right),\tag{5.73}$$

$$\sigma_{13}=\frac{\mu b}{2\pi}\left(\frac{-X_2}{(X_1-a)^2+{X_2}^2}+\frac{X_2}{(X_1+a)^2+{X_2}^2}\right),\tag{5.74}$$

$$\sigma_{32}=\frac{\mu b}{2\pi}\left(\frac{(X_1-a)}{(X_1-a)^2+{X_2}^2}-\frac{(X_1+a)}{(X_1+a)^2+{X_2}^2}+\int_{-\infty}^{\infty}\frac{2s^2}{\left(s^2+\frac{1}{l^2}\right)}e^{-(a|s|+X_1\sqrt{s^2+\frac{1}{l^2}})}e^{isX_2}ds\right), \quad (5.75)$$

$$\sigma_{23}=\frac{\mu b}{2\pi}\left(\frac{X_1-a}{(X_1-a)^2+{X_2}^2}-\frac{X_1+a}{(X_1+a)^2+{X_2}^2}\right), \quad (5.76)$$

and the couple stress components,

$$\mu_{11}=\frac{\gamma b}{2\pi}\left(\frac{{X_2}^2-\left(X_1-a\right)^2}{\left(\left(X_1-a\right)^2+{X_2}^2\right)^2}-\frac{{X_2}^2-\left(X_1+a\right)^2}{\left(\left(X_1+a\right)^2+{X_2}^2\right)^2}+\int_{-\infty}^{\infty}\frac{-s^2}{\sqrt{s^2+\frac{1}{l^2}}}e^{-(a|s|+\sqrt{s^2+\frac{1}{l^2}}X_1)}e^{isX_2}ds\right), \quad (5.77)$$

$$\mu_{22}=\frac{\gamma b}{2\pi}\left(\frac{-{X_2}^2+\left(X_1-a\right)^2}{\left(\left(X_1-a\right)^2+{X_2}^2\right)^2}-\frac{-{X_2}^2+\left(X_1+a\right)^2}{\left(\left(X_1+a\right)^2+{X_2}^2\right)^2}+\int_{-\infty}^{\infty}\frac{s^2}{\sqrt{s^2+\frac{1}{l^2}}}e^{-(a|s|+\sqrt{s^2+\frac{1}{l^2}}X_1)}e^{isX_2}ds\right), \quad (5.78)$$

$$\mu_{12}=\frac{\gamma b}{2\pi}\left(\frac{-2\left(X_1-a\right)X_2}{\left(\left(X_1-a\right)^2+{X_2}^2\right)^2}+\frac{2\left(X_1+a\right)X_2}{\left(\left(X_1+a\right)^2+{X_2}^2\right)^2}+\int_{-\infty}^{\infty}ise^{-(a|s|+\sqrt{s^2+\frac{1}{l^2}}X_1)}e^{isX_2}ds\right), \quad (5.79)$$

$$\mu_{21}=\frac{\gamma b}{2\pi}\left(\frac{-2\left(X_1-a\right)X_2}{\left(\left(X_1-a\right)^2+{X_2}^2\right)^2}+\frac{2\left(X_1+a\right)X_2}{\left(\left(X_1+a\right)^2+{X_2}^2\right)^2}+\int_{-\infty}^{\infty}\frac{-is^3}{\left(s^2+\frac{1}{l^2}\right)}e^{-(a|s|+\sqrt{s^2+\frac{1}{l^2}}X_1)}e^{isX_2}ds\right). \quad (5.80)$$

It is obvious from (5.74) and (5.76) that the stress components on every plane parallel to the X_3-direction do not differ from the classical solution and regarding the assumed Cartesian coordinates the couple stress effects appear only in σ_{31} and σ_{32} components of the stress field.

5.4 Numerical evaluation of couple stress effects

In this section, we numerically evaluate the improper integrals in the expressions (5.51). Subsequently, we present results for the stress field components and compare them to the existing classical solutions. We use normalized parameters in the numerical evaluation.

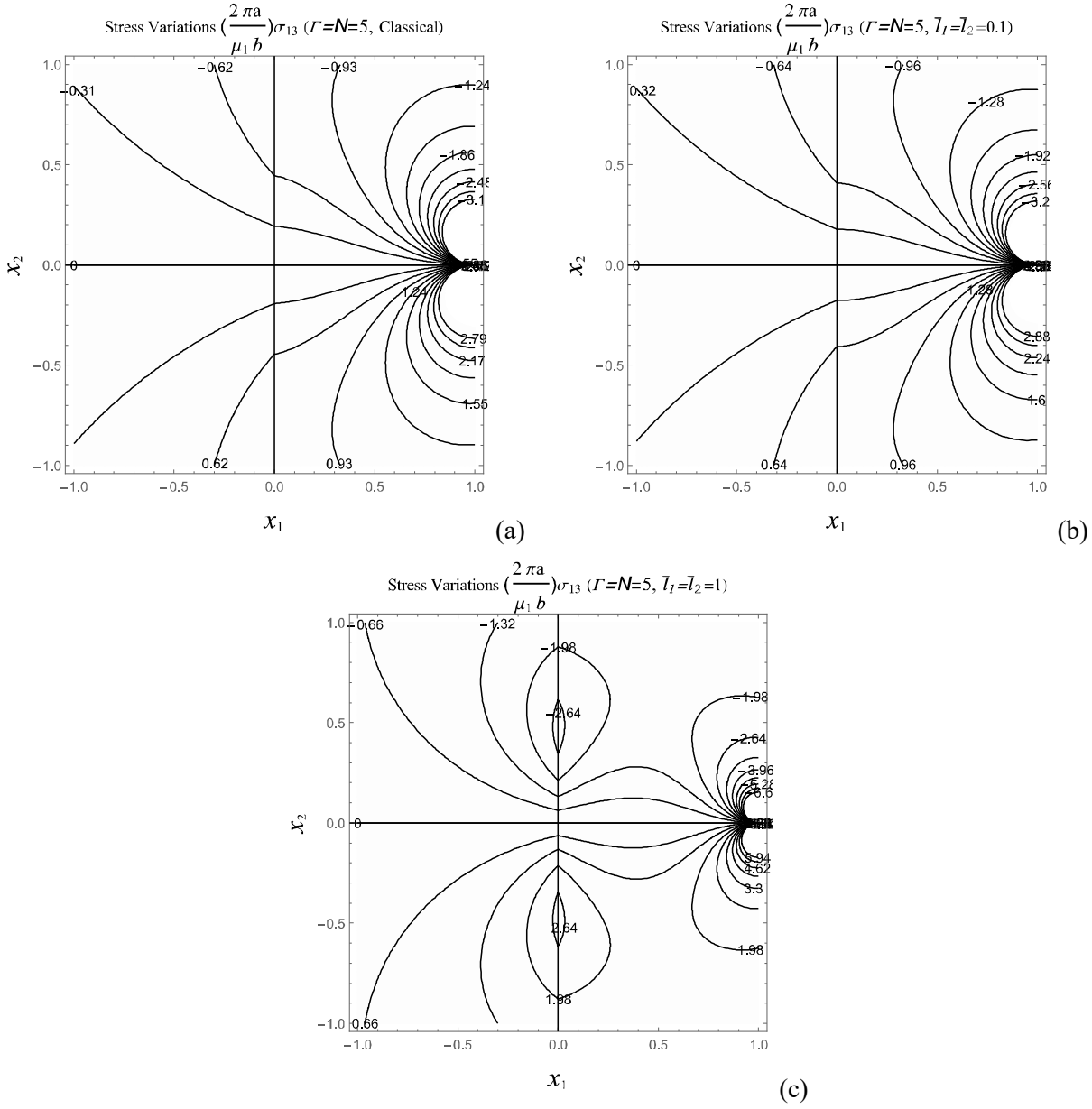

Fig. 5-2- Normalized distribution of stress component σ_{13} for length of materials $\bar{l}_1 = \bar{l}_2 = 0, 0.1, 1$

Note that in choosing the parameters we must consider the interrelation between mismatch coefficients Γ and N, and characteristic lengths $\bar{l}_1$ and $\bar{l}_2$ of the two material phases;

$$\bar{l}_2 = \sqrt{\frac{N}{\Gamma}}\bar{l}_1. \tag{5.81}$$

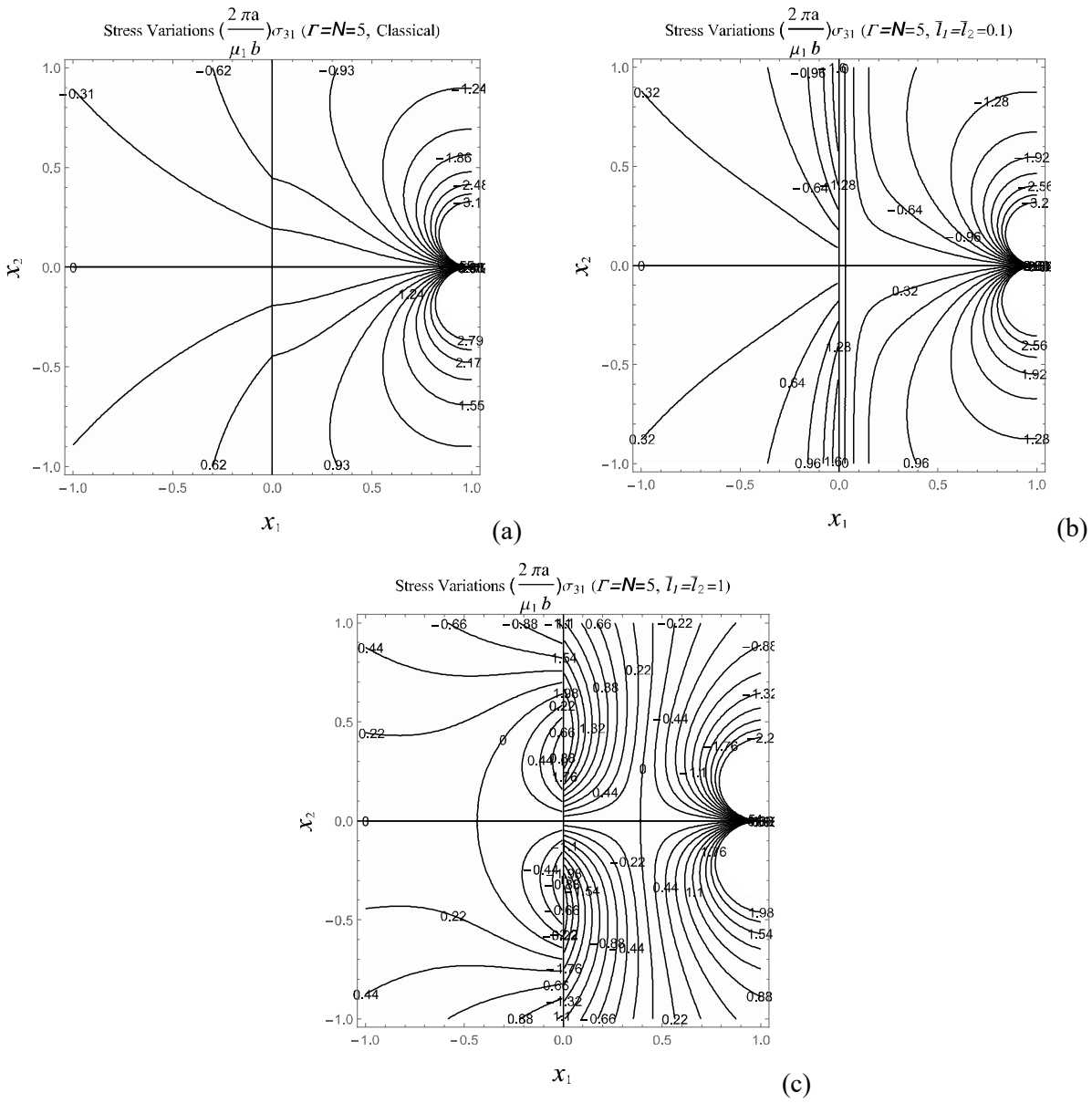

Fig. 5-3- Normalized distribution of stress component σ_{31} for length of materials $\bar{l}_1 = \bar{l}_2 = 0, 0.1, 1$

The stress results in the case of $\Gamma = N = 5$, for $\bar{l}_1 = \bar{l}_2 = 0.1$ and $\bar{l}_1 = \bar{l}_2 = 1$ as well as classical solutions ($\bar{l}_1 = \bar{l}_2 = 0$) are compared through Figs.5-2 to 5-5.

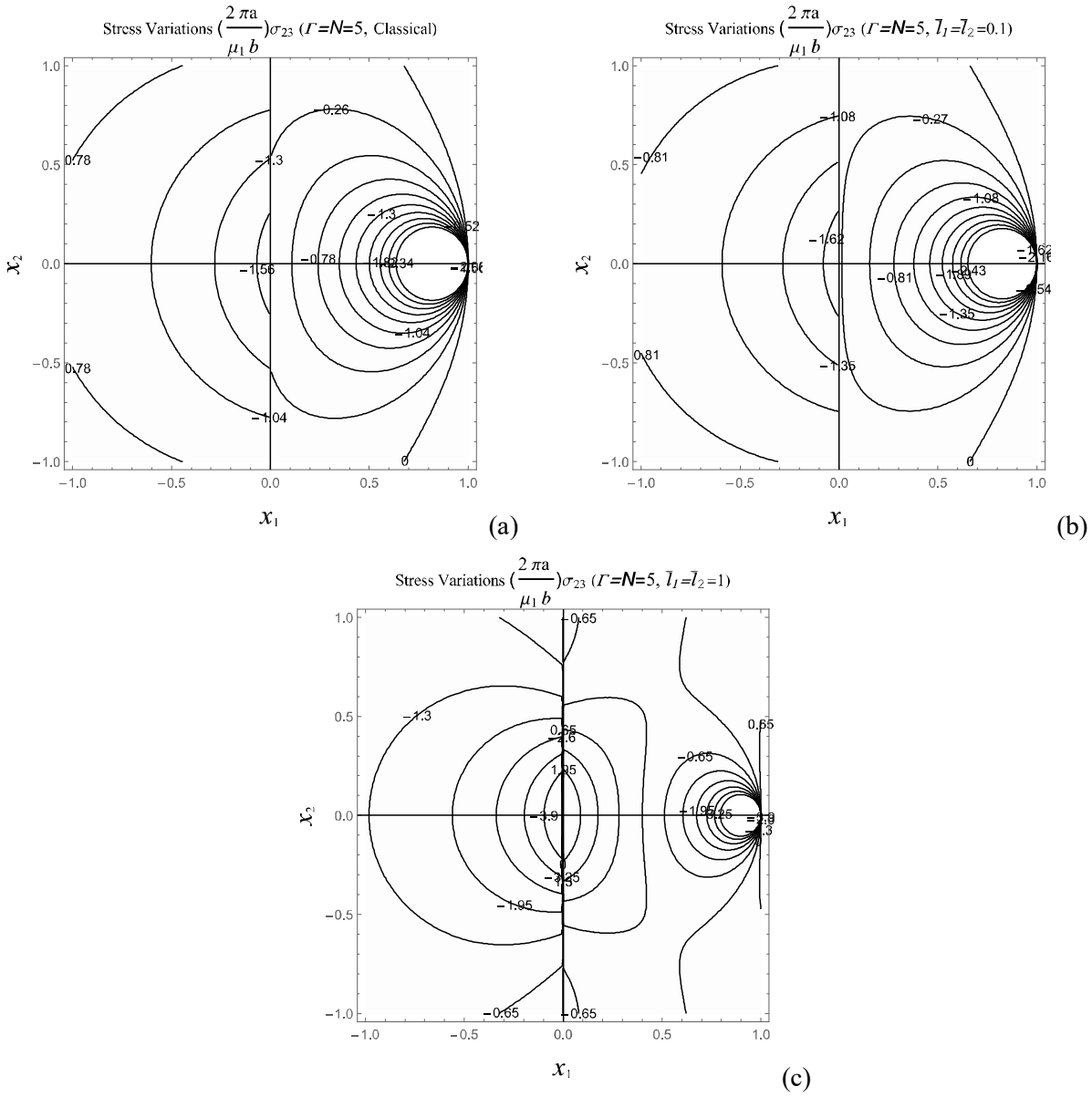

Fig. 5-4- Normalized distribution of stress component σ_{23} for length of materials $\bar{l}_1 = \bar{l}_2 = 0, 0.1, 1$

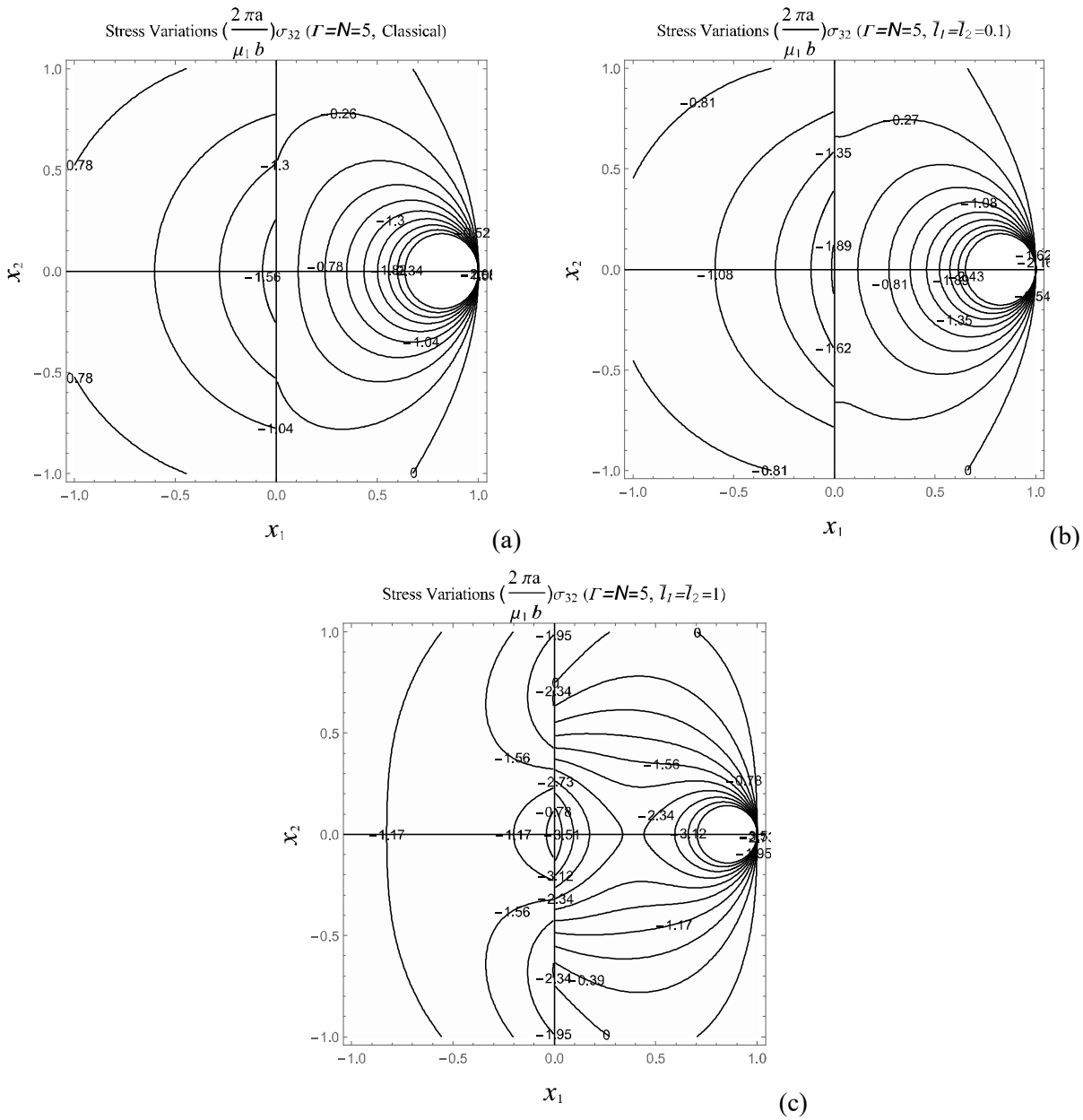

Fig. 5-5- Normalized distribution of stress component σ_{32} for length of materials $\bar{l}_1 = \bar{l}_2 = 0, 0.1, 1$

We can see from Figs. 5-2(a) and (b), that for a relatively small characteristic length of material, the distribution of σ_{13} differs only slightly from that of the classical solution. However, for larger values of $\bar{l}_1$ and $\bar{l}_2$ (comparable to the dislocation's distance from the interface), we observe a quite different distribution of σ_{13} with overall larger, and at some points, localized values. In particular, for the case of $\bar{l}_1 = \bar{l}_2 = 1$ (taken to represent a relatively 'large' characteristic length of material in Fig. 5-2(c)), σ_{13} attains extreme values on the interface

around $x_2 = \pm 0.45$. From Fig. 5-3 we see that, in contrast to the classical results, in the case of the couple stress solution, the stress component σ_{31} is always discontinuous on the interface. Similarly, for 'small values' of $\bar{l}_1$ and $\bar{l}_2$, the overall distribution of σ_{31} does not change significantly but it does exhibit a localized nature around the interface (Figs. 5-3(a) and (b)). Additionally, a neutral surface ($\sigma_{31} = 0$) appears parallel to the interface with a distance nearly half of the characteristic length of material. In contrast, in the case of a larger characteristic length, a significant change in the distribution of σ_{31} is observed (Fig. 5-3(c)). A neutral surface again emerges at approximately half of the characteristic length of material from the interface and the stress distribution becomes concentrated to give extreme values on the interface.

Fig. 5-4 shows the σ_{23} component of the stress field. This component also undergoes a significant change when the characteristic length of material is of the order of the dislocation's distance from the interface or higher (say $\bar{l}_1 = \bar{l}_2 = 1$ as in Fig. 5-4(c)). In addition, we observe a rapid variation of σ_{23} on the interface ($x_1 = 0$), as well as stress concentrations at the origin ($x_1 = x_2 = 0$), that is, the nearest point of the interface to the dislocation. The stress component σ_{32} is also shown in Fig. 5-5. Comparing Figs. 5-4 and 5-5 demonstrates that the two components σ_{23} and σ_{32} deviate from each other as the characteristic length becomes larger. For $\bar{l}_1 = \bar{l}_2 = 1$ in Fig. 5-5, we can again observe a concentration of σ_{32} at the origin but the distribution differs from that of σ_{23}.

5.5 Interaction force on the screw dislocation near the interface

In Chapter 4, we showed that the energy changes due to the translation of a singularity can be expressed by the idea of path independent J-integrals. In this section, we use this idea to calculate the interaction force on the screw dislocation. The J-integral in couple stress theory which is equivalent to the force is given in (4.32). We rewrite the formula,

$$F_n = \oint_S \left(\delta_{nj} w - \mu_{ji} \omega_{i,n} - \sigma_{ji} u_{i,n} \right) n_j dS, \tag{5.82}$$

where w is the strain energy density given as

$$w = \mu \varepsilon_{ij} \varepsilon_{ij} + \frac{\lambda}{2} \varepsilon_{kk} \varepsilon_{nn} + \gamma \omega_{j,i} \omega_{j,i}, \tag{5.83}$$

in couple stress theory. For the anti-plane problem, (5.83) reduces to

$$w = \mu \varepsilon_{ij} \varepsilon_{ij} + \gamma \omega_{j,i} \omega_{j,i}. \tag{5.84}$$

We choose a path that conforms to the conditions mentioned in Chapter 4. Thus, the chosen path lies completely in Phase 1. Additionally, we define a rectangular path to take advantage of the defined rectangular Cartesian coordinates to formulate the integral in (5.82). Therefore, using (2.86) and (2.87), for the only component of the force in the X_1-direction, we may write

$$\begin{aligned} F_1 = & \int_{S_2} \left(\frac{\mu_1}{2} \left(u_{3,1}^{(1)2} + u_{3,2}^{(1)2} \right) + \frac{\gamma_1}{4} \left(u_{3,11}^{(1)\,2} + u_{3,22}^{(1)\,2} + 2 u_{3,12}^{(1)\,2} \right) - \sigma_{13} u_{3,1}^{(1)} - \mu_{11} \omega_{1,1}^{(1)} - \mu_{12} \omega_{2,1}^{(1)} \right) dX_2 \\ & + \int_{S_1} \left(\sigma_{23} u_{3,1}^{(1)} + \mu_{21} \omega_{1,1}^{(1)} + \mu_{22} \omega_{2,1}^{(1)} \right) dX_1, \end{aligned} \tag{5.85}$$

where S_1 and S_2 are the sums of the path segments parallel to the X_1 and X_2-axis, respectively, such that $S_1 + S_2 = S$. S is shown in Fig. 5-6. We may rephrase the expression (5.85) in terms of the normalized forms introduced earlier in (5.46) and (5.47):

$$\begin{aligned} \frac{F_1}{\left(\frac{\mu_1 b^2}{4\pi a} \right)} = & \int_{\bar{S}_2} \left(\frac{1}{2\pi} \left(\bar{u}_{3,1}^{(1)2} + \bar{u}_{3,2}^{(1)2} - 2 \bar{\sigma}_{13}^{(1)} \bar{u}_{3,1}^{(1)} \right) + \frac{\bar{l}_1^{\,2}}{2\pi} \left(\bar{u}_{3,22}^{(1)2} - \bar{u}_{3,11}^{(1)2} \right) \right) dx_2 \\ & + \int_{\bar{S}_1} \left(\frac{1}{\pi} \left(\bar{\sigma}_{23}^{(1)} \bar{u}_{3,1}^{(1)} \right) + \frac{\bar{l}_1^{\,2}}{\pi} \left(\bar{u}_{3,22}^{(1)} + \bar{u}_{3,11}^{(1)} \right) \bar{u}_{3,12}^{(1)} \right) dx_1, \end{aligned} \tag{5.86}$$

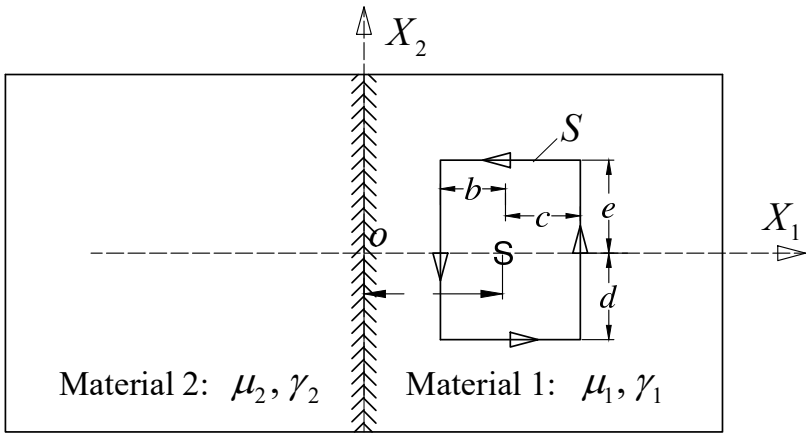

Fig. 5-6-An arbitrary rectangular path of integration enclosing the screw dislocation

In (5.86),

$$\bar{u}_{3,j}^{(1)} = \frac{u_{3,j}^{(1)}}{\left(\frac{b}{2\pi a}\right)}, \quad \bar{u}_{3,ij}^{(1)} = \frac{u_{3,ij}^{(1)}}{\left(\frac{b}{2\pi a^2}\right)}, \quad \bar{S}_1 = \frac{S_1}{a}, \quad \bar{S}_2 = \frac{S_2}{a}. \tag{5.87}$$

Taking the characteristic lengths as $\bar{l}_1 = \bar{l}_2 = 0$, (5.86) can be determined analytically for the special case of a classical elastic material,

$$\frac{F_1}{\left(\frac{\mu_1 b^2}{4\pi a}\right)} = \frac{1}{2\pi}\int_{\bar{S}_2}\left(\bar{u}_{3,1}^{(1)2} + \bar{u}_{3,2}^{(1)2} - 2\bar{\sigma}_{13}^{(1)}\bar{u}_{3,1}^{(1)}\right)dx_2 + \frac{1}{\pi}\int_{\bar{S}_1}\left(\bar{\sigma}_{23}^{(1)}\bar{u}_{3,1}^{(1)}\right)dx_1, \tag{5.88}$$

In order to determine (5.88) analytically, we consider a general rectangular path as shown in Fig. 5-6. However, we normalize the dimensions in Fig. 5-6 with respect to the distance of the dislocation to the interface. Therefore, we have

$$\begin{aligned}\frac{F_1}{\left(\frac{\mu_1 b^2}{4\pi a}\right)} = \frac{1}{2\pi}\int_{-\bar{d}}^{\bar{e}}\left(\left(\bar{u}_{3,1}^{(1)2} + \bar{u}_{3,2}^{(1)2} - 2\bar{\sigma}_{13}^{(1)}\bar{u}_{3,1}^{(1)}\right)_{x_1=1+\bar{c}} - \left(\bar{u}_{3,1}^{(1)2} + \bar{u}_{3,2}^{(1)2} - 2\bar{\sigma}_{13}^{(1)}\bar{u}_{3,1}^{(1)}\right)_{x_1=1-\bar{b}}\right)dx_2 \\ + \frac{1}{\pi}\int_{1-\bar{b}}^{1+\bar{c}}\left(\left(\bar{\sigma}_{23}^{(1)}\bar{u}_{3,1}^{(1)}\right)_{x_2=-\bar{d}} - \left(\bar{\sigma}_{23}^{(1)}\bar{u}_{3,1}^{(1)}\right)_{x_2=\bar{e}}\right)dx_1,\end{aligned} \tag{5.89}$$

with b, c, d and e defined in Fig. 5-6, and

$$\bar{b}=\frac{b}{a},\quad \bar{c}=\frac{c}{a},\quad \bar{d}=\frac{d}{a},\quad \bar{e}=\frac{e}{a}. \tag{5.90}$$

Calculating the integral (5.89) analytically gives us

$$\begin{aligned}\frac{F_1}{\left(\frac{\mu_1 b^2}{4\pi a}\right)}=\frac{K}{2\pi}\Bigg[&\tan^{-1}\left(\frac{2-b}{d}\right)+\tan^{-1}\left(\frac{d}{2-b}\right)-\tan^{-1}\left(\frac{2+c}{d}\right)-\tan^{-1}\left(\frac{d}{2+c}\right)\\&+\tan^{-1}\left(\frac{2-b}{e}\right)+\tan^{-1}\left(\frac{e}{2-b}\right)-\tan^{-1}\left(\frac{2+c}{e}\right)-\tan^{-1}\left(\frac{e}{2+c}\right)\\&+\tan^{-1}\left(\frac{b}{d}\right)+\tan^{-1}\left(\frac{d}{b}\right)+\tan^{-1}\left(\frac{b}{e}\right)+\tan^{-1}\left(\frac{e}{b}\right)\\&+\tan^{-1}\left(\frac{c}{d}\right)+\tan^{-1}\left(\frac{d}{c}\right)+\tan^{-1}\left(\frac{c}{e}\right)+\tan^{-1}\left(\frac{e}{c}\right)\Bigg]=K,\end{aligned} \tag{5.91}$$

which, by referring to (3.28), is exactly as expected (Dundurs [15]). The general integral (5.86), however, cannot be determined analytically. We use the displacement and stress distributions from (5.49), (5.51) and (5.53) to calculate sampling points on the path of integration. Then, we employ numerical integration methods (for example the Gauss-Kronrod formula) to estimate the force on the dislocation in different cases.

The effects of mismatch ratio on the interaction force are illustrated in Fig. 5-7. It is evident that for $\Gamma = N = 0$, which is equivalent to the free surface case, the interaction force is equal to the force determined by classical elasticity theory. This proposition is always true, regardless of the value of $\bar{l}$ in a couple stress semi-infinite medium. We can reach the same conclusion if we use the direct results from the free surface solution ((5.72) to (5.76)). With $\Gamma = N = 1$, the material properties of both phases become identical and they make up a uniform, infinite medium. In this case, as expected, the interaction force is zero. For high values of the mismatch ratios ($\Gamma, N >> 1$), the results show that, in couple stress materials, a higher interaction force repels the dislocation from the interface. However, for small values of $\bar{l}_1$ and $\bar{l}_2$ the change in force is not significant. For example, in the case of $\bar{l}_1 = \bar{l}_2 = 0.1$, we can continue to use classical solutions with only a reasonable loss of accuracy. Moreover, the higher the characteristic length, the greater the difference between the classical and couple stress solutions.

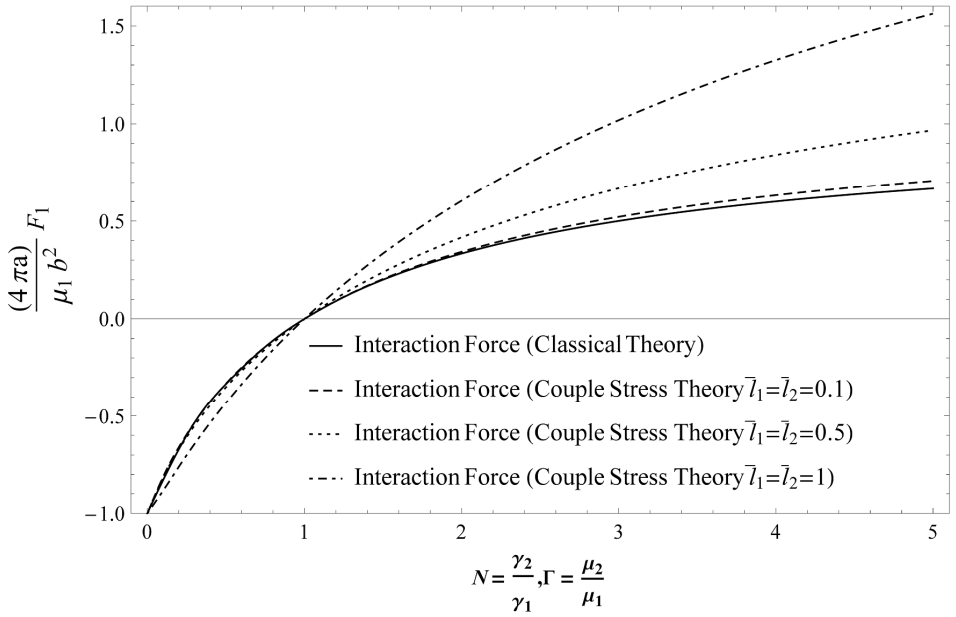

Fig. 5-7- Variations of interaction force with mismatch ratio

Another interesting aspect addressed in Fig. 5-8 is the variation of interaction force with the characteristic length of the material. Evidently for $\Gamma, N < 0$, when phase 2 of the material is softer, the interaction force is intensified as $\bar{l}_1$ and $\bar{l}_2$ increase, but the nature of the force is attraction towards the interface. It should be noted that when phase 2 is extremely soft relative to phase 1 (say $\Gamma = N = 0.01$) the negative force increases at a lower rate. For higher values of Γ and N, while phase 2 remains softer than phase 1 ($\Gamma, N < 0$), the negative force intensifies more rapidly as $\bar{l}_1$ and $\bar{l}_2$ grow. Moreover, we observe from Fig. 5-8 that when phase 2 of the material is softer than phase 1, there are certain values of $\bar{l}_1$ and $\bar{l}_2$ at which the force becomes equal to the force acting on a screw dislocation near a free surface (the curves meet the gray line in Fig. 5-8). For $\Gamma, N > 0$, that is, for a relatively harder phase 2 material, the force is again intensified at higher material lengths, however, the force repels the dislocation from the interface.

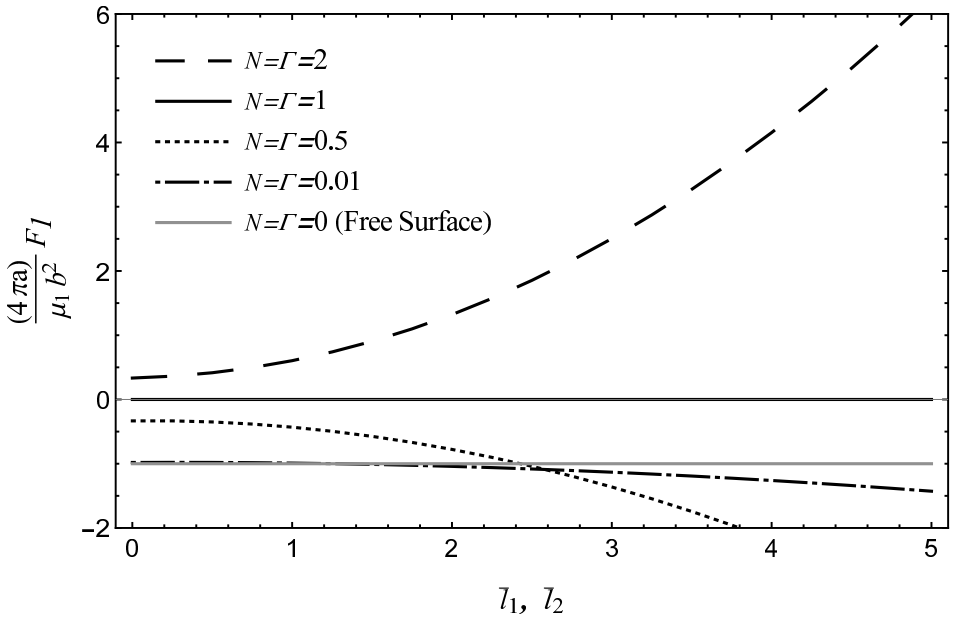

Fig. 5-8- Variations of interaction force characteristic length of materials

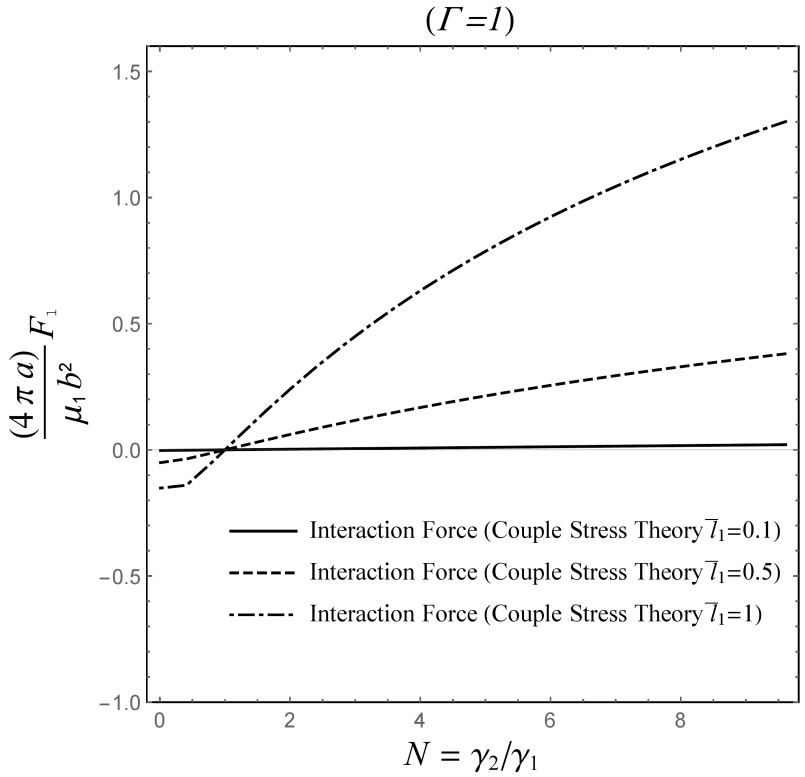

Fig. 5-9-Variation of force with mismatch between characteristic lengths

The variations of interaction force with the mismatch between characteristic lengths are demonstrated in the Fig. 5-9. Since the relation (5.81) between the two media must be satisfied,

we choose $\bar{l}_1$ as a constant and change $\bar{l}_2$ by regulating N. Therefore, the variations of force versus N are the subject of study in Fig. 5-9. In other words, we generate the mismatch between two semi-infinite media by bending-twisting moduli γ_1 and γ_2 only, and from the view of the classical shear moduli μ_1 and μ_2, we deal with a uniform infinite medium, hence $\Gamma = 1$. The advantage of this choice is to remove the effects of mismatch ratio in classical elasticity and identify the pure couple stress effects. It can be observed from Fig. 5-9 that when $N < 1$, meaning that $\bar{l}_1 > \bar{l}_2$, the mismatch causes a negative force meaning attraction towards the interface. Conversely, for the values $N > 1$, that is when $\bar{l}_1 < \bar{l}_2$, the interface repels the dislocation. In addition, we see that the interaction force induced by this kind of mismatch is highly dependent on the order of the characteristic length of material. Thus, when the characteristic lengths of the two materials are relatively large compared to the dislocation's distance from the interface, the effect of mismatch on the force is obviously higher. For a small value of $\bar{l}_1$ (for example $\bar{l}_1 = 0.1$), however, the effect of mismatch between characteristic lengths of materials is negligible. This conclusion agrees with the results from Fig. 5-7, where we can see that for $\bar{l}_1 = 0.1$ the force variations approximately follow the curve of the classical solution.

In this chapter, we have introduced an integral transform approach and concluded a thorough investigation of the classical problem of a screw dislocation near the interface of a bi-material in couple stress elasticity. In the following chapters, we employ the same approach to solve problems of particular relevance to engineering applications. In the next two chapters, we consider a screw dislocation in a substrate interacting with a thin film in couple stress elasticity. In the later chapter, we discuss a dislocation in an isolated thin film in couple stress elasticity.

6 A Screw Dislocation in a Substrate Near a Thin Film

Many industrial and technological devices require the application of thin films over substrates in manufacturing. For example, in solar cells, semiconductors, and optical products, certain materials are used in the form of thin films with thickness ranging from a few micro to a few hundred nanometers coated over a substrate. Therefore, the study of the mechanical properties of these structures is of significant importance in engineering applications. In particular, when the dimension of a thin film is of the order of microns the use of couple stress theory seems most appropriate. In this chapter, we use an approach similar to that used in the previous chapter to study a more general case involving the interaction of a screw dislocation in a substrate with a thin film.

6.1 Solving the boundary value problem

We adopt the layout presented in Fig. 6-1. As before, we assume that the anti-plane parameters act in the X_3-direction, while the X_2 axis lies on the substrate-film interface and a right-handed screw dislocation is located at the point $(a,0)$ in the substrate. In this case, μ_S and γ_S designate the elastic properties of the substrate material and the film of thickness h has the elastic shear and twisting-bending moduli of μ_F and γ_F.

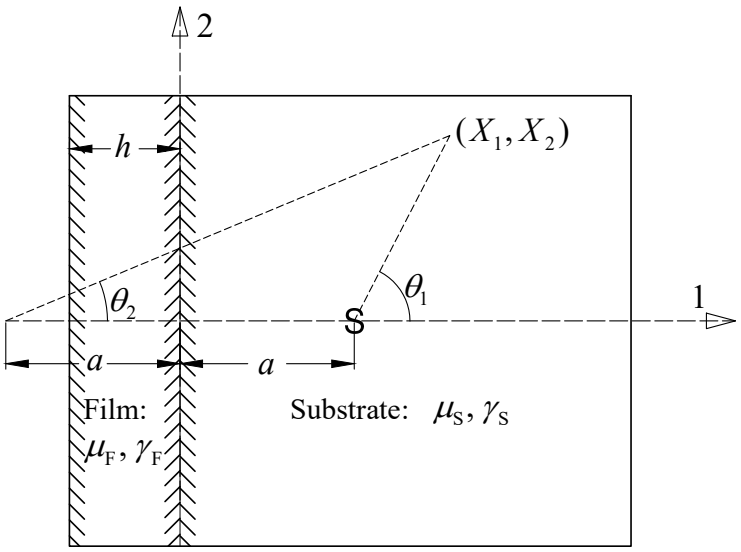

Fig. 6-1- Configuration of the problem of a screw dislocation in a substrate near a thin film

Again, using the superposition principle we separate the classical solution corresponding to a screw dislocation near a bi-material interface from the total solution of interest. That means

$$
\begin{aligned}
u_3^{(\mathsf{S})} &= \frac{b}{2\pi}\left(\tan^{-1}\left(\frac{X_2}{X_1-a}\right)+K\tan^{-1}\left(\frac{X_2}{X_1+a}\right)\right)+\hat{u}_3^{(\mathsf{S})},\\
u_3^{(\mathsf{F})} &= \frac{b}{2\pi}\left((1-K)\tan^{-1}\left(\frac{X_2}{X_1-a}\right)+K\pi\right)+\hat{u}_3^{(\mathsf{F})},
\end{aligned}
\tag{6.1}
$$

where the superscripts "(S)" and "(F)" indicate correspondence to the substrate and the film, respectively. The additional terms $\hat{u}_3^{(\mathsf{S})}$ and $\hat{u}_3^{(\mathsf{F})}$ involve both the effects of couple stresses and thin layer geometry. The governing displacement field equations

$$
\begin{aligned}
&\nabla^2(1-l_{\mathsf{S}}^2\nabla^2)u_3^{(\mathsf{S})}=0, \quad X_1\geq 0,\\
&\nabla^2(1-l_{\mathsf{F}}^2\nabla^2)u_3^{(\mathsf{F})}=0, \quad -h\leq X_1<0,
\end{aligned}
\tag{6.2}
$$

must be satisfied in the substrate and in the film, respectively. In (6.2), $l_{\mathsf{S}}^2=\gamma_{\mathsf{S}}/2\mu_{\mathsf{S}}$ and $l_{\mathsf{F}}^2=\gamma_{\mathsf{F}}/2\mu_{\mathsf{F}}$. First, substituting (6.1) into (6.2), we have

$$
\begin{aligned}
&\nabla^2(1-l_{\mathsf{S}}^2\nabla^2)\hat{u}_3^{(\mathsf{S})}=0,\\
&\nabla^2(1-l_{\mathsf{F}}^2\nabla^2)\hat{u}_3^{(\mathsf{F})}=0.
\end{aligned}
\tag{6.3}
$$

Then, we apply the Fourier transform defined in (5.25) to (6.3) to obtain

$$\left(\frac{\partial^2}{\partial X_1^{\,2}}-s^2\right)\left(\frac{1}{l_{\mathsf{S}}^2}+s^2-\frac{\partial^2}{\partial X_1^{\,2}}\right)\tilde{U}_3^{(\mathsf{S})}(X_1,s)=0,$$
$$\left(\frac{\partial^2}{\partial X_1^{\,2}}-s^2\right)\left(\frac{1}{l_{\mathsf{F}}^2}+s^2-\frac{\partial^2}{\partial X_1^{\,2}}\right)\tilde{U}_3^{(\mathsf{F})}(X_1,s)=0. \tag{6.4}$$

The solution to the two ordinary differential equations (6.4) is given by

$$\tilde{U}_3^{(\mathrm{S})}=B_1(s)e^{-|s|X_1}+D_1(s)e^{-\beta_1(s)X_1},\ \text{for } X_1\geq 0,$$
$$\tilde{U}_3^{(\mathrm{F})}=A_2(s)e^{|s|X_1}+B_2(s)e^{-|s|X_1}+C_2(s)e^{\beta_2(s)X_1}+D_2(s)e^{-\beta_2(s)X_1},\ \text{for } -h\leq X_1<0, \tag{6.5}$$

where,

$$\beta_1(s)=\sqrt{s^2+\frac{1}{l_{\mathsf{S}}^2}},\quad \beta_2(s)=\sqrt{s^2+\frac{1}{l_{\mathsf{F}}^2}}. \tag{6.6}$$

At this point, for brevity we refer to the coefficients "$B_1(s)$, $D_1(s)$, …", as "B_1, D_1,…". The boundary conditions at the perfectly bonded interface between the substrate and the film are as follows:

$$\mu_{12}^{(\mathsf{S})}(0,X_2)=\mu_{12}^{(\mathsf{F})}(0,X_2),\quad \sigma_{13}^{(\mathsf{S})}(0,X_2)=\sigma_{13}^{(\mathsf{F})}(0,X_2),$$
$$u_3^{(\mathsf{S})}(0,X_2)=u_3^{(\mathsf{F})}(0,X_2),\quad u_{3,1}^{(\mathsf{S})}(0,X_2)=u_{3,1}^{(\mathsf{F})}(0,X_2). \tag{6.7}$$

Also, the following boundary conditions are established on the traction-free surface of the thin film:

$$\mu_{12}^{(\mathsf{F})}(-h,X_2)=0,\quad \sigma_{13}^{(\mathsf{F})}(-h,X_2)=0. \tag{6.8}$$

Considering the expressions given in (5.11) and (5.12) for the stress and couple stress components in each medium (the substrate and the film), we expand the boundary conditions as

$$\sigma_{13}^{(\mathsf{S})}(0,X_2)=\sigma_{13}^{(\mathsf{F})}(0,X_2)\Rightarrow$$
$$\mu_{\mathsf{S}}\hat{u}_{3,1}^{(\mathsf{S})}(0,X_2)-\mu_{\mathsf{F}}\hat{u}_{3,1}^{(\mathsf{F})}(0,X_2)-\frac{\gamma_{\mathsf{S}}}{2}\nabla^2\hat{u}_{3,1}^{(\mathsf{S})}(0,X_2)+\frac{\gamma_{\mathsf{F}}}{2}\nabla^2\hat{u}_{3,1}^{(\mathsf{F})}(0,X_2)=0, \tag{6.9}$$

$$\mu_{12}^{(\mathsf{S})}(0,X_2)=\mu_{12}^{(\mathsf{F})}(0,X_2)\Rightarrow$$
$$\gamma_{\mathsf{S}}\hat{u}_{3,11}^{(\mathsf{S})}(0,X_2)-\gamma_{\mathsf{F}}\hat{u}_{3,11}^{(\mathsf{F})}(0,X_2)=\frac{b}{2\pi}\left((\gamma_{\mathsf{S}}-\gamma_{\mathsf{F}})(1-K)\frac{2X_2a}{(a^2+X_2^2)^2}\right), \tag{6.10}$$

$$u_3^{(\mathsf{S})}(0,X_2)=u_3^{(\mathsf{F})}(0,X_2)\Rightarrow \hat{u}_3^{(\mathsf{S})}(0,X_2)=\hat{u}_3^{(\mathsf{F})}(0,X_2), \tag{6.11}$$

$$u_{3,1}^{(\mathsf{S})}(0,X_2)=u_{3,1}^{(\mathsf{F})}(0,X_2)\Rightarrow \hat{u}_{3,1}^{(\mathsf{S})}(0,X_2)-\hat{u}_{3,1}^{(\mathsf{F})}(0,X_2)=\frac{b}{2\pi}\left(\frac{2KX_2}{a^2+X_2^2}\right), \tag{6.12}$$

$$\begin{aligned}&\sigma_{13}^{(\mathsf{F})}(-h,X_2)=0\Rightarrow\\&\mu_{\mathsf{F}}u_{3,1}^{(\mathsf{F})}(-h,X_2)-\frac{\gamma_{\mathsf{F}}}{2}\nabla^2u_{3,1}^{(\mathsf{F})}(-h,X_2)=0,\end{aligned} \tag{6.13}$$

$$\begin{aligned}&\mu_{12}^{(\mathsf{F})}(-h,X_2)=0\Rightarrow\\&\gamma_{\mathsf{F}}\hat{u}_{3,11}^{(\mathsf{F})}(-h,X_2)=\frac{b\gamma_{\mathsf{F}}}{2\pi}\left((1-K)\frac{2(h+a)X_2}{\left((a+h)^2+X_2^2\right)^2}\right),\end{aligned} \tag{6.14}$$

Applying the Fourier transform to (6.9)-(6.14) results in

$$\begin{aligned}&\mu_{\mathsf{S}}\left(-|s|B_1-\beta_1D_1\right)-\mu_{\mathsf{F}}\left(|s|A_2-|s|B_2+\beta_2C_2-\beta_2D_2\right)\\&-\frac{\gamma_{\mathsf{S}}}{2}\left(-\beta_1^3+s^2\beta_1\right)D_1-\frac{\gamma_{\mathsf{F}}}{2}\left((s^2\beta_2-\beta_2^3)C_2+(\beta_2^3-s^2\beta_2)D_2\right)=0,\end{aligned} \tag{6.15}$$

$$\gamma_{\mathsf{S}}\left(s^2B_1+\beta_1^2D_1\right)-\gamma_{\mathsf{F}}\left(s^2A_2+s^2B_2+\beta_2^2C_2+\beta_2^2D_2\right)=\frac{-(\gamma_{\mathsf{S}}-\gamma_{\mathsf{F}})(1-K)b}{2\sqrt{2\pi}}\left(ise^{-a|s|}\right), \tag{6.16}$$

$$B_1+D_1-A_2-B_2-C_2-D_2=0, \tag{6.17}$$

$$|s|B_1+\beta_1D_1+|s|A_2-|s|B_2+\beta_2C_2-\beta_2D_2=\frac{bK}{\sqrt{2\pi}}\left(i\,\mathrm{sgn}(s)e^{-a|s|}\right), \tag{6.18}$$

$$\begin{aligned}&\left(|s|A_2e^{-|s|h}-|s|B_2e^{|s|h}+\beta_2C_2e^{-\beta_2h}-\beta_2D_2e^{\beta_2h}\right)\\&-l_{\mathsf{F}}^2\left((\beta_2^3-s^2\beta_2)C_2e^{-\beta_2h}+(s^2\beta_2-\beta_2^3)D_2e^{\beta_2h}\right)=-\frac{b(1-K)}{2\sqrt{2\pi}}\left(i\,\mathrm{sgn}(s)e^{-(a+h)|s|}\right),\end{aligned} \tag{6.19}$$

$$s^2A_2e^{-|s|h}+s^2B_2e^{|s|h}+\beta_2^2C_2e^{-\beta_2h}+\beta_2^2D_2e^{\beta_2h}=-\frac{b(1-K)}{2\sqrt{2\pi}}\left(ise^{-(h+a)|s|}\right), \tag{6.20}$$

respectively. Clearly, the equations (6.15) to (6.20) form a set of six algebraic equations in terms of six unknowns B_1, D_1, A_2, B_2, C_2 and D_2. After normalizing in terms of a, such that,

$$\bar{l}_S = \frac{l_S}{a}, \quad \bar{l}_F = \frac{l_F}{a}, \quad \bar{h} = \frac{h}{a}, \quad \bar{s} = as$$
$$\bar{\beta}_1 = a\beta_1 \Rightarrow \bar{\beta}_1 = \sqrt{\bar{s}^2 + \frac{1}{\bar{l}_S^{\,2}}}, \quad \bar{\beta}_2 = a\beta_2 \Rightarrow \bar{\beta}_2 = \sqrt{\bar{s}^2 + \frac{1}{\bar{l}_F^{\,2}}}. \tag{6.21}$$

We solve the system of equations to obtain,

$$\begin{aligned}
&\bar{B}_1 = \frac{a\sqrt{2\pi}}{b} B_1 = \frac{B_1^*}{D}, \quad \bar{D}_1 = \frac{a\sqrt{2\pi}}{b} D_1 = \frac{D_1^*}{D}, \\
&\bar{A}_2 = \frac{a\sqrt{2\pi}}{b} A_2 = \frac{A_2^*}{D}, \quad \bar{B}_2 = \frac{a\sqrt{2\pi}}{b} B_2 = \frac{B_2^*}{D}, \\
&\bar{C}_2 = \frac{a\sqrt{2\pi}}{b} C_2 = \frac{C_2^*}{\bar{\beta}_2(\bar{s})D}, \quad \bar{D}_2 = \frac{a\sqrt{2\pi}}{b} D_2 = \frac{D_2^*}{\bar{\beta}_2(\bar{s})D},
\end{aligned} \tag{6.22}$$

the normalized forms of B_1, D_1, A_2, B_2, C_2 and D_2. In relations (6.22),

$$\begin{aligned}
D = 2|\bar{s}|\Big\{&(\bar{\beta}_1^{\,2} - N\bar{\beta}_2^{\,2})\Big[4\bar{s}^2 e^{\bar{h}(\bar{\beta}_2+|\bar{s}|)} - (e^{2\bar{h}\bar{\beta}_2} - 1)(e^{2\bar{h}|\bar{s}|} - 1)\bar{\beta}_2(\Gamma - 1)|\bar{s}|\Big] \\
&+\bar{s}^2\bar{\beta}_2\Big[N(e^{2\bar{h}|\bar{s}|} + 1) + \Gamma(e^{2\bar{h}|\bar{s}|} - 1)\Big]\Big[e^{2\bar{h}\bar{\beta}_2}(\bar{\beta}_1 + \bar{\beta}_2) + (\bar{\beta}_2 - \bar{\beta}_1)\Big] \\
&+\Big[(\Gamma - 1) - (\Gamma + 1)e^{2\bar{h}|\bar{s}|}\Big]\Big[(N\bar{\beta}_1\bar{\beta}_2^{\,3} + \bar{\beta}_1^{\,2}\bar{\beta}_2^{\,2})e^{2\bar{h}\bar{\beta}_2} - (N\bar{\beta}_1\bar{\beta}_2^{\,3} - \bar{\beta}_1^{\,2}\bar{\beta}_2^{\,2})\Big]\Big\},
\end{aligned} \tag{6.23}$$

$$\begin{aligned}
B_1^* = ie^{-|\bar{s}|}\Gamma\Big\{&(\bar{\beta}_1^{\,2} - N\bar{\beta}_2^{\,2})\big[4\bar{s}|\bar{s}|(1-K)e^{\bar{h}\bar{\beta}_2}\sinh(\bar{h}|\bar{s}|) \\
&+4(1-K)\operatorname{sgn}(\bar{s})\bar{s}^2 e^{\bar{h}\bar{\beta}_2}\cosh(\bar{h}|\bar{s}|) - 2K|\bar{s}|\bar{\beta}_2\operatorname{sgn}(\bar{s})(e^{2\bar{h}\bar{\beta}_2} - 1)(e^{2\bar{h}|\bar{s}|} - 1)\Big] \\
&+\Big((\bar{\beta}_1 + \bar{\beta}_2)e^{2\bar{h}\bar{\beta}_2} - (\bar{\beta}_1 - \bar{\beta}_2)\Big)(1-K)\bar{\beta}_2\Big[\bar{s}|\bar{s}|(N-1)(e^{2\bar{h}|\bar{s}|} - 1) + 2\bar{s}^2 N\operatorname{sgn}(\bar{s})\Big] \\
&+2(K-1)\operatorname{sgn}(\bar{s})\bar{\beta}_1\bar{\beta}_2^{\,2}\Big[\bar{\beta}_1(e^{2\bar{h}\bar{\beta}_2} + 1) + \bar{\beta}_2 N(e^{2\bar{h}\bar{\beta}_2} - 1)\Big]\Big\},
\end{aligned} \tag{6.24}$$

$$
\begin{aligned}
D_1^* = ie^{-|\bar{s}|}\Big\{&(K-1)(N-1)(\Gamma-1)\bar{\beta}_2\bar{s}\,|\bar{s}|^2\,(e^{2\bar{h}\bar{\beta}_2}-1)(e^{2\bar{h}|\bar{s}|}-1)\\
&+(K-1)(N-1)\bar{\beta}_2{}^2(e^{2\bar{h}\bar{\beta}_2}+1)\Big[-\bar{s}\,|\bar{s}|\Big((\Gamma-1)-(\Gamma+1)e^{2\bar{h}|\bar{s}|}\Big)+2\Gamma\bar{s}^2\,\mathrm{sgn}(\bar{s})\Big]\\
&+2\bar{s}(K-1)e^{\bar{h}(\bar{\beta}_2+|\bar{s}|)}\Big[\bar{s}^3\,\mathrm{sgn}(\bar{s})(N+\Gamma)-\bar{s}\,\bar{\beta}_2{}^2N\,\mathrm{sgn}(\bar{s})(\Gamma+1)\\
&\qquad-\bar{s}^2\,|\bar{s}|(N-\Gamma)-|\bar{s}|\,\bar{\beta}_2{}^2N(\Gamma+1)+2\bar{s}^2\,|\bar{s}|\Big]\\
&+2\bar{s}(K-1)e^{\bar{h}(\bar{\beta}_2-|\bar{s}|)}\Big[-\bar{s}^3\,\mathrm{sgn}(\bar{s})(N-\Gamma)-\bar{s}\,\bar{\beta}_2{}^2N\,\mathrm{sgn}(\bar{s})(\Gamma-1)\\
&\qquad+\bar{s}^2\,|\bar{s}|(N-\Gamma)+|\bar{s}|\,\bar{\beta}_2{}^2N(\Gamma-1)\Big]\\
&-2\bar{\beta}_2(e^{2\bar{h}\bar{\beta}_2}-1)|\bar{s}|\,\mathrm{sgn}(\bar{s})\Big[\bar{s}^2K\Gamma(1-e^{2\bar{h}|\bar{s}|})+KN\Gamma(\bar{\beta}_2{}^2e^{2\bar{h}|\bar{s}|}-\bar{s}^2)\\
&+N(\bar{\beta}_2{}^2-\bar{s}^2)\Big((1-\Gamma)+Ke^{2\bar{h}|\bar{s}|}\Big)\Big]\Big\},
\end{aligned}
\tag{6.25}
$$

$$
\begin{aligned}
A_2^* = \\
&ie^{\bar{h}|\bar{s}|}\Big\{(\bar{\beta}_1{}^2-N\bar{\beta}_2{}^2)\Big[(K-1)\,\mathrm{sgn}(\bar{s})e^{-(1+\bar{h})|\bar{s}|}\Big(2\bar{s}^2e^{\bar{h}(\bar{\beta}_2+|\bar{s}|)}+\bar{\beta}_2(\Gamma-1)|\bar{s}|(e^{2\bar{h}\bar{\beta}_2}-1)\Big)\\
&+2|\bar{s}|\,e^{(-1+\bar{h})|\bar{s}|}\Big(\bar{s}(K-1)e^{\bar{h}(\bar{\beta}_2-|\bar{s}|)}+K\bar{\beta}_2\,\mathrm{sgn}(\bar{s})(e^{2\bar{h}\bar{\beta}_2}-1)\Big)\Big]\\
&+\Big[(\bar{\beta}_1+\bar{\beta}_2)e^{2\bar{h}\bar{\beta}_2}+(\bar{\beta}_2-\bar{\beta}_1)\Big]\Big[N\bar{s}^2\bar{\beta}_2(K-1)\,\mathrm{sgn}(\bar{s})\,e^{-(1+\bar{h})|\bar{s}|}\\
&-\Gamma\bar{s}^2\bar{\beta}_2(K-1)\,\mathrm{sgn}(\bar{s})e^{-(1+\bar{h})|\bar{s}|}+(K-1)(N-1)\bar{\beta}_2\bar{s}\,|\bar{s}|\,e^{(-1+\bar{h})|\bar{s}|}\Big]\\
&+(K-1)(\Gamma-1)\,\mathrm{sgn}(\bar{s})e^{-(1+\bar{h})|\bar{s}|}\Big[N\bar{\beta}_1\bar{\beta}_2{}^3(e^{2\bar{h}\bar{\beta}_2}-1)+\bar{\beta}_1{}^2\bar{\beta}_2{}^2(e^{2\bar{h}\bar{\beta}_2}+1)\Big]\Big\},
\end{aligned}
\tag{6.26}
$$

$$
\begin{aligned}
B_2^* = -ie^{-|\bar{s}|}\Big\{&(\bar{\beta}_1{}^2-N\bar{\beta}_2{}^2)\Big[2(1-K)e^{\bar{h}(\bar{\beta}_2-|\bar{s}|)}\Big(\bar{s}\,|\bar{s}|-\bar{s}^2\,\mathrm{sgn}(\bar{s})\Big)\\
&+|\bar{s}|\,\mathrm{sgn}(\bar{s})\bar{\beta}_2(e^{2\bar{h}\bar{\beta}_2}-1)\Big((\Gamma-1)-K(\Gamma+1)\Big)\Big]\\
&-(1-K)\Big[(\bar{\beta}_2-\bar{\beta}_1)+(\bar{\beta}_1+\bar{\beta}_2)e^{2\bar{h}\bar{\beta}_2}\Big]\Big[\bar{s}^2\,\mathrm{sgn}(\bar{s})\bar{\beta}_2(\Gamma+N)+\bar{s}\,|\bar{s}|\,\bar{\beta}_2(1-N)\Big]\\
&+(1-K)(\Gamma+1)\,\mathrm{sgn}(\bar{s})\Big[\bar{\beta}_1{}^2\bar{\beta}_2{}^2(e^{2\bar{h}\bar{\beta}_2}+1)+N\bar{\beta}_1\bar{\beta}_2{}^3(e^{2\bar{h}\bar{\beta}_2}-1)\Big]\Big\},
\end{aligned}
\tag{6.27}
$$

$$
\begin{aligned}
C_2^* = ie^{\bar{h}\bar{\beta}_2-(1+\bar{h})|\bar{s}|}\Big\{&(K-1)(\Gamma-1)\bar{s}\,|\bar{s}|^2\,(e^{2\bar{h}|\bar{s}|}-1)\Big(\bar{\beta}_1^{\,2}-N\bar{\beta}_2^{\,2}+(N-1)\bar{\beta}_2^{\,2}e^{\bar{h}(\bar{\beta}_2+|\bar{s}|)}\Big)\\
&-\bar{s}^2\,\mathrm{sgn}(\bar{s})(K-1)\Big[\,\bar{s}^2(\bar{\beta}_1-\bar{\beta}_2)\Big(\Gamma(e^{2\bar{h}|\bar{s}|}+1)+N(e^{2\bar{h}|\bar{s}|}-1)\Big)\\
&+2\bar{\beta}_1\bar{\beta}_2^{\,2}\Gamma(N-1)e^{\bar{h}(\bar{\beta}_2+|\bar{s}|)}+\bar{\beta}_1\bar{\beta}_2(\bar{\beta}_1-N\bar{\beta}_2)\Big((\Gamma+1)e^{2\bar{h}|\bar{s}|}+(\Gamma-1)\Big)\Big]\\
&+(K-1)\bar{s}\,|\bar{s}|\Big[\,(\Gamma-N)\bar{s}^2(\bar{\beta}_2-\bar{\beta}_1)(e^{2\bar{h}|\bar{s}|}-1)\\
&+\bar{\beta}_1\bar{\beta}_2(\bar{\beta}_1-N\bar{\beta}_2)\Big((\Gamma-1)-(\Gamma+1)e^{2\bar{h}|\bar{s}|}\Big)\\
&+2\bar{s}^2(\bar{\beta}_2-\bar{\beta}_1)e^{2\bar{h}|\bar{s}|}+(N-1)\bar{\beta}_1\bar{\beta}_2^{\,2}\Big((\Gamma-1)e^{\bar{h}(\bar{\beta}_2+|\bar{s}|)}-(\Gamma+1)e^{\bar{h}(\bar{\beta}_2+3|\bar{s}|)}\Big)\Big]\\
&+|\bar{s}|\,\mathrm{sgn}(\bar{s})\Big[\,2(\Gamma-1)\bar{\beta}_1^{\,2}\bar{\beta}_2^{\,2}e^{\bar{h}(\bar{\beta}_2+|\bar{s}|)}-2K\bar{\beta}_2^{\,2}e^{\bar{h}(\bar{\beta}_2+3|\bar{s}|)}\Big((\Gamma+1)\bar{\beta}_1^{\,2}-N\bar{s}^2\Big)\\
&+\bar{s}^2(\bar{\beta}_1^{\,2}-N\bar{\beta}_2^{\,2})\Big(\big((1-\Gamma)+K(\Gamma+3)\big)e^{2\bar{h}|\bar{s}|}+(K-1)(\Gamma-1)\Big)\\
&-2N\bar{\beta}_2^{\,2}\bar{s}^2\big((\Gamma-1)-\Gamma K\big)e^{\bar{h}(\bar{\beta}_2+|\bar{s}|)}+2\bar{\beta}_2^{\,2}\bar{s}^2\Gamma K\Big(e^{\bar{h}(\bar{\beta}_2+3|\bar{s}|)}-e^{\bar{h}(\bar{\beta}_2+|\bar{s}|)}\Big)\Big]\Big\},
\end{aligned}
$$

$$
\begin{aligned}
D_2^* = ie^{-|\bar{s}|}\Big\{&(\bar{\beta}_1^{\,2}-N\bar{\beta}_2^{\,2})\Big[\,(K-1)(\Gamma-1)\bar{s}\,|\bar{s}|^2\Big(e^{\bar{h}(\bar{\beta}_2-|\bar{s}|)}-e^{\bar{h}(\bar{\beta}_2+|\bar{s}|)}\Big)\\
&-\bar{s}^2\,|\bar{s}|\,\mathrm{sgn}(\bar{s})\big((1-\Gamma)+K(\Gamma+3)\big)e^{\bar{h}(\bar{\beta}_2+|\bar{s}|)}-\bar{s}^2\,|\bar{s}|\,\mathrm{sgn}(\bar{s})(K-1)(\Gamma-1)e^{\bar{h}(\bar{\beta}_2-|\bar{s}|)}\Big]\\
&+(K-1)(\Gamma-1)(N-1)\bar{s}\,|\bar{s}|^2\,\bar{\beta}_2^{\,2}(1-e^{2\bar{h}|\bar{s}|})+(K-1)\bar{s}^2\,\mathrm{sgn}(\bar{s})\Big[\,2(N-1)\Gamma\bar{\beta}_1\bar{\beta}_2^{\,2}\\
&+\bar{s}^2(\bar{\beta}_1+\bar{\beta}_2)\Big((N+\Gamma)e^{\bar{h}(\bar{\beta}_2+|\bar{s}|)}-(N-\Gamma)e^{\bar{h}(\bar{\beta}_2-|\bar{s}|)}\Big)\\
&+\bar{\beta}_1\bar{\beta}_2(\bar{\beta}_1+N\bar{\beta}_2)\Big((1-\Gamma)e^{\bar{h}(\bar{\beta}_2-|\bar{s}|)}-(1+\Gamma)e^{\bar{h}(\bar{\beta}_2+|\bar{s}|)}\Big)\Big]\\
&+(1-K)\bar{s}\,|\bar{s}|\Big[\,(N-1)\bar{\beta}_1\bar{\beta}_2^{\,2}\Big((\Gamma-1)-(\Gamma+1)e^{2\bar{h}|\bar{s}|}\Big)\\
&+\bar{s}^2(\bar{\beta}_1+\bar{\beta}_2)\Big(\big(N-(\Gamma+2)\big)e^{\bar{h}(\bar{\beta}_2+|\bar{s}|)}+(\Gamma-N)e^{\bar{h}(\bar{\beta}_2-|\bar{s}|)}\Big)\\
&+\bar{\beta}_1\bar{\beta}_2(\bar{\beta}_1+N\bar{\beta}_2)\Big((1-\Gamma)e^{\bar{h}(\bar{\beta}_2-|\bar{s}|)}+(1+\Gamma)e^{\bar{h}(\bar{\beta}_2+|\bar{s}|)}\Big)\Big]\\
&+|\bar{s}|\,\mathrm{sgn}(\bar{s})\Big[\,2\bar{s}^2\bar{\beta}_2^{\,2}\Big(-K(N+\Gamma)e^{2\bar{h}|\bar{s}|}+N(\Gamma-1)+K\Gamma(1-N)\Big)\\
&-2\bar{\beta}_1^{\,2}\bar{\beta}_2^{\,2}\Big(-K(1+\Gamma)e^{2\bar{h}|\bar{s}|}+(\Gamma-1)\Big)\Big]\Big\},
\end{aligned}
\tag{6.29}
$$

where, $N=\gamma_{\mathsf{F}}/\gamma_{\mathsf{S}}$ and $\Gamma=\mu_{\mathsf{F}}/\mu_{\mathsf{S}}$. Now, using the coefficients (6.22) and the inverse transform (5.26), the expressions for the displacement component in the substrate and the film are obtained as

$$u_3^{(S)} = \frac{b}{2\pi}\left(\tan^{-1}\left(\frac{x_2}{x_1-1}\right) + K\tan^{-1}\left(\frac{x_2}{x_1+1}\right) + \int_{-\infty}^{\infty}\left(\overline{B}_1(\overline{s})e^{-|\overline{s}|x_1} + \overline{D}_1(\overline{s})e^{-\overline{\beta}_1(\overline{s})x_1}\right)e^{i\overline{s}x_2}d\overline{s}\right), \quad (6.30)$$

$$\begin{aligned} u_3^{(F)} &= \frac{b}{2\pi}\left((1-K)\tan^{-1}\left(\frac{x_2}{x_1-1}\right) + K\pi \right. \\ &\left. + \int_{-\infty}^{\infty}\left(\overline{A}_2(\overline{s})e^{|\overline{s}|x_1} + \overline{B}_2(\overline{s})e^{-|\overline{s}|x_1} + \overline{C}_2(\overline{s})e^{\overline{\beta}_2(\overline{s})x_1} + \overline{D}_2(\overline{s})e^{-\overline{\beta}_2(\overline{s})x_1}\right)e^{i\overline{s}x_2}d\overline{s}\right). \end{aligned} \quad (6.31)$$

Accordingly, through the relations (5.11), the stress components in terms of normalized parameters are

$$\sigma_{13}^{(S)} = \frac{\mu_S b}{2\pi a}\left(\frac{-x_2}{(x_1-1)^2+{x_2}^2} + K\frac{-x_2}{(x_1+1)^2+{x_2}^2} + \int_{-\infty}^{\infty}\left(-|\overline{s}|\,\overline{B}_1 e^{-|\overline{s}|x_1}\right)e^{i\overline{s}x_2}d\overline{s}\right), \quad (6.32)$$

$$\begin{aligned} &\sigma_{31}^{(S)} \\ &= \frac{\mu_S b}{2\pi a}\left(\frac{-x_2}{(x_1-1)^2+{x_2}^2} + K\frac{-x_2}{(x_1+1)^2+{x_2}^2} + \int_{-\infty}^{\infty}\left(-|\overline{s}|\,\overline{B}_1 e^{-|\overline{s}|x_1} - 2\overline{\beta}_1\overline{D}_1 e^{-\overline{\beta}_1 x_1}\right)e^{i\overline{s}x_2}d\overline{s}\right), \end{aligned} \quad (6.33)$$

$$\sigma_{23}^{(S)} = \frac{\mu_S b}{2\pi a}\left(\frac{x_1-1}{(x_1-1)^2+{x_2}^2} + K\frac{x_1+1}{(x_1+1)^2+{x_2}^2} + \int_{-\infty}^{\infty}\left(i\overline{s}\overline{B}_1 e^{-|\overline{s}|x_1}\right)e^{i\overline{s}x_2}d\overline{s}\right), \quad (6.34)$$

$$\begin{aligned} &\sigma_{32}^{(S)} \\ &= \frac{\mu_S b}{2\pi a}\left(\frac{x_1-1}{(x_1-1)^2+{x_2}^2} + K\frac{x_1+1}{(x_1+1)^2+{x_2}^2} + \int_{-\infty}^{\infty} i\overline{s}\left(\overline{B}_1 e^{-|\overline{s}|x_1} + 2\overline{D}_1 e^{-\overline{\beta}_1 x_1}\right)e^{i\overline{s}x_2}d\overline{s}\right), \end{aligned} \quad (6.35)$$

for the substrate and,

$$\sigma_{13}^{(F)} = \frac{\mu_F b}{2\pi a}\left((1-K)\frac{-x_2}{(x_1-1)^2+{x_2}^2} + \int_{-\infty}^{\infty}|\overline{s}|\left(\overline{A}_2(\overline{s})e^{|\overline{s}|x_1} - \overline{B}_2(\overline{s})e^{-|\overline{s}|x_1}\right)e^{i\overline{s}x_2}d\overline{s}\right), \quad (6.36)$$

$$\begin{aligned} \sigma_{31}^{(F)} &= \frac{\mu_F b}{2\pi a}\left((1-K)\frac{-x_2}{(x_1-1)^2+{x_2}^2} \right. \\ &\left. + \int_{-\infty}^{\infty}\left(|\overline{s}|\,\overline{A}_2(\overline{s})e^{|\overline{s}|x_1} - |\overline{s}|\,\overline{B}_2(\overline{s})e^{-|\overline{s}|x_1} + 2\overline{\beta}_2\overline{C}_2(\overline{s})e^{\overline{\beta}_2 x_1} - 2\overline{\beta}_2\overline{D}_2(\overline{s})e^{-\overline{\beta}_2 x_1}\right)e^{i\overline{s}x_2}d\overline{s}\right), \end{aligned} \quad (6.37)$$

$$\sigma_{23}^{(\mathsf{F})}=\frac{\mu_{\mathsf{F}}b}{2\pi a}\left((1-K)\frac{x_1-1}{(x_1-1)^2+{x_2}^2}+\int_{-\infty}^{\infty}i\bar{s}\left(\bar{A}_2(\bar{s})e^{|\bar{s}|x_1}+\bar{B}_2(\bar{s})e^{-|\bar{s}|x_1}\right)e^{i\bar{s}x_2}d\bar{s}\right), \tag{6.38}$$

$$\begin{aligned}\sigma_{32}^{(\mathsf{F})}=&\frac{\mu_{\mathsf{F}}b}{2\pi a}\left((1-K)\frac{x_1-1}{(x_1-1)^2+{x_2}^2}\right.\\&\left.+\int_{-\infty}^{\infty}i\bar{s}\left(\bar{A}_2(\bar{s})e^{|\bar{s}|x_1}+\bar{B}_2(\bar{s})e^{-|\bar{s}|x_1}+2\bar{C}_2(\bar{s})e^{\bar{\beta}_2x_1}+2\bar{D}_2(\bar{s})e^{-\bar{\beta}_2x_1}\right)e^{i\bar{s}x_2}d\bar{s}\right),\end{aligned} \tag{6.39}$$

for the film. In order to verify the presented results, we determine the displacement fields (6.30) and (6.31) for the extreme case when $\{l_{\mathsf{S}},l_{\mathsf{F}}\to 0\}$. We observe then that the results reduce to the existing solution in classical elasticity [15]. That is

$$u_3^{(\mathsf{S})}=\frac{b}{2\pi}\left(\tan^{-1}\left(\frac{x_2}{x_1-1}\right)+K\tan^{-1}\left(\frac{x_2}{x_1+1}\right)+\int_{-\infty}^{\infty}\left(\frac{-i(1+K)}{2\Gamma|\bar{s}|}\bar{A}(\bar{s})e^{-(\bar{h}+1+x_1)|\bar{s}|}\right)e^{i\bar{s}x_2}d\bar{s}\right), \tag{6.40}$$

$$\begin{aligned}u_3^{(\mathsf{F})}=&\frac{b}{2\pi}\left((1-K)\tan^{-1}\left(\frac{x_2}{x_1-1}\right)+K\pi\right.\\&\left.+\int_{-\infty}^{\infty}\left(\frac{-i(1+K)}{2\Gamma|\bar{s}|}\left(\bar{B}(\bar{s})\cosh(\bar{s}x_1)+\bar{C}(\bar{s})\sinh(\bar{s}x_1)\right)e^{-(\bar{h}+1)|\bar{s}|}\right)e^{i\bar{s}x_2}d\bar{s}\right),\end{aligned} \tag{6.41}$$

where,

$$\begin{aligned}\bar{A}(\bar{s})=\bar{B}(\bar{s})&=\frac{-\Gamma\bar{h}\bar{s}}{|\bar{h}\bar{s}|\cosh(\bar{h}\bar{s})+\Gamma\bar{h}\bar{s}\sinh(\bar{h}\bar{s})},\\ \bar{C}(\bar{s})&=\frac{|\bar{h}\bar{s}|}{|\bar{h}\bar{s}|\cosh(\bar{h}\bar{s})+\Gamma\bar{h}\bar{s}\sinh(\bar{h}\bar{s})}.\end{aligned} \tag{6.42}$$

Additionally, if we let $\bar{h}\to\infty$, the result will be equal to that of the bi-material interface discussed in Chapter 5.

6.2 Numerical evaluation of stress field

As in Section 5.4, we estimate the integrals in the expressions (6.32) to (6.41) by numerical procedures. Selected results are shown in (Figs. 6-2 to 6-5) to demonstrate the effects of couple stresses on the stress field in different cases.

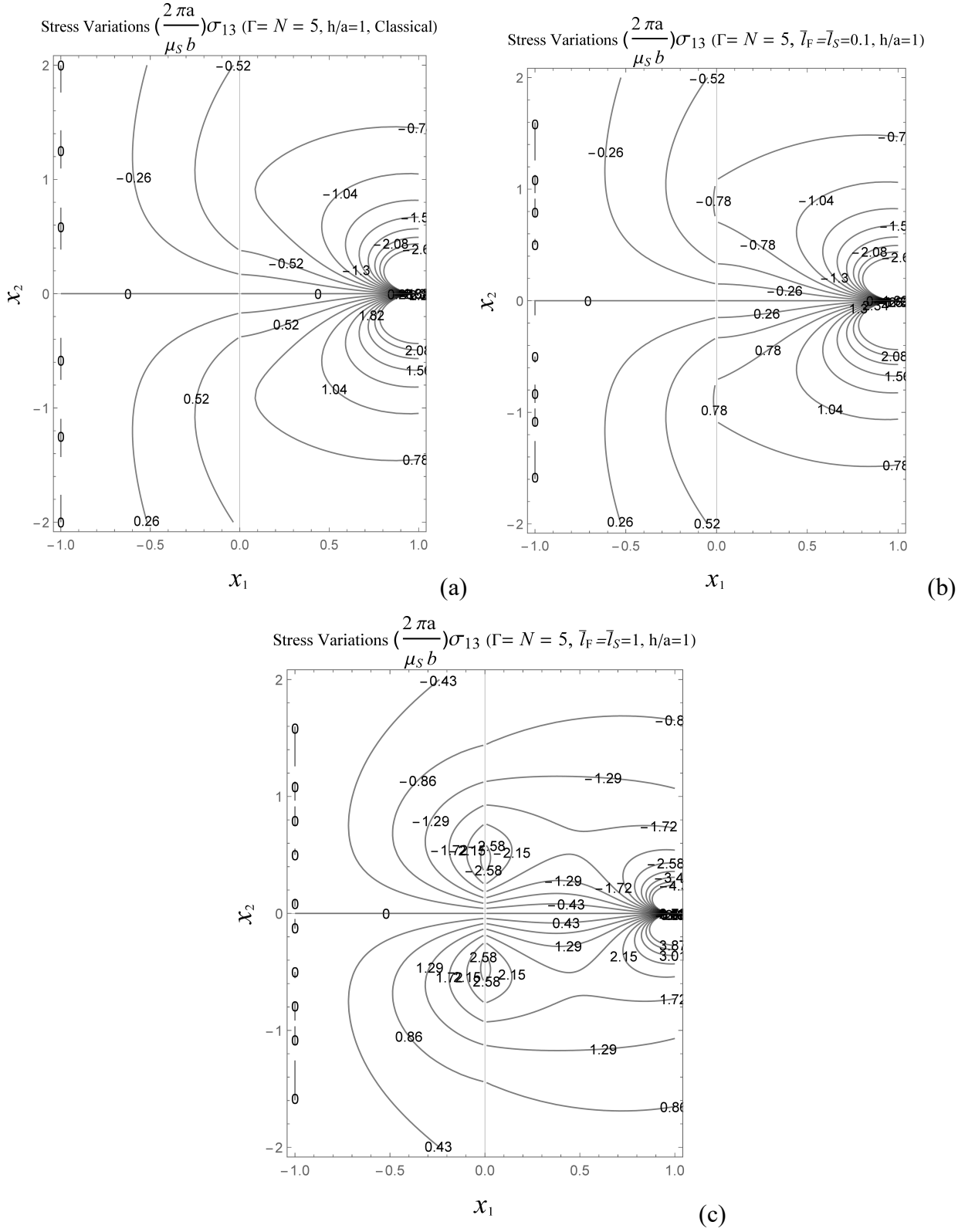

Fig. 6-2-Normalized distribution of stress component σ_{13} for length of materials $\bar{l}_1 = \bar{l}_2 = 0, 0.1, 1$, and $\bar{h} = 1$

In Fig. 6-2, the normalized values of the stress component σ_{13} are shown in contour plots. The mismatch ratios are chosen as $\Gamma = N = 5$, so that the film is stiffer than the substrate. Considering the plots in Fig. 6-2, we realize that the stress field is subjected to dramatic changes when the characteristic length of material is large compared to the distance of the dislocation from the interface ($\bar{l}_S = \bar{l}_F = 1$). For small relative characteristic lengths of material (say $\bar{l}_S = \bar{l}_F = 0.1$), however, σ_{13} varies slightly between classical and couple stress solutions. The changes from the classical solution for σ_{31} stress component are shown in Fig. 6-3. In the case of relatively large characteristic lengths of materials, $\bar{l}_S = \bar{l}_F = 1$, we observe a discontinuity of stress distribution as well as stress concentration at the interface.

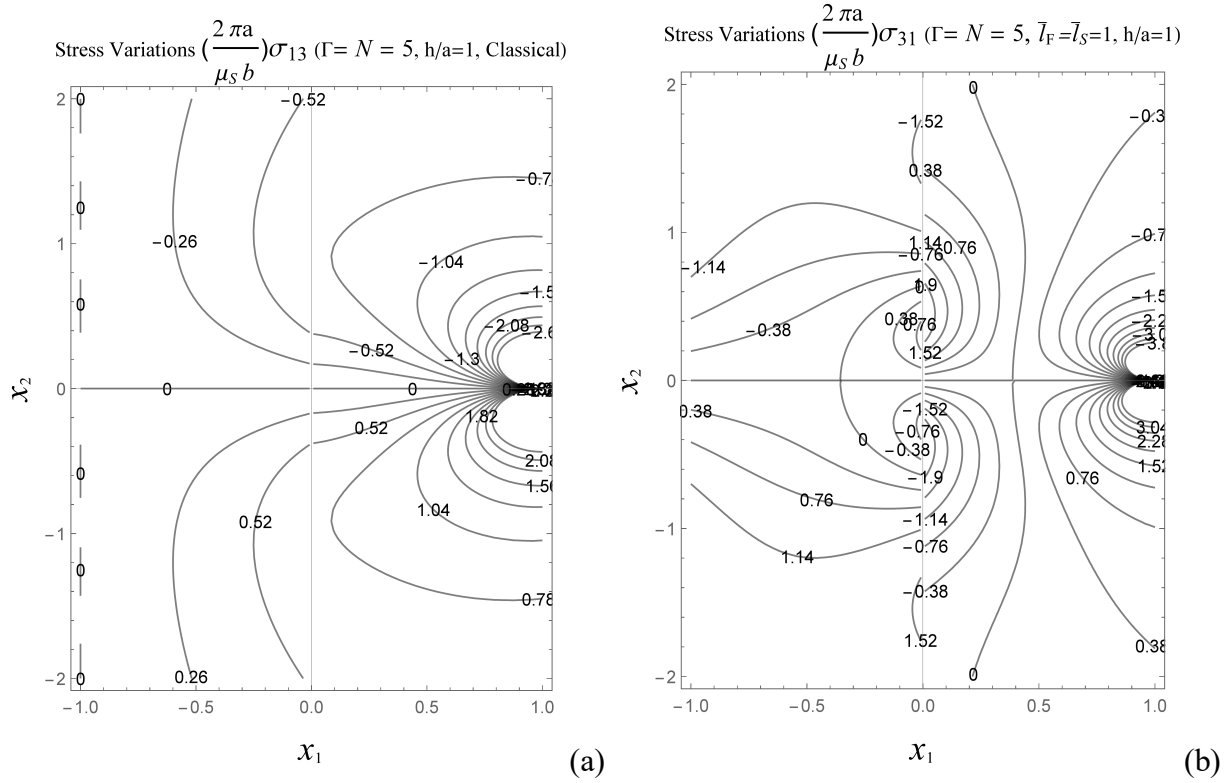

Fig. 6-3-Normalized distribution of stress component σ_{31} for length of materials $\bar{l}_1 = \bar{l}_2 = 0, 1$, and $\bar{h} = 1$

Figs. 6-3 and 6-4 illustrate the stress components σ_{23} and σ_{32}. A pronounced deviation from the classical solution is obvious in these figures. Notice that the discontinuity and stress magnitudes are intensified at the interface for these components.

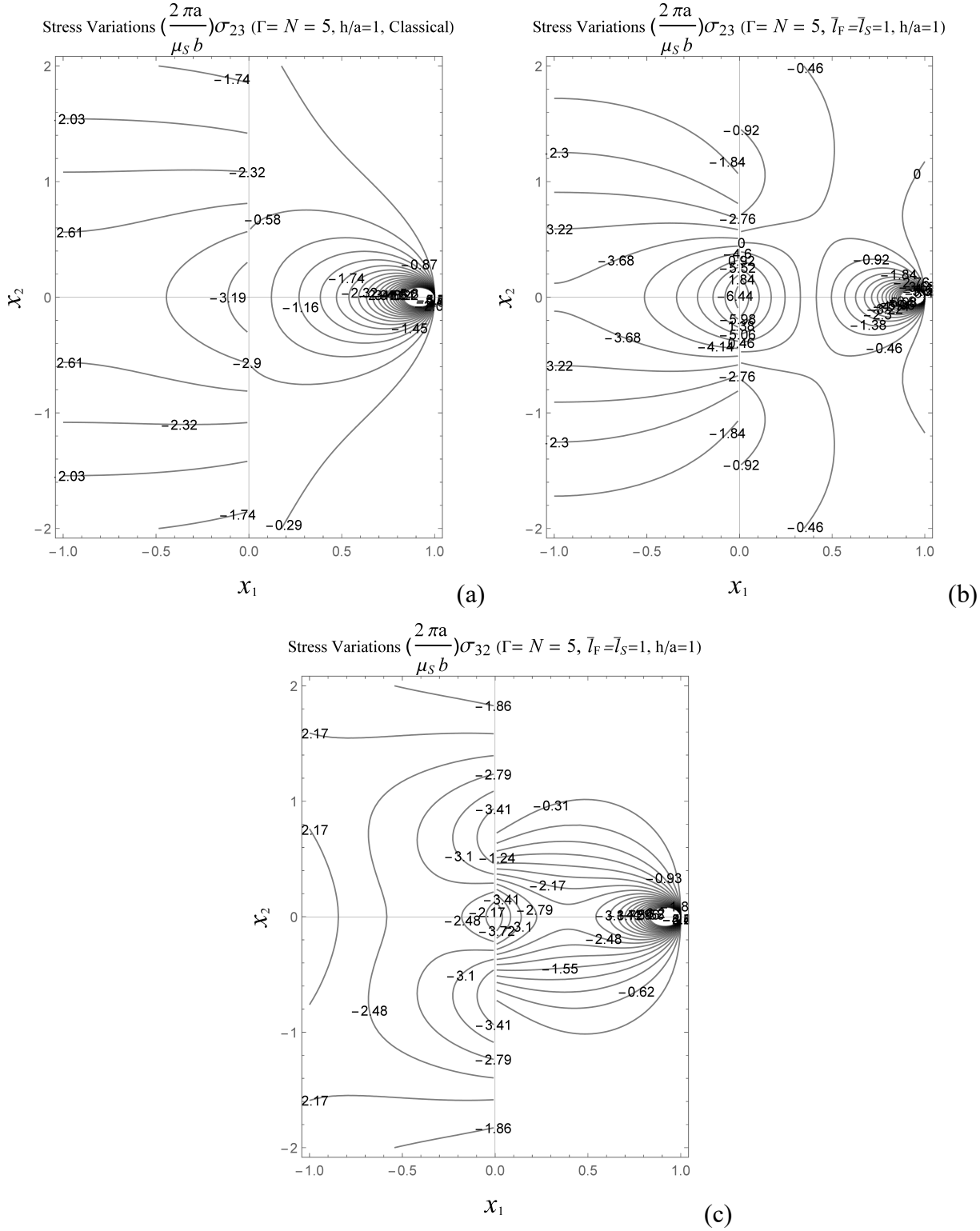

Fig. 6-4- Normalized distribution of stress components σ_{23} and σ_{32} for length of materials $\bar{l}_1=\bar{l}_2=0,1$, and $\bar{h}=1$

To evaluate the effect of thickness $\bar{h}$ of the film on the stress field, we may illustrate representative results for two more different cases namely $\bar{h} = 0.5$ and $\bar{h} = 0.1$. In each case we choose the characteristic length of materials to be equal to the thickness of the film. Again, the mismatch ratios are taken as $\Gamma = N = 5$ so that the film is stiffer than the substrate. We see from Fig. 6-5 that the stress distribution is highly dependent on the proportion of characteristic length to the dislocation's distance from the interface. However, the distribution shows less sensitivity to the thickness of the film, even though the relative characteristic length is large compared to the thickness. We observe from Fig. 6-5(a) and (b) that for $\bar{h} = 0.5$ the effect of couple stresses on both the film and the substrate is more pronounced, because the ratio $\bar{l}_F = \bar{l}_S = 0.5$ is relatively large. For the case of $\bar{h} = 0.1$ as shown in Fig. 6-5(c) and (d), however, couple stress theory imposes no tangible effect on the stress distribution. In this case, despite being of the order of the thickness $\bar{h} = 0.1$, the relative characteristic length ($\bar{l}_F = \bar{l}_S = 0.1$) is still far from comparable to the dislocation's distance from the interface. With reference to Fig. 6-2(c), on the other hand, we observe that the stress distribution is significantly influenced by couple stresses for $\bar{h} = \bar{l}_F = \bar{l}_S = 1$.

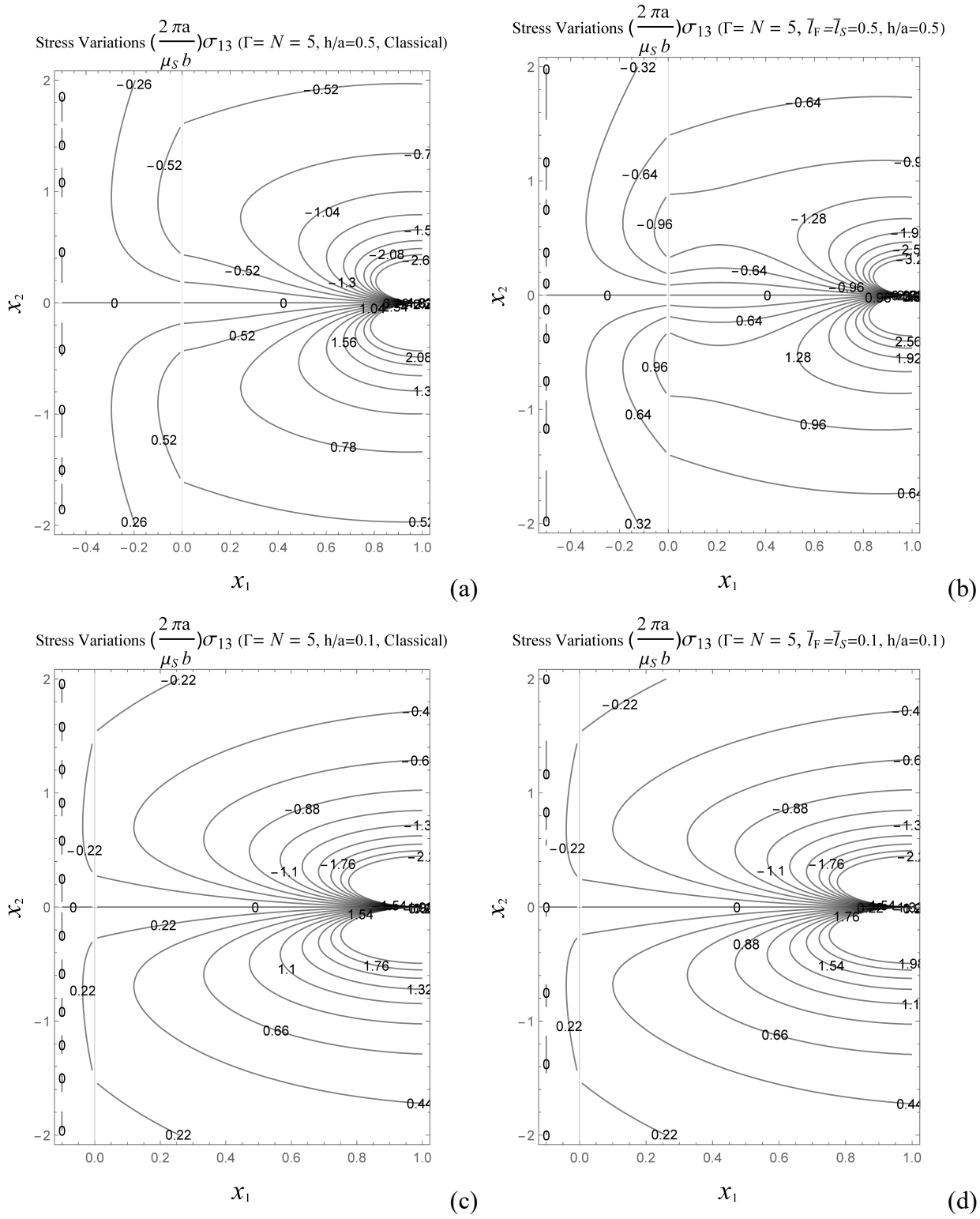

Fig. 6-5-Couple stress effects on the stress component σ_{13} for different film thicknesses

6.3 Interaction force in substrate-film configuration

We use the same approach as in Section 5.5 to calculate the force. The equation (5.86) which represents the interaction force in normalized form is then adopted and we may write:

$$\frac{F_1}{\left(\frac{\mu_S b^2}{4\pi a}\right)} = \int_{\bar{S}_2}\left(\frac{1}{2\pi}\left(\bar{u}_{3,1}^{(S)2}+\bar{u}_{3,2}^{(S)2}-2\bar{\sigma}_{13}^{(S)}\bar{u}_{3,1}^{(S)}\right)+\frac{\bar{l}_S^2}{2\pi}\left(\bar{u}_{3,22}^{(S)2}-\bar{u}_{3,11}^{(S)2}\right)\right)dx_2$$
$$+\int_{\bar{S}_1}\left(\frac{1}{\pi}\left(\bar{\sigma}_{23}^{(S)}\bar{u}_{3,1}^{(S)}\right)+\frac{\bar{l}_S^2}{\pi}\left(\bar{u}_{3,22}^{(S)}+\bar{u}_{3,11}^{(S)}\right)\bar{u}_{3,12}^{(S)}\right)dx_1, \tag{6.43}$$

for the case of the substrate-film interface. In the expression (6.43),

$$\bar{u}_{3,j}^{(S)}=\frac{u_{3,j}^{(S)}}{\left(\frac{b}{2\pi a}\right)},\quad \bar{u}_{3,ij}^{(S)}=\frac{u_{3,ij}^{(S)}}{\left(\frac{b}{2\pi a^2}\right)},\quad \bar{\sigma}_{23}^{(S)}=\frac{\sigma_{23}^{(S)}}{\left(\frac{\mu_S b}{2\pi a}\right)},$$
$$\bar{\sigma}_{13}^{(S)}=\frac{\sigma_{13}^{(S)}}{\left(\frac{\mu_S b}{2\pi a}\right)},\quad \bar{S}_1=\frac{S_1}{a},\quad \bar{S}_2=\frac{S_2}{a}, \tag{6.44}$$

and $u_3^{(S)}$, $\sigma_{23}^{(S)}$ and $\sigma_{13}^{(S)}$ are obtained from (6.30), (6.32) and (6.34). Again, S_1 and S_2 are the sums of the segments parallel to the X_1 and X_2-axes, respectively so that $S_1+S_2=S$ comprises an enclosing path around the screw dislocation. We notice that this arbitrary rectangular path lies completely in the substrate region as in Fig. 6-6.

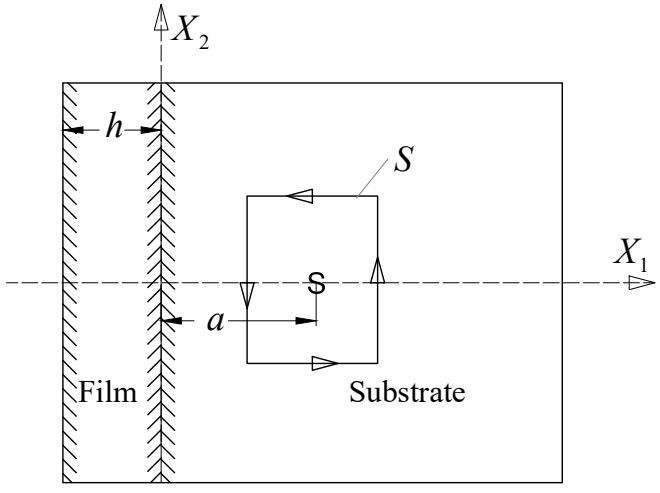

Fig. 6-6-Path of integration for calculating the force

We employ the displacement and stress expressions given in Section 6.1 to determine sampling points for evaluating the integral (6.44) over an arbitrary rectangular path within the substrate. Fig. 6-7 illustrates numerical results for the interaction force varying with the relative thickness of the film, $\overline{h}$. We can see that for each of the mismatch coefficients Γ and N, as $\overline{h}$ takes larger values, the normalized force approaches its value for the bi-material case. In Fig. 6-7, the force variations are presented for a relatively soft film over a stiff substrate where $\Gamma = N = 0.5$, as well as, for the case when the film is made of a stiffer material than the substrate $\Gamma = N = 5$. In each of these states, we compare the forces for $\overline{l}_F = \overline{l}_S = 0.5$ and $\overline{l}_F = \overline{l}_S = 1$ to the classical solutions in Dundurs [15]. It can also be shown using numerical analysis that if $\overline{l}_F = \overline{l}_S \to 0$ the results reproduce those found in Dundurs [15] as

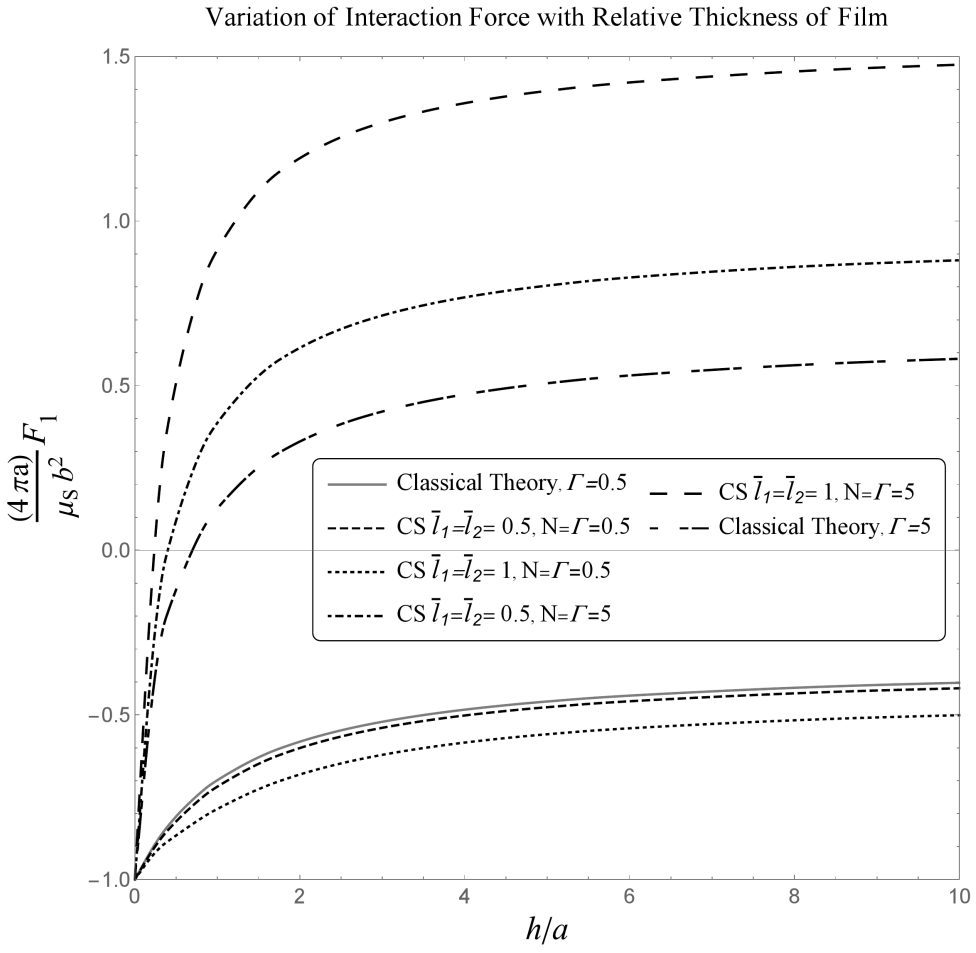

Fig. 6-7-Variations of normalized force with relative thickness of the film.

$$\frac{F_1}{\left(\frac{\mu_S b^2}{4\pi a}\right)} = \left(K - (1+K)\frac{2}{\bar{h}}\int_0^\infty \frac{e^{-\left(1+\frac{2}{\bar{h}}\right)\bar{s}}}{\cosh(\bar{h}\bar{s}) + \Gamma \sinh(\bar{h}\bar{s})} d\bar{s} \right), \tag{6.45}$$

for the case of classical elasticity. It can be deduced from Fig. 6-7, that as in the case of a bi-material, the higher values of $\bar{l}_F$ and $\bar{l}_S$, intensify the absolute value of the force on the dislocation. However, for $\Gamma, N > 1$, when we increase the thickness $\bar{h}$ from zero (which is equivalent to a half-plane medium), the force decreases until it vanishes indicating that the dislocation reaches a state of equilibrium. This particular value of thickness imposing equilibrium on the dislocation decreases for higher values of relative characteristic lengths $\bar{l}_F$ and $\bar{l}_S$. Physically, this means that for couple stress materials a thinner coating is required to immobilize the dislocation.

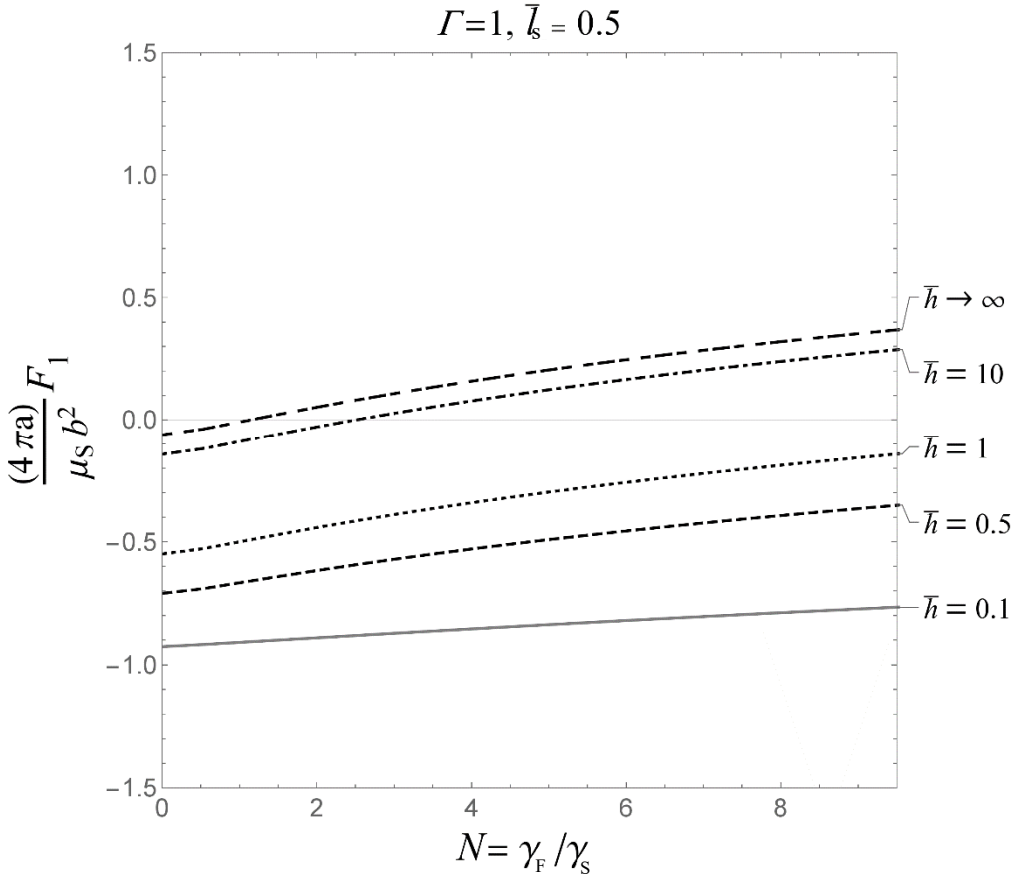

Fig. 6-8 Variation of force with mismatch between characteristic lengths for different thicknesses and $\bar{l}_S = 0.5$

As another interesting aspect of the problem, we consider the combined effects of couple stresses and thickness of the film on the force. Figs. 6-8 and 6-9, illustrate the variations of force when the mismatch of the substrate-film is produced only by the difference in the characteristic lengths of materials occupying the two regions. Again, we choose the parameters so that they satisfy the relation (5.81). In this regard, we keep the characteristic length of material in the substrate as a constant in each case and change the bending-twisting moduli ratio N as well as the thickness of the film.

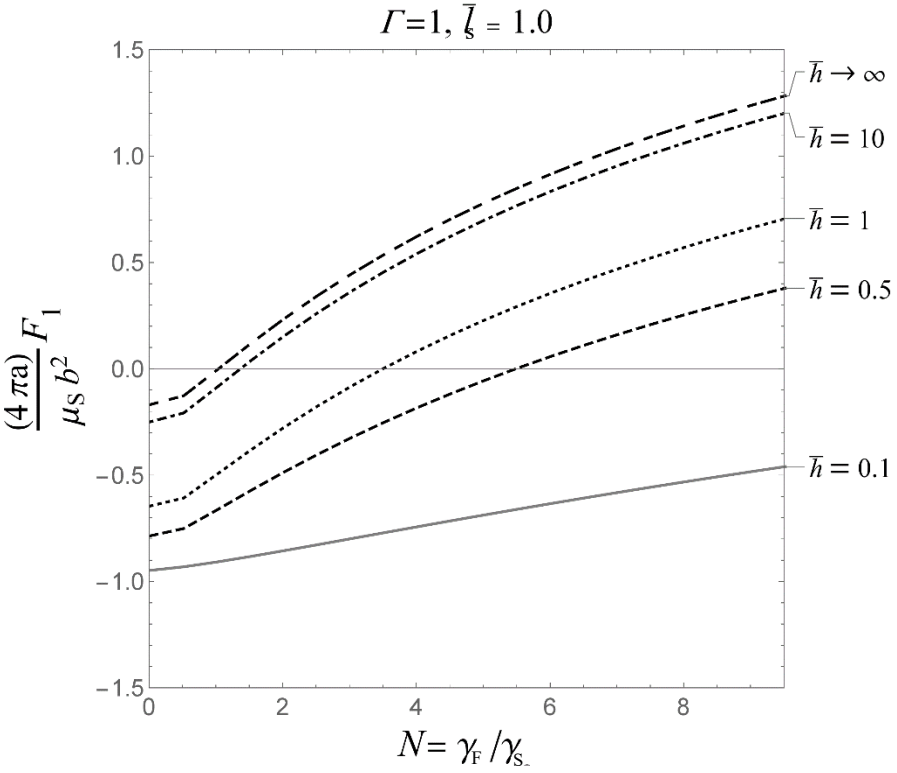

Fig. 6-9- Variation of force with mismatch between characteristic lengths for different thicknesses and $\bar{l}_S = 1$

From Fig. 6-8 and 6-9, it is clear that while the relative characteristic length of material in the substrate is definite, increasing N from a very small value (approximately classical theory) to higher values, decreases the absolute value of the attraction force towards the interface until a state of equilibrium is reached. This balance point occurs at a smaller N for higher thicknesses. The minimum N where the balance occurs is at $N = 1$ when $\bar{h} \to \infty$, which is consistent with the case of a dislocation in a uniform infinite medium. Then, if we continue to increase N after the balance point, a repulsive force appears and increases accordingly. The repulsive force is also

higher for higher thicknesses of the film. Comparing Fig. 6-8 with Fig. 6-9, we deduce that the rate of change in force is higher for a larger characteristic length of material in the substrate. In addition, we can compare Figs. 6-8 and 6-9 with Fig. 5-9 for the case when $\overline{h} \to \infty$ to verify that our results are reducible to the case of the interface interaction for a bi-material presented in Chapter 5.

7 A Screw Dislocation in a Film over a Substrate

In this chapter, we present the second possible case of the screw dislocation-interface interaction for a thin film and a substrate configuration. In this case, the dislocation is positioned inside the film region. We use the same Fourier integral transform approach to tackle the problem.

7.1 Solving the boundary value problem

Assuming again that the anti-plane parameters act in the X_3-direction and that the X_2 axis coincides with the film- substrate interface, we place a right-handed screw dislocation at the point $(a,0)$ inside the thin film of thickness h $(h>a)$. Again, we assign the shear and twisting-bending moduli μ_{S} and γ_{S}, respectively, to the substrate region while these parameters for the film region are denoted by μ_{F} and γ_{F}. The geometry of the problem, in this case, is shown in Fig. 7-1. As before, by taking the classical displacement solution for a dislocation near a bi-material interface as a base solution, we introduce a perturbation displacement term that encompasses the effects of the confined film as well as the couple stresses. Therefore, we may write:

$$\begin{aligned} u_3^{(\mathsf{F})} &= \frac{b}{2\pi}\left(\tan^{-1}\left(\frac{X_2}{X_1-a}\right)+K\tan^{-1}\left(\frac{X_2}{X_1+a}\right)\right)+\hat{u}_3^{(\mathsf{F})}, \\ u_3^{(\mathsf{S})} &= \frac{b}{2\pi}\left((1-K)\tan^{-1}\left(\frac{X_2}{X_1-a}\right)+K\pi\right)+\hat{u}_3^{(\mathsf{S})}, \end{aligned} \tag{7.1}$$

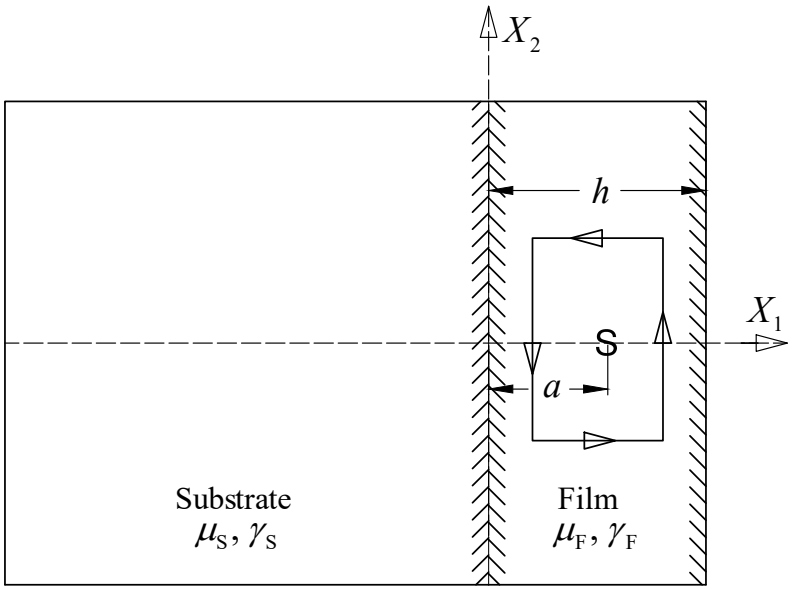

Fig. 7-1-Configuration of the problem of a screw dislocation in a film over a substrate.

where, the superscripts "(S)" and "(F)" again refer to the substrate and film, respectively. For this anti-plane problem, we express the governing field equations as

$$\begin{aligned} &\nabla^2(1-l_F^2\nabla^2)u_3^{(F)}=0, \quad 0\le X_1\le h,\\ &\nabla^2(1-l_S^2\nabla^2)u_3^{(S)}=0, \quad X_1<0, \end{aligned} \tag{7.2}$$

for the film and the substrate respectively. Upon inserting (7.1) into (7.2), we have

$$\begin{aligned} &\nabla^2(1-l_F^2\nabla^2)\hat{u}_3^{(F)}=0, \quad 0\le X_1\le h,\\ &\nabla^2(1-l_S^2\nabla^2)\hat{u}_3^{(S)}=0, \quad X_1<0, \end{aligned} \tag{7.3}$$

As in the previous chapters, for both material media (the substrate and the film, respectively), the characteristic lengths are denoted by $l_S^2=\gamma_S/2\mu_S$ and $l_F^2=\gamma_F/2\mu_F$. The boundary conditions for the two governing equations (7.2) can be written as

$$\begin{aligned} &\mu_{12}^{(S)}(0,X_2)=\mu_{12}^{(F)}(0,X_2), \quad \sigma_{13}^{(S)}(0,X_2)=\sigma_{13}^{(F)}(0,X_2),\\ &u_3^{(S)}(0,X_2)=u_3^{(F)}(0,X_2), \quad u_{3,1}^{(S)}(0,X_2)=u_{3,1}^{(F)}(0,X_2), \end{aligned} \tag{7.4}$$

at the interface ($X_1=0$) and

$$\mu_{12}^{(F)}(h,X_2)=0, \quad \sigma_{13}^{(F)}(h,X_2)=0, \tag{7.5}$$

for the traction-free surface of the thin film at $X_1=h$. Taking (7.1) into consideration and

making use of (5.11) and (5.12) we may express the boundary conditions (7.4) and (7.5) in terms of the additional displacement parameters $\hat{u}_3^{(\mathsf{F})}$ and $\hat{u}_3^{(\mathsf{S})}$ as

$$\begin{aligned}&\sigma_{13}^{(\mathsf{F})}(0,X_2)=\sigma_{13}^{(\mathsf{S})}(0,X_2)\\&\Rightarrow \hat{u}_{3,1}^{(\mathsf{F})}(0,X_2)-\Gamma\hat{u}_{3,1}^{(\mathsf{S})}(0,X_2)-{l_{\mathsf{F}}}^2\nabla^2\hat{u}_{3,1}^{(\mathsf{F})}(0,X_2)+\Gamma{l_{\mathsf{S}}}^2\nabla^2\hat{u}_{3,1}^{(\mathsf{S})}(0,X_2)=0,\end{aligned} \tag{7.6}$$

$$\begin{aligned}&\mu_{12}^{(\mathsf{F})}(0,X_2)=\mu_{12}^{(\mathsf{S})}(0,X_2)\\&\Rightarrow \hat{u}_{3,11}^{(\mathsf{F})}(0,X_2)-N\hat{u}_{3,11}^{(\mathsf{S})}(0,X_2)=\frac{b}{2\pi}\left((1-N)(1-K)\frac{2X_2a}{(a^2+X_2^2)^2}\right),\end{aligned} \tag{7.7}$$

$$u_3^{(\mathsf{F})}(0,X_2)=u_3^{(\mathsf{S})}(0,X_2)\Rightarrow \hat{u}_3^{(\mathsf{F})}(0,X_2)=\hat{u}_3^{(\mathsf{S})}(0,X_2), \tag{7.8}$$

$$\begin{aligned}&u_{3,1}^{(\mathsf{F})}(0,X_2)=u_{3,1}^{(\mathsf{S})}(0,X_2)\\&\Rightarrow \hat{u}_{3,1}^{(\mathsf{F})}(0,X_2)-\hat{u}_{3,1}^{(\mathsf{S})}(0,X_2)=\frac{b}{2\pi}\left(\frac{2KX_2}{a^2+X_2^2}\right),\end{aligned} \tag{7.9}$$

$$\begin{aligned}&\sigma_{13}^{(\mathsf{F})}(h,X_2)=0\\&\Rightarrow \hat{u}_{3,1}^{(\mathsf{F})}(h,X_2)-{l_{\mathsf{F}}}^2\nabla^2\hat{u}_{3,1}^{(\mathsf{F})}(h,X_2)=\frac{b}{2\pi}\left(\frac{X_2}{(h-a)^2+X_2^2}+\frac{KX_2}{(h+a)^2+X_2^2}\right),\end{aligned} \tag{7.10}$$

$$\begin{aligned}&\mu_{12}^{(\mathsf{F})}(h,X_2)=0\\&\Rightarrow \hat{u}_{3,11}^{(\mathsf{F})}(h,X_2)=\frac{-b}{2\pi}\left(\frac{2X_2(h-a)}{\left((h-a)^2+X_2^2\right)^2}+\frac{2X_2(h+a)}{\left((h+a)^2+X_2^2\right)^2}\right).\end{aligned} \tag{7.11}$$

Applying the Fourier integral transform given in (5.25) and (5.26) to the governing equations (7.3), we obtain the two ordinary differential equations,

$$\begin{aligned}&\left(\frac{\partial^2}{\partial {X_1}^2}-s^2\right)\left(\frac{1}{l_{\mathsf{F}}^2}+s^2-\frac{\partial^2}{\partial {X_1}^2}\right)\tilde{U}_3^{(\mathsf{F})}(X_1,s)=0,\\&\left(\frac{\partial^2}{\partial {X_1}^2}-s^2\right)\left(\frac{1}{l_{\mathsf{S}}^2}+s^2-\frac{\partial^2}{\partial {X_1}^2}\right)\tilde{U}_3^{(\mathsf{S})}(X_1,s)=0,\end{aligned} \tag{7.12}$$

which, regarding the bounded displacement condition as $X_1\to\infty$, have solutions

$$\begin{aligned}\tilde{U}_3^{(\mathrm{F})} &= A_1(s)e^{|s|X_1} + B_1(s)e^{-|s|X_1} + C_1(s)e^{\beta_1(s)X_1} + D_1(s)e^{-\beta_1(s)X_1}, \text{ for } 0 \le X_1 < h, \\ \tilde{U}_3^{(\mathrm{S})} &= B_2(s)e^{|s|X_1} + D_2(s)e^{\beta_2(s)X_1}, \text{ for } X_1 < 0,\end{aligned} \tag{7.13}$$

where,

$$\beta_1(s) = \sqrt{s^2 + \frac{1}{l_{\mathrm{S}}^2}}, \quad \beta_2(s) = \sqrt{s^2 + \frac{1}{l_{\mathrm{F}}^2}}. \tag{7.14}$$

The boundary conditions introduced through (7.6) to (7.11) can also be transformed by (5.25), which result in

$$A_1 - B_1 - \Gamma B_2 = 0, \tag{7.15}$$

$$s^2 A_1 + s^2 B_1 + \beta_1{}^2 C_1 + \beta_1{}^2 D_1 - N\left(s^2 B_2 + \beta_2{}^2 D_2\right) = \frac{b}{2\sqrt{2\pi}}\left(-(1-N)(1-K)ise^{-a|s|}\right), \tag{7.16}$$

$$A_1 + B_1 + C_1 + D_1 - B_2 - D_2 = 0, \tag{7.17}$$

$$|s|A_1 - |s|B_1 + \beta_1 C_1 - \beta_1 D_1 - |s|B_2 - \beta_2 D_2 = \frac{-bK}{\sqrt{2\pi}}\left(i\,\mathrm{sgn}(s)e^{-a|s|}\right), \tag{7.18}$$

$$|s|A_1 e^{|s|h} - |s|B_1 e^{-|s|h} = -\frac{b}{2\sqrt{2\pi}}\left(i\,\mathrm{sgn}(s)(e^{-(h-a)|s|} + Ke^{-(h+a)|s|})\right), \tag{7.19}$$

$$s^2 A_1 e^{|s|h} + s^2 B_1 e^{-|s|h} + \beta_1^2 C_1 e^{\beta_1 h} + \beta_1^2 D_1 e^{-\beta_1 h} = \frac{b}{2\sqrt{2\pi}}\left(is(e^{-(h-a)|s|} + Ke^{-(h+a)|s|})\right), \tag{7.20}$$

respectively. We solve the set of algebraic equations (7.15) to (7.20) for the coefficients A_1, B_1, C_1, D_1, B_2 and D_2, and we simultaneously use the substitutions,

$$\begin{aligned}&\bar{l}_{\mathrm{S}} = \frac{l_{\mathrm{S}}}{a}, \quad \bar{l}_{\mathrm{F}} = \frac{l_{\mathrm{F}}}{a}, \quad \bar{h} = \frac{h}{a}, \quad \bar{s} = as \\ &\bar{\beta}_1 = a\beta_1 \Rightarrow \bar{\beta}_1 = \sqrt{\bar{s}^2 + \frac{1}{\bar{l}_{\mathrm{F}}{}^2}}, \quad \bar{\beta}_2 = a\beta_2 \Rightarrow \bar{\beta}_2 = \sqrt{\bar{s}^2 + \frac{1}{\bar{l}_{\mathrm{S}}{}^2}},\end{aligned} \tag{7.21}$$

to express the results in the following form:

$$
\begin{aligned}
&\bar{A}_1 = \frac{a\sqrt{2\pi}}{b} A_1 = \frac{A_1^*}{D}, \quad \bar{B}_1 = \frac{a\sqrt{2\pi}}{b} B_1 = \frac{B_1^*}{D}, \\
&\bar{C}_1 = \frac{a\sqrt{2\pi}}{b} C_1 = \frac{C_1^*}{\bar{\beta}_1(\bar{s})D}, \quad \bar{D}_1 = \frac{a\sqrt{2\pi}}{b} D_1 = \frac{D_1^*}{\bar{\beta}_1(\bar{s})D}, \\
&\bar{B}_2 = \frac{a\sqrt{2\pi}}{b} B_2 = \frac{B_2^*}{D}, \quad \bar{D}_2 = \frac{a\sqrt{2\pi}}{b} D_2 = \frac{D_2^*}{D},
\end{aligned}
\tag{7.22}
$$

where,

$$
\begin{aligned}
D = 2|\bar{s}|\Big\{ & \bar{s}^2 N\left(-\bar{\beta}_1^2\left(e^{2\bar{\beta}_1\bar{h}}+1\right)\left(e^{2\bar{h}|\bar{s}|}-1\right)-4\bar{\beta}_2^2\Gamma e^{\bar{h}(|\bar{s}|+\bar{\beta}_1)}-\bar{\beta}_1\bar{\beta}_2\left(e^{2\bar{\beta}_1\bar{h}}-1\right)\left(e^{2\bar{h}|\bar{s}|}-1\right)\right) \\
& +\bar{\beta}_1^2\bar{\beta}_2^2 N\left(e^{2\bar{\beta}_1\bar{h}}+1\right)\left((\Gamma+1)e^{2\bar{h}|\bar{s}|}+\Gamma-1\right) \\
& +\bar{\beta}_1(\Gamma-1)|\bar{s}|\left(e^{2\bar{\beta}_1\bar{h}}-1\right)\left(e^{2\bar{h}|\bar{s}|}-1\right)\left(\bar{\beta}_1^2-\bar{\beta}_2^2 N\right)+\bar{\beta}_2\bar{\beta}_1\Gamma\bar{s}^2\left(1-e^{2\bar{\beta}_1\bar{h}}\right)\left(e^{2\bar{h}|\bar{s}|}+1\right) \\
& -\bar{\beta}_1^2\Gamma\bar{s}^2\left(-4e^{\bar{h}(|\bar{s}|+\bar{\beta}_1)}+e^{2\bar{h}(|\bar{s}|+\bar{\beta}_1)}+e^{2\bar{h}|\bar{s}|}+e^{2\bar{\beta}_1\bar{h}}+1\right) \\
& +\bar{\beta}_1^3\bar{\beta}_2\left(e^{2\bar{\beta}_1\bar{h}}-1\right)\left((\Gamma+1)e^{2\bar{h}|\bar{s}|}+\Gamma-1\right)\Big\},
\end{aligned}
\tag{7.23}
$$

$$
\begin{aligned}
& A_1^* = \\
& ie^{-(\bar{h}+1)|\bar{s}|}\Big\{\operatorname{sgn}(\bar{s})\left(e^{2|\bar{s}|}+K\right)\Big[-\beta_1 e^{\bar{h}(|\bar{s}|+2\bar{\beta}_1)}\left((\Gamma+1)\bar{\beta}_1\bar{\beta}_2\left(\bar{\beta}_1+N\bar{\beta}_2\right)-\bar{s}^2(N+\Gamma)(\bar{\beta}_1+\bar{\beta}_2)\right) \\
& +\bar{\beta}_1 e^{\bar{h}|\bar{s}|}\left(\bar{\beta}_1^2\bar{\beta}_2(\Gamma+1)+N\left(\bar{s}^2\left(\bar{\beta}_1-\bar{\beta}_2\right)-\bar{\beta}_1\bar{\beta}_2^2(\Gamma+1)\right)+\Gamma\bar{s}^2(\bar{\beta}_1-\bar{\beta}_2)\right) \\
& -\bar{\beta}_1(\Gamma-1)|\bar{s}|\left(e^{2\bar{\beta}_1\bar{h}}-1\right)e^{\bar{h}|\bar{s}|}\left(\bar{\beta}_1^2-N\bar{\beta}_2^2\right)-2\Gamma\bar{s}^2 e^{\bar{\beta}_1\bar{h}}\left(\bar{\beta}_1^2-N\bar{\beta}_2^2\right)\Big] \\
& +\Gamma|\bar{s}|\Big[\bar{s}\left(\bar{\beta}_1(K-1)(N-1)\left(\left(\bar{\beta}_1-\bar{\beta}_2\right)e^{\bar{h}|\bar{s}|}+\left(\bar{\beta}_1+\bar{\beta}_2\right)e^{\bar{h}(|\bar{s}|+2\bar{\beta}_1)}\right)\right. \\
& \left.+\left(2e^{2|\bar{s}|+\bar{\beta}_1\bar{h}}+2Ke^{\bar{\beta}_1\bar{h}}\right)\left(\bar{\beta}_1^2-N\bar{\beta}_2^2\right)\right)+2\bar{\beta}_1 K\left(e^{2\bar{\beta}_1\bar{h}}-1\right)\operatorname{sgn}(\bar{s})e^{\bar{h}|\bar{s}|}\left(\bar{\beta}_1^2-N\bar{\beta}_2^2\right)\Big]\Big\},
\end{aligned}
\tag{7.24}
$$

$$
\begin{aligned}
B_1^* = -ie^{-|\bar{s}|}\Big\{ & \operatorname{sgn}(\bar{s})\Big[-2\Gamma\bar{s}^2\left(\bar{\beta}_1^2 - N\bar{\beta}_2^2\right)\left(Ke^{\bar{h}(|\bar{s}|+\bar{\beta}_1)} + e^{(\bar{h}+2)|\bar{s}|+\bar{\beta}_1\bar{h}}\right) \\
& -\bar{\beta}_1\left(e^{2(|\bar{s}|+\bar{\beta}_1\bar{h})} + Ke^{2\bar{\beta}_1\bar{h}}\right)\left(\bar{\beta}_1\bar{\beta}_2(\Gamma-1)\left(\bar{\beta}_1 - N\bar{\beta}_2\right) + \bar{s}^2(N-\Gamma)\left(\bar{\beta}_1+\bar{\beta}_2\right)\right) \\
& +\bar{\beta}_1\left(K + e^{2|\bar{s}|}\right)\left(\bar{\beta}_1\bar{\beta}_2(\Gamma-1)\left(\bar{\beta}_1 - N\bar{\beta}_2\right) + \bar{s}^2(N-\Gamma)\left(\bar{\beta}_2 - \bar{\beta}_1\right)\right)\Big] \\
& +|\bar{s}|\Big[\Gamma\bar{s}\left(-2K\left(\bar{\beta}_1^2 - N\bar{\beta}_2^2\right)e^{\bar{h}(|\bar{s}|+\bar{\beta}_1)} - e^{2\bar{h}|\bar{s}|}\bar{\beta}_1(K-1)(N-1)\left(\bar{\beta}_1 - \bar{\beta}_2\right)\right. \\
& \left.-\bar{\beta}_1(K-1)(N-1)\left(\bar{\beta}_1+\bar{\beta}_2\right)e^{2\bar{h}(|\bar{s}|+\bar{\beta}_1)} - 2\left(\bar{\beta}_1^2 - N\bar{\beta}_2^2\right)e^{(\bar{h}+2)|\bar{s}|+\bar{\beta}_1\bar{h}}\right) \\
& +\bar{\beta}_1\operatorname{sgn}(\bar{s})\left(e^{2\bar{\beta}_1\bar{h}} - 1\right)\left(\bar{\beta}_1^2 - N\bar{\beta}_2^2\right)\left(-2\Gamma Ke^{2\bar{h}|\bar{s}|} + (\Gamma-1)e^{2|\bar{s}|} + (\Gamma-1)K\right)\Big]\Big\},
\end{aligned}
\tag{7.25}
$$

$$
\begin{aligned}
C_1^* = ie^{-(\bar{h}+1)|\bar{s}|}\Big\{ & \bar{s}^2\operatorname{sgn}(\bar{s})\Big[2e^{(\bar{h}+2)|\bar{s}|}(N-1)\bar{\beta}_2\bar{\beta}_1^2 + 2e^{\bar{h}|\bar{s}|}K(N-1)\bar{\beta}_2\bar{\beta}_1^2 \\
& +\left(e^{\bar{h}\bar{\beta}_1}K + e^{\bar{h}\bar{\beta}_1+2|\bar{s}|}\right)\left(\bar{s}^2(\Gamma-N)\left(\bar{\beta}_1+\bar{\beta}_2\right) - \bar{\beta}_1\bar{\beta}_2(\Gamma-1)\left(\bar{\beta}_1 + N\bar{\beta}_2\right)\right) \\
& +\left(e^{\bar{h}\bar{\beta}_1+2(\bar{h}+1)|\bar{s}|} + e^{\bar{h}(\bar{\beta}_1+2|\bar{s}|)}K\right)\left(-\bar{s}^2(\Gamma+N)\left(\bar{\beta}_1+\bar{\beta}_2\right) + \bar{\beta}_1\bar{\beta}_2(\Gamma+1)\left(\bar{\beta}_1+N\bar{\beta}_2\right)\right)\Big] \\
& +\bar{s}|\bar{s}|^2(\Gamma-1)\left(e^{2\bar{h}|\bar{s}|}-1\right)\left(e^{\bar{h}|\bar{s}|}(K-1)(N-1)\bar{\beta}_1^2 + \left(e^{\bar{h}\bar{\beta}_1+2|\bar{s}|} + e^{\bar{h}\bar{\beta}_1}K\right)\left(\bar{\beta}_1^2 - N\bar{\beta}_2^2\right)\right) \\
& +|\bar{s}|\bar{s}\Big[(K-1)(N-1)\bar{\beta}_1^2\bar{\beta}_2\left((\Gamma-1)e^{\bar{h}|\bar{s}|} + (\Gamma+1)e^{3\bar{h}|\bar{s}|}\right) \\
& +\left(e^{\bar{h}\bar{\beta}_1+2|\bar{s}|} + e^{\bar{h}\bar{\beta}1}K\right)\left(\bar{s}^2(N-\Gamma)\left(\bar{\beta}_1+\bar{\beta}_2\right) + \bar{\beta}_1\bar{\beta}_2(\Gamma-1)\left(\bar{\beta}_1+N\bar{\beta}_2\right)\right) \\
& +e^{\bar{h}\bar{\beta}1+2(\bar{h}+1)|\bar{s}|}\left(-\bar{s}^2(\Gamma+N)\left(\bar{\beta}_1+\bar{\beta}_2\right) + \bar{\beta}_1\bar{\beta}_2(\Gamma+1)\left(\bar{\beta}_1+N\bar{\beta}_2\right)\right) \\
& +e^{\bar{h}(\bar{\beta}1+2|\bar{s}|)}\left(2(N-1)\left(\bar{\beta}_1+\bar{\beta}_2\right)\Gamma\bar{s}^2 + K\left(\bar{s}^2\left(\bar{\beta}_1+\bar{\beta}_2\right)\left(\Gamma - N(2\Gamma+1)\right) + \bar{\beta}_1\bar{\beta}_2(\Gamma+1)\left(\bar{\beta}_1+N\bar{\beta}_2\right)\right)\right)\Big] \\
& +|\bar{s}|\operatorname{sgn}(\bar{s})\Big[-2e^{\bar{h}|\bar{s}|}K(N-1)\bar{\beta}_1^2\bar{s}^2 + \left(e^{\bar{h}\bar{\beta}_1+2|\bar{s}|} + e^{\bar{h}\bar{\beta}_1+2(\bar{h}+1)|\bar{s}|} + e^{\bar{h}\bar{\beta}_1}K\right)(\Gamma-1)\bar{s}^2\left(\bar{\beta}_1^2 - N\bar{\beta}_2^2\right) \\
& -\left(e^{\bar{h}(\bar{\beta}_1+2|\bar{s}|)}K(3\Gamma+1)\bar{s}^2 + 2e^{(\bar{h}+2)|\bar{s}|}\bar{\beta}_1^2(\Gamma-1)\right)\left(\bar{s}^2 - N\bar{\beta}_2^2\right) \\
& +2e^{3\bar{h}|\bar{s}|}K\bar{\beta}_1^2\left(\Gamma\bar{s}^2 + N\left(\bar{s}^2 - \bar{\beta}_2^2(\Gamma+1)\right)\right)\Big]\Big\},
\end{aligned}
\tag{7.26}
$$

$$
\begin{aligned}
D_1^* = {} & ie^{\bar{h}\bar{\beta}_1-(\bar{h}+1)|\bar{s}|}\Big\{\bar{s}^2\,\mathrm{sgn}(\bar{s})\Big[2\Big(e^{\bar{h}\bar{\beta}_1+(\bar{h}+2)|\bar{s}|}+e^{\bar{h}(\bar{\beta}_1+|\bar{s}|)}K\Big)(1-N)\,\bar{\beta}_2\bar{\beta}_1^{\,2} \\
& +\Big(e^{2|\bar{s}|}+K\Big)\Big((N-\Gamma)\bar{s}^2\left(\bar{\beta}_2-\bar{\beta}_1\right)+\bar{\beta}_1\bar{\beta}_2\left(\Gamma-1\right)\left(\bar{\beta}_1-N\bar{\beta}_2\right)\Big) \\
& +\Big(e^{2(\bar{h}+1)|\bar{s}|}+e^{2\bar{h}|\bar{s}|}K\Big)\Big((N+\Gamma)\bar{s}^2\left(\bar{\beta}_2-\bar{\beta}_1\right)-\bar{\beta}_1\bar{\beta}_2\left(\Gamma+1\right)\left(\bar{\beta}_1-N\bar{\beta}_2\right)\Big)\Big] \\
& +(\Gamma-1)\bar{s}\,|\bar{s}|^2\left(1-e^{2\bar{h}|\bar{s}|}\right)\Big(e^{\bar{h}(\bar{\beta}_1+|\bar{s}|)}\left(K-1\right)\left(N-1\right)\bar{\beta}_1^{\,2}+(e^{2|\bar{s}|}+K)\left(\bar{\beta}_1^{\,2}-N\bar{\beta}_2^{\,2}\right)\Big) \\
& +\bar{s}\,|\bar{s}|\Big[-\Big(e^{\bar{h}(\bar{\beta}_1+|\bar{s}|)}\left(\Gamma-1\right)+e^{\bar{h}(\bar{\beta}_1+3|\bar{s}|)}\left(\Gamma+1\right)\Big)\left(K-1\right)\left(N-1\right)\bar{\beta}_1^{\,2}\bar{\beta}_2 \\
& +\Big(e^{2|\bar{s}|}+K\Big)\Big((N-\Gamma)\bar{s}^2\left(\bar{\beta}_1-\bar{\beta}_2\right)+\bar{\beta}_1\bar{\beta}_2\left(1-\Gamma\right)\left(\bar{\beta}_1-N\bar{\beta}_2\right)\Big) \\
& +e^{2(\bar{h}+1)|\bar{s}|}\Big((N+\Gamma)\bar{s}^2\left(\bar{\beta}_2-\bar{\beta}_1\right)-\bar{\beta}_1\bar{\beta}_2\left(1+\Gamma\right)\left(\bar{\beta}_1-N\bar{\beta}_2\right)\Big) \\
& +e^{2\bar{h}|\bar{s}|}\Big(2\left(N-1\right)\left(\bar{\beta}_1-\bar{\beta}_2\right)\Gamma\bar{s}^2+K\Big(\left(\Gamma-N\left(2\Gamma+1\right)\right)\bar{s}^2\left(\bar{\beta}_1-\bar{\beta}_2\right)-\bar{\beta}_1\bar{\beta}_2\left(1+\Gamma\right)\left(\bar{\beta}_1-N\bar{\beta}_2\right)\Big)\Big)\Big] \\
& +|\bar{s}|\,\mathrm{sgn}\left(\bar{s}\right)\Big[2e^{\bar{h}(\bar{\beta}_1+|\bar{s}|)}K\left(N-1\right)\bar{\beta}_1^{\,2}\bar{s}^2-(e^{2|\bar{s}|}+e^{2(\bar{h}+1)|\bar{s}|}+K)\left(\bar{\beta}_1^{\,2}-N\bar{\beta}_2^{\,2}\right)\left(\Gamma-1\right)\bar{s}^2 \\
& +e^{2\bar{h}|\bar{s}|}K\left(\bar{\beta}_1^{\,2}-N\bar{\beta}_2^{\,2}\right)\left(3\Gamma+1\right)\bar{s}^2+2e^{\bar{h}\bar{\beta}_1+(\bar{h}+2)|\bar{s}|}\bar{\beta}_1^{\,2}\left(\bar{s}^2-N\bar{\beta}_2^{\,2}\right)\left(\Gamma-1\right) \\
& -2e^{\bar{h}(\bar{\beta}_1+3|\bar{s}|)}K\bar{\beta}_1^{\,2}\left(\Gamma\bar{s}^2+N\left(\bar{s}^2-\bar{\beta}_2^{\,2}\left(\Gamma+1\right)\right)\right)\Big]\Big\},
\end{aligned}
\tag{7.27}
$$

$$
\begin{aligned}
B_2^* = {} & ie^{-(\bar{h}+1)|\bar{s}|}\Big\{2\,\mathrm{sgn}(\bar{s})\Big[-K\bar{s}^2\left(\bar{\beta}_1^{\,2}-N\bar{\beta}_2^{\,2}\right)e^{\bar{h}(2|\bar{s}|+\bar{\beta}_1)} \\
& -\bar{\beta}_1(Ke^{\bar{h}(|\bar{s}|+2\bar{\beta}_1)}+e^{(\bar{h}+2)|\bar{s}|+2\bar{\beta}_1\bar{h}})\left(\bar{\beta}_1\bar{\beta}_2\left(\bar{\beta}_1+N\bar{\beta}_2\right)-\bar{s}^2\left(\bar{\beta}_1+\bar{\beta}_2\right)\right) \\
& +\bar{\beta}_1\left(Ke^{\bar{h}|\bar{s}|}+e^{(\bar{h}+2)|\bar{s}|}\right)\left(\bar{\beta}_1\bar{\beta}_2\left(\bar{\beta}_1-N\bar{\beta}_2\right)+\bar{s}^2\left(\bar{\beta}_1-\bar{\beta}_2\right)\right) \\
& -\left(e^{2(\bar{h}+1)|\bar{s}|+\bar{\beta}_1\bar{h}}+e^{2|\bar{s}|+\bar{\beta}_1\bar{h}}-Ke^{\bar{\beta}_1\bar{h}}\right)\bar{s}^2\left(\bar{\beta}_1^{\,2}-N\bar{\beta}_2^{\,2}\right)\Big] \\
& +|\bar{s}|\,\bar{s}\Big[\left(e^{\bar{h}|\bar{s}|}-e^{3\bar{h}|\bar{s}|}\right)\bar{\beta}_1\left(K-1\right)\left(N-1\right)\left(\bar{\beta}_1-\bar{\beta}_2\right) \\
& +\left(e^{\bar{h}(|\bar{s}|+2\bar{\beta}_1)}-e^{3\bar{h}|\bar{s}|+2\bar{\beta}_1\bar{h}}\right)\bar{\beta}_1\left(K-1\right)\left(N-1\right)\left(\bar{\beta}_1+\bar{\beta}_2\right) \\
& +2\left(e^{2|\bar{s}|+\bar{\beta}_1\bar{h}}-e^{2(\bar{h}+1)|\bar{s}|+\bar{\beta}_1\bar{h}}+Ke^{\bar{\beta}_1\bar{h}}-Ke^{\bar{h}(2|\bar{s}|+\bar{\beta}_1)}\right)\left(\bar{\beta}_1^{\,2}-N\bar{\beta}_2^{\,2}\right)\Big] \\
& -2\bar{\beta}_1K\,|\bar{s}|\,\mathrm{sgn}(\bar{s})\left(e^{2\bar{\beta}_1\bar{h}}-1\right)\left(e^{3\bar{h}|\bar{s}|}-e^{\bar{h}|\bar{s}|}\right)\left(\bar{\beta}_1^{\,2}-N\bar{\beta}_2^{\,2}\right)\Big\},
\end{aligned}
\tag{7.28}
$$

$$
\begin{aligned}
D_2^{*} = &-ie^{-(\bar{h}+1)|\bar{s}|}\Big\{2\bar{s}^2\,\mathrm{sgn}(\bar{s})\Big[-\Big(Ke^{\bar{h}(2|\bar{s}|+\bar{\beta}_1)}+e^{2(\bar{h}+1)|\bar{s}|+\bar{\beta}_1\bar{h}}\Big)\Big(\bar{\beta}_1^{\,2}\left(\Gamma+1\right)-(N+\Gamma)\bar{s}^2\Big)\\
&+\Big(e^{2|\bar{s}|+\bar{\beta}_1\bar{h}}+Ke^{\bar{\beta}_1\bar{h}}\Big)\Big(\bar{\beta}_1^{\,2}\left(\Gamma-1\right)+(N-\Gamma)\bar{s}^2\Big)\\
&+\bar{\beta}_1^{\,2}\left(N-1\right)\Big(Ke^{\bar{h}|\bar{s}|}+Ke^{\bar{h}(|\bar{s}|+2\bar{\beta}_1)}+e^{(\bar{h}+2)|\bar{s}|+2\bar{\beta}_1\bar{h}}+e^{(\bar{h}+2)|\bar{s}|}\Big)\Big]\\
&+\bar{s}\,|\bar{s}|\Big[-2e^{\bar{h}(2|\bar{s}|+\bar{\beta}_1)}\left(\bar{\beta}_1^{\,2}K\left(\Gamma+1\right)-KN\left(2\Gamma+1\right)\bar{s}^2+\Gamma K\bar{s}^2+2\Gamma\left(N-1\right)\bar{s}^2\right)\\
&-\bar{\beta}_1^{\,2}\left(K-1\right)\left(N-1\right)\Big(\left(\Gamma-1\right)\Big(e^{\bar{h}(|\bar{s}|+2\bar{\beta}_1)}+e^{\bar{h}|\bar{s}|}\Big)+\left(\Gamma+1\right)\Big(e^{3\bar{h}|\bar{s}|}+e^{3\bar{h}|\bar{s}|+2\bar{\beta}_1\bar{h}}\Big)\Big)\\
&-2\Big(e^{2|\bar{s}|+\bar{\beta}_1\bar{h}}+Ke^{\bar{\beta}_1\bar{h}}\Big)\Big(\bar{\beta}_1^{\,2}\left(\Gamma-1\right)+\bar{s}^2(N-\Gamma)\Big)-2e^{2(\bar{h}+1)|\bar{s}|+\bar{\beta}_1\bar{h}}\left(\bar{\beta}_1^{\,2}\left(\Gamma+1\right)-(N+\Gamma)\bar{s}^2\right)\Big]\\
&+2\bar{\beta}_1\,\mathrm{sgn}(\bar{s})\,|\bar{s}|\Big[\Big(Ke^{3\bar{h}|\bar{s}|}-Ke^{3\bar{h}|\bar{s}|+2\bar{\beta}_1\bar{h}}\Big)\Big(\bar{\beta}_1^{\,2}\left(\Gamma+1\right)-(N+\Gamma)\bar{s}^2\Big)\\
&-K\left(N-1\right)\bar{s}^2\Big(e^{\bar{h}(|\bar{s}|+2\bar{\beta}_1)}-e^{\bar{h}|\bar{s}|}\Big)+\left(\Gamma-1\right)\Big(\bar{s}^2-\bar{\beta}_1^{\,2}\Big)\Big(e^{(\bar{h}+2)|\bar{s}|}-e^{(\bar{h}+2)|\bar{s}|+2\bar{\beta}_1\bar{h}}\Big)\Big]\\
&+\bar{\beta}_1\left(\Gamma-1\right)\left(K-1\right)\left(N-1\right)\bar{s}\,|\bar{s}|^2\left(e^{2\bar{\beta}_1\bar{h}}-1\right)\Big(e^{3\bar{h}|\bar{s}|}-e^{\bar{h}|\bar{s}|}\Big)\Big\},
\end{aligned}
\tag{7.29}
$$

and, as opposed to Chapter 6, we define $N=\gamma_{\mathsf{S}}/\gamma_{\mathsf{F}}$ and $\Gamma=\mu_{\mathsf{S}}/\mu_{\mathsf{F}}$, since the dislocation is located in the film. Similar to the previous chapters, we use the coefficients (7.22), and the inverse transform (5.26) to express the displacement solution as

$$
\begin{aligned}
u_3^{(\mathsf{F})} = \frac{b}{2\pi}\Bigg(&\tan^{-1}\left(\frac{X_2}{X_1-a}\right)+K\tan^{-1}\left(\frac{X_2}{X_1+a}\right)\\
&+\int_{-\infty}^{\infty}\Big(\bar{A}_1(\bar{s})e^{|\bar{s}|x_1}+\bar{B}_1(\bar{s})e^{-|\bar{s}|x_1}+\bar{C}_1(\bar{s})e^{\bar{\beta}_1(\bar{s})x_1}+\bar{D}_1(\bar{s})e^{-\bar{\beta}_1(\bar{s})x_1}\Big)e^{i\bar{s}x_2}d\bar{s}\Bigg),
\end{aligned}
\tag{7.30}
$$

$$
u_3^{(\mathsf{S})} = \frac{b}{2\pi}\left((1-K)\tan^{-1}\left(\frac{X_2}{X_1-a}\right)+K\pi+\int_{-\infty}^{\infty}\Big(\bar{B}_2(\bar{s})e^{|\bar{s}|x_1}+\bar{D}_2(\bar{s})e^{\bar{\beta}_2(\bar{s})x_1}\Big)e^{i\bar{s}x_2}d\bar{s}\right),
\tag{7.31}
$$

for the film and the substrate respectively. In addition, using (5.11) the stress components can be expressed in terms of the coefficients given in (7.22), as follows:

$$
\sigma_{13}^{(\mathsf{F})} = \frac{\mu_{\mathsf{F}}b}{2\pi a}\left(\frac{-x_2}{(x_1-1)^2+x_2^{\,2}}+K\frac{-x_2}{(x_1+1)^2+x_2^{\,2}}+\int_{-\infty}^{\infty}\Big(|\bar{s}|\,\bar{A}_1e^{|\bar{s}|x_1}-|\bar{s}|\,\bar{B}_1e^{-|\bar{s}|x_1}\Big)e^{i\bar{s}x_2}d\bar{s}\right),
\tag{7.32}
$$

$$
\sigma_{13}^{(\mathsf{S})} = \frac{\mu_{\mathsf{S}}b}{2\pi a}\left((1-K)\frac{-x_2}{(x_1-1)^2+x_2^{\,2}}+\int_{-\infty}^{\infty}\Big(|\bar{s}|\,\bar{B}_2e^{|\bar{s}|x_1}\Big)e^{i\bar{s}x_2}d\bar{s}\right),
\tag{7.33}
$$

$$\sigma_{31}^{(\mathrm{F})}=\frac{\mu_{\mathrm{F}}b}{2\pi a}\Bigg(\frac{-x_2}{(x_1-1)^2+x_2{}^2}+K\frac{-x_2}{(x_1+1)^2+x_2{}^2}+\int_{-\infty}^{\infty}\Big(|\bar{s}|\,\bar{A}_1e^{|\bar{s}|x_1}-|\bar{s}|\,\bar{B}_1e^{-|\bar{s}|x_1}+2\bar{\beta}_1\bar{C}_1e^{\bar{\beta}_1x_1}-2\bar{\beta}_1\bar{D}_1e^{-\bar{\beta}_1x_1}\Big)e^{i\bar{s}x_2}d\bar{s}\Bigg),\tag{7.34}$$

$$\sigma_{31}^{(\mathrm{S})}=\frac{\mu_{\mathrm{S}}b}{2\pi a}\Bigg((1-K)\frac{-x_2}{(x_1-1)^2+x_2{}^2}+\int_{-\infty}^{\infty}\Big(|\bar{s}|\,\bar{B}_2e^{|\bar{s}|x_1}+2\bar{\beta}_2\bar{D}_2e^{\bar{\beta}_2x_1}\Big)e^{i\bar{s}x_2}d\bar{s}\Bigg),\tag{7.35}$$

$$\sigma_{23}^{(\mathrm{F})}=\frac{\mu_{\mathrm{F}}b}{2\pi a}\Bigg(\frac{x_1-1}{(x_1-1)^2+x_2{}^2}+K\frac{x_1+1}{(x_1+1)^2+x_2{}^2}+\int_{-\infty}^{\infty}is\Big(\bar{A}_1e^{|\bar{s}|x_1}+\bar{B}_1e^{-|\bar{s}|x_1}\Big)e^{i\bar{s}x_2}d\bar{s}\Bigg),\tag{7.36}$$

$$\sigma_{23}^{(\mathrm{S})}=\frac{\mu_{\mathrm{S}}b}{2\pi a}\Bigg((1-K)\frac{x_1-1}{(x_1-1)^2+x_2{}^2}+\int_{-\infty}^{\infty}is\Big(\bar{B}_2e^{|\bar{s}|x_1}\Big)e^{i\bar{s}x_2}d\bar{s}\Bigg),\tag{7.37}$$

$$\sigma_{32}^{(\mathrm{F})}=\frac{\mu_{\mathrm{F}}b}{2\pi a}\Bigg(\frac{x_1-1}{(x_1-1)^2+x_2{}^2}+K\frac{x_1+1}{(x_1+1)^2+x_2{}^2}+\int_{-\infty}^{\infty}is\Big(\bar{A}_1e^{|\bar{s}|x_1}+\bar{B}_1e^{-|\bar{s}|x_1}+2\bar{C}_1e^{\bar{\beta}_1x_1}+2\bar{D}_1e^{-\bar{\beta}_1x_1}\Big)e^{i\bar{s}x_2}d\bar{s}\Bigg),\tag{7.38}$$

$$\sigma_{32}^{(\mathrm{S})}=\frac{\mu_{\mathrm{S}}b}{2\pi a}\Bigg((1-K)\frac{x_1-1}{(x_1-1)^2+x_2{}^2}+\int_{-\infty}^{\infty}is\Big(\bar{B}_2e^{|\bar{s}|x_1}+2\bar{D}_2e^{\bar{\beta}_2x_1}\Big)e^{i\bar{s}x_2}d\bar{s}\Bigg).\tag{7.39}$$

With the use of the foregoing expressions, we may analyze the effects of couple stresses in the case of a screw dislocation inside the film.

7.2 Numerical solutions for the stress field

We evaluate the integral representations (7.32) to (7.39) in order to identify the specific contributions made by the use of couple stress theory. The illustrative results are presented in Figs. 7-2 to 7-4. Note that since the dislocation lies in the film, the stress components, in this case, are normalized in terms of the parameters of the film region. We can observe that the effect of couple stress is significant when the characteristic lengths of the materials are comparable to the dislocation's distance to the film-substrate interface. The dislocation's distance from the free surface, however, seems not to be a factor in the influence of couple stresses on σ_{13} and σ_{23},

meaning that if the characteristic length of the material is comparable to the distance from the free surface, but still small compared to the distance from the interface, the couple stress effect is negligible on σ_{13} and σ_{23}. The effect is significant on σ_{31} and σ_{32}, however, if the size of the characteristic length of material is comparable to the dislocation's distance to the free surface, but still small compared to the dislocation's distance to the interface. This conclusion becomes clearer in the next chapter where we analyze a dislocation in an isolated thin film. Comparing Fig. 7-2(a) with Fig. 7-2(b), which illustrate the stress distribution around the dislocation for the mismatch ratios $\Gamma = N = 0.2$, that is when the film is stiffer than the substrate, we observe a concentration of shear stress σ_{13} accompanied by a change of sign along the interface, for the couple stress materials with $\overline{l}_F = \overline{l}_S = 1$.

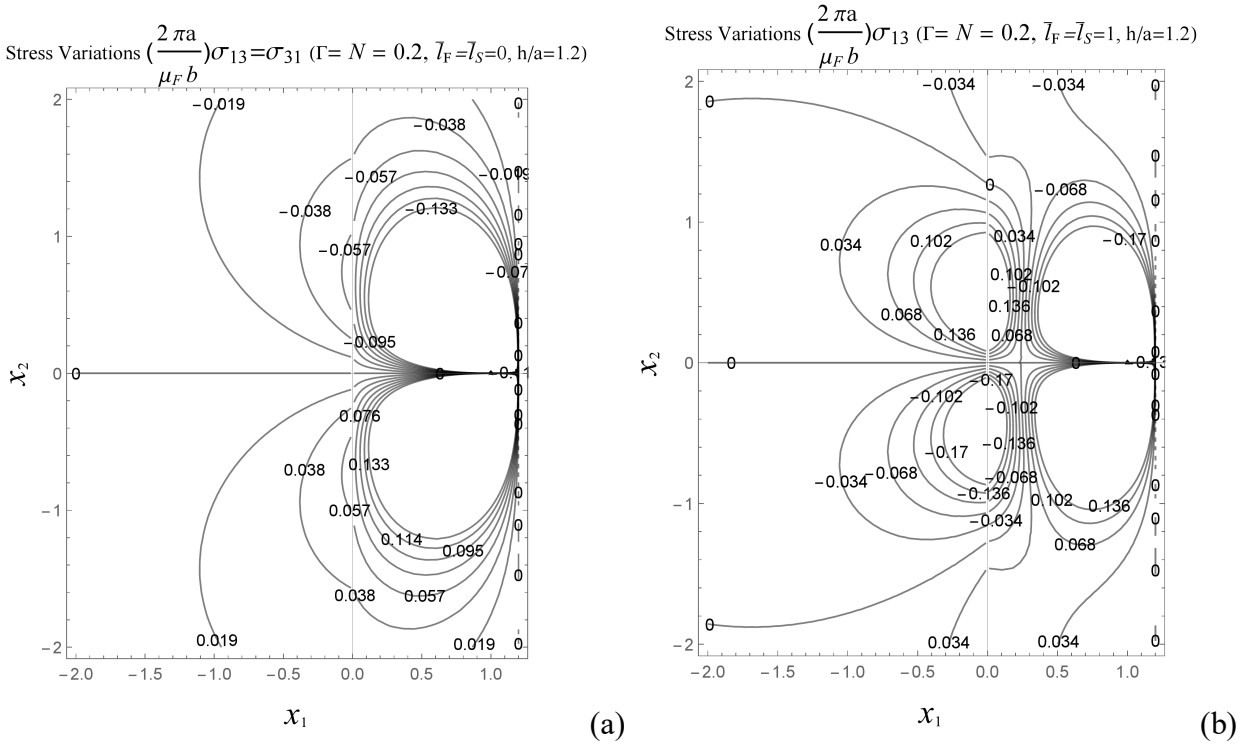

Fig. 7-2- Normalized distribution of stress components σ_{13} and σ_{31} for $\overline{l}_F = \overline{l}_S = 0, 1$, $\overline{h} = 1.2$, $\Gamma = N = 0.2$

From Fig. 7-3 illustrating the stress components σ_{13} and σ_{31} for the case where $\overline{h} = 1.5$, we deduce that, as in the classical case, development of the stress field of a dislocation from a stiffer medium (the film) to a softer medium (the substrate) is limited. However, for the σ_{13} component there still exists a concentration area on the interface. In contrast, for the case of a stiffer

substrate, shown in Fig. 7-4, the dislocation inside the film imposes a greater effect on the substrate medium and specifically for high values of relative characteristic lengths (say $\overline{l}_F = \overline{l}_S = 1$), the stress concentration on the interface becomes higher.

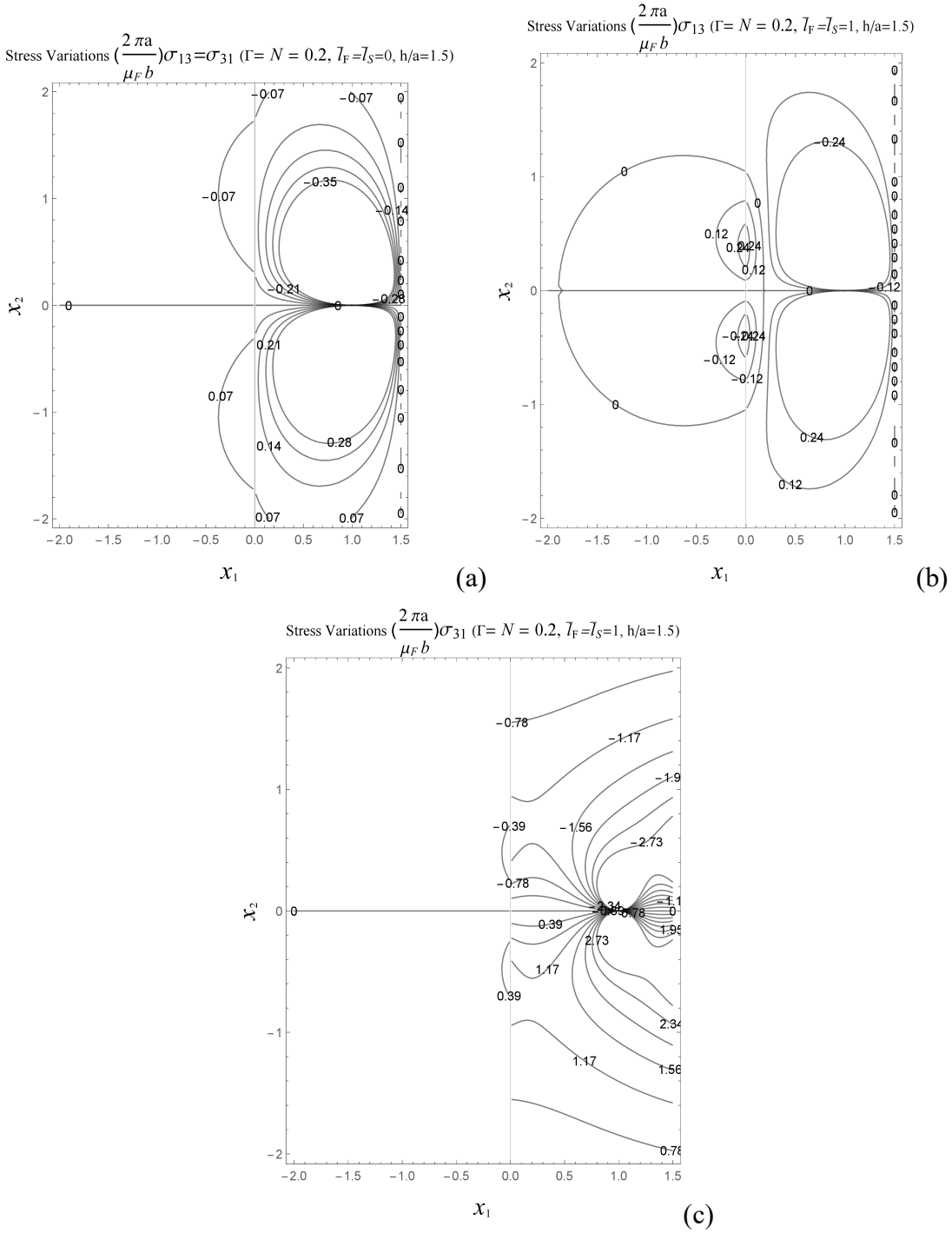

Fig. 7-3- Normalized distribution of stress components σ_{13} and σ_{31} for $\overline{l}_F = \overline{l}_S = 0,1$, $\overline{h} = 1.5$, $\Gamma = N = 0.2$

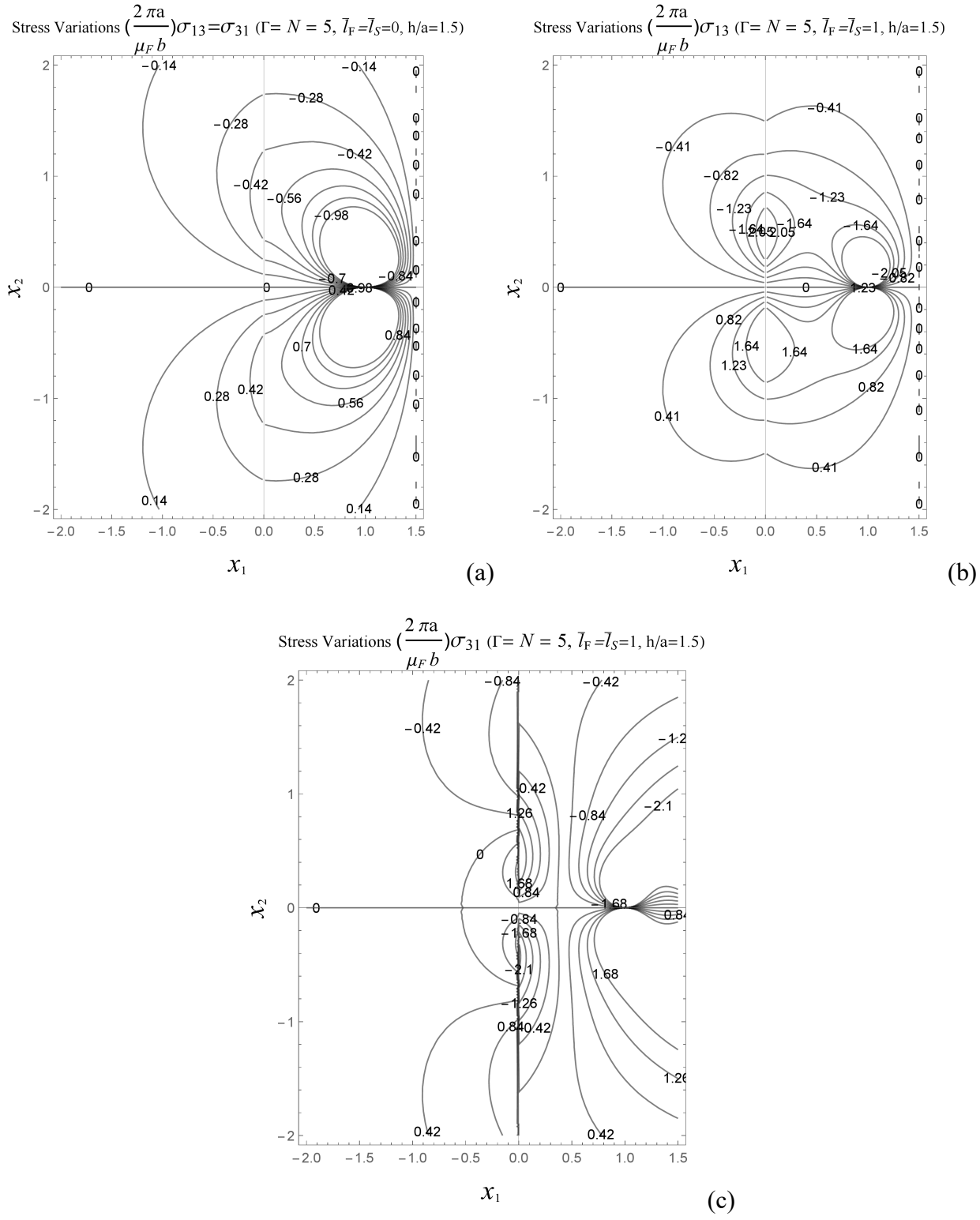

Fig. 7-4- Normalized distribution of stress components σ_{13} and σ_{31} for $\bar{l}_F=\bar{l}_S=0,1$, $\bar{h}=1.5$, $\Gamma=N=5$

7.3 Interaction force on the screw dislocation

Following the procedure introduced in Section 5.5, here we evaluate the force acting on the dislocation inside the thin film. The force on the screw dislocation, in this case, is a combination of the forces induced by the film-substrate interface and the film's free surface. We use the following integral formula to determine the force:

$$\begin{aligned}\frac{F_1}{\left(\frac{\mu_F b^2}{4\pi a}\right)} &= \int_{\bar{S}_2}\left(\frac{1}{2\pi}\left(\bar{u}_{3,1}^{(F)2}+\bar{u}_{3,2}^{(F)2}-2\bar{\sigma}_{13}^{(F)}\bar{u}_{3,1}^{(F)}\right)+\frac{\bar{l}_F^2}{2\pi}\left(\bar{u}_{3,22}^{(F)2}-\bar{u}_{3,11}^{(F)2}\right)\right)dx_2 \\ &+\int_{\bar{S}_1}\left(\frac{1}{\pi}\left(\bar{\sigma}_{23}^{(F)}\bar{u}_{3,1}^{(F)}\right)+\frac{\bar{l}_F^2}{\pi}\left(\bar{u}_{3,22}^{(F)}+\bar{u}_{3,11}^{(F)}\right)\bar{u}_{3,12}^{(F)}\right)dx_1,\end{aligned} \tag{7.40}$$

with the schematic path given in Fig. 7-1 and the parameters defined as

$$\bar{u}_{3,j}^{(F)}=\frac{u_{3,j}^{(F)}}{\left(\frac{b}{2\pi a}\right)},\quad \bar{u}_{3,ij}^{(S)}=\frac{u_{3,ij}^{(F)}}{\left(\frac{b}{2\pi a^2}\right)},\quad \bar{\sigma}_{23}^{(F)}=\frac{\sigma_{23}^{(F)}}{\left(\frac{\mu_F b}{2\pi a}\right)},\quad \bar{\sigma}_{13}^{(F)}=\frac{\sigma_{13}^{(F)}}{\left(\frac{\mu_F b}{2\pi a}\right)}. \tag{7.41}$$

Using the displacement and stress expressions given in (7.30) to (7.39) we determine sampling points for the evaluation of the integral (7.40) over an arbitrary rectangular path which encloses the screw dislocation and lies completely inside the film region. The interaction force on the screw dislocation inside the thin film on a substrate is calculated for a variety of cases. First, consider the variations of normalized force with changes of film thickness. As we see in Fig. 7-5, when the relative thickness increases from $\bar{h}=1$, the force declines from an infinite value and approaches asymptotically to the forces achieved for the case of an infinite plane of a bi-material. In particular, when the thin film is of a softer material than the substrate (say $N=\Gamma=5$), the force declines more slowly for a higher characteristic length of material and approaches a higher positive value, which indicates repulsion from the interface. On the other hand, for $N=\Gamma=0.5$, when the thin film is of a stiffer material, the force declines from an infinite repulsive value to approach a negative value, meaning that the dislocation is attracted to the interface. We observe that in this case, there is a certain thickness at which the dislocation is in the equilibrium state. This equilibrium thickness is smaller for higher characteristic lengths of material. Therefore, the

force analysis of a screw dislocation in couple stress theory predicts a smaller thickness for which the stability of the dislocation inside a thin film is achieved.

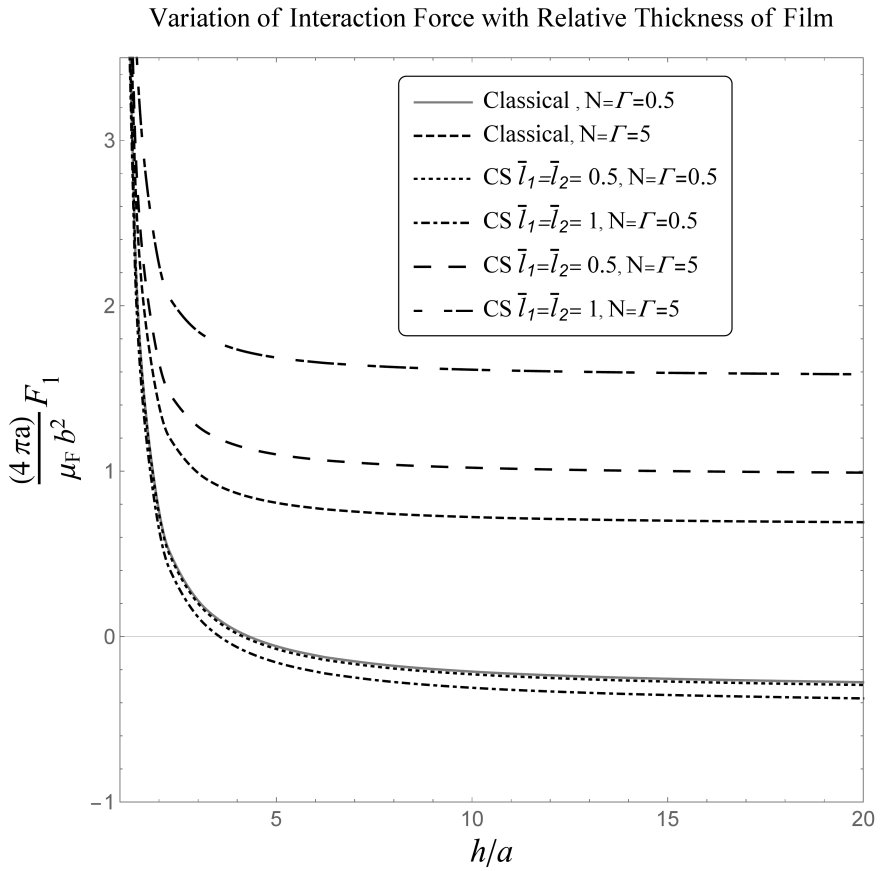

Fig. 7-5- Variations of normalized force with relative thickness of the film.

Additionally, as in Chapter 6 we illustrate the pure effect of mismatch in characteristic lengths of materials in the film and the substrate. Recall that the relation between mismatch ratios and characteristic lengths of the film and the substrate is

$$\bar{l}_S = \sqrt{\frac{N}{\Gamma}}\bar{l}_F. \tag{7.42}$$

Hence, using (7.42) we can determine the characteristic length of the material in the substrate for each given N, by the given characteristic length of the film in Figs. 7-6 and 7-7. We take $\Gamma = 1$ so that the shear moduli of the material regions become uniform and the only influence inducing mismatch parameter will be the different characteristic lengths of the film and the substrate region.

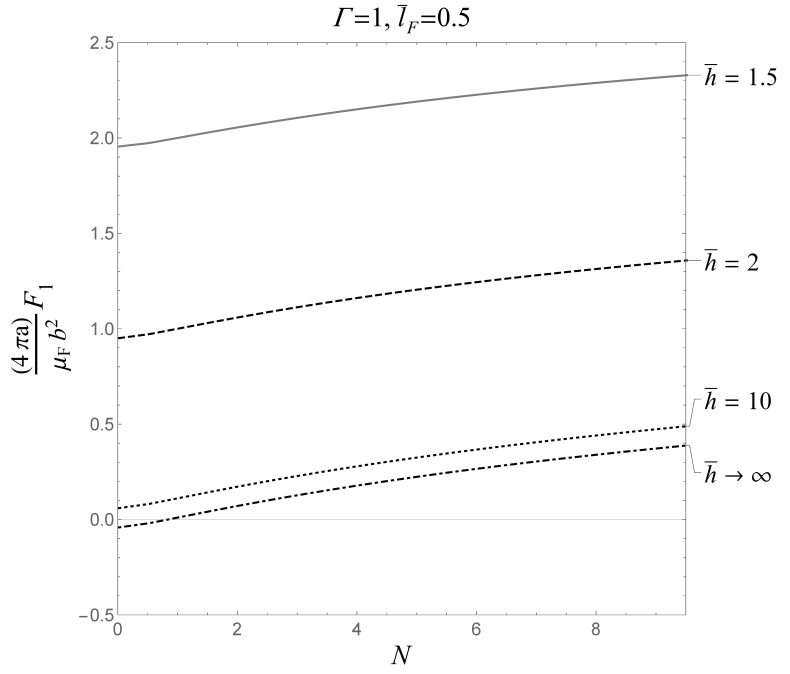

Fig. 7-6- Variation of force with mismatch between characteristic lengths for different thicknesses and $\bar{l}_F = 0.5$

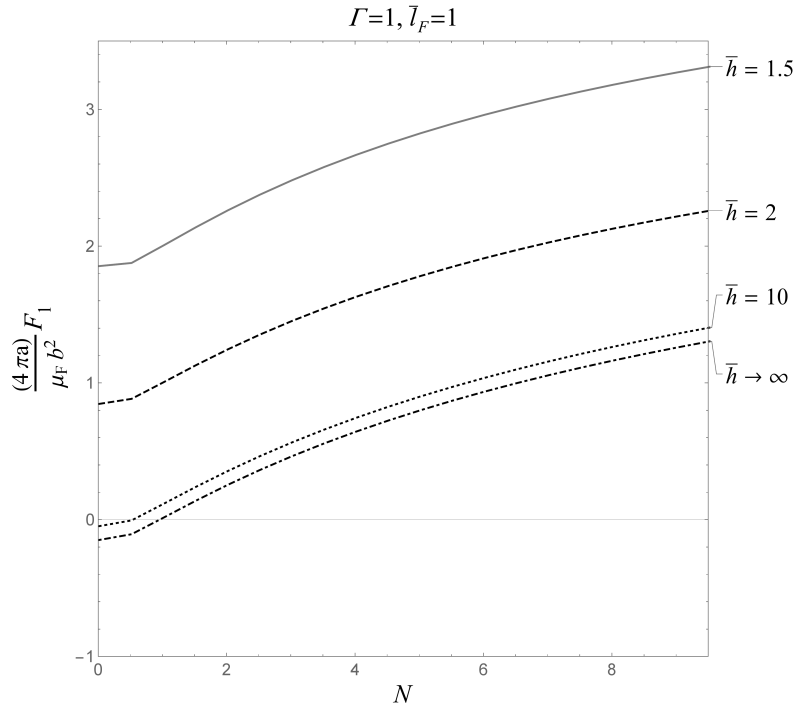

Fig. 7-7- Variation of force with mismatch between characteristic lengths for different thicknesses and $\bar{l}_F = 1$

From Figs. 7-6 and 7-7, we find that in general, the magnitude of the force is greater for the smaller film thickness. This higher force is caused by the presence of the free surface near the

dislocation for a thinner film which makes a substantial contribution to the force in the X_1-direction towards the free surface. In addition, as opposed to the case evaluated in Section 6.3, for both $\bar{l}_F = 0.5$ and $\bar{l}_F = 1$, respectively (shown in Figs. 7-6 and 7-7), the equilibrium of the dislocation is possible only for a very high value of the relative thickness (practically infinite thickness). Also, to confirm the results, notice that the graphs shown for $\bar{h} \to \infty$, representing the infinite bi-material case, coincide with their counterparts in Figs. 6-8 and 6-9.

8 A Screw Dislocation in an Unconfined Film

The problem of a single screw dislocation in an unconfined couple stress film is considered here. So far, we have analyzed geometries in which the dislocation was located in a semi-infinite medium. In the present configuration, however, the dislocation takes place in an infinite film with parallel planar free surfaces. We use the same approach to solve the problem of an isolated film containing a screw dislocation. As shown in Fig. 8-1, the screw dislocation is located at a distance a from the left-side free surface in a strip of a thickness h ($h > a$). This time, we place the origin of the Cartesian coordinates at the dislocation so that the X_3-axis coincides with the dislocation line. The infinitely extended film is filled with a linear elastic couple stress material with elastic properties described by μ_F and γ_F.

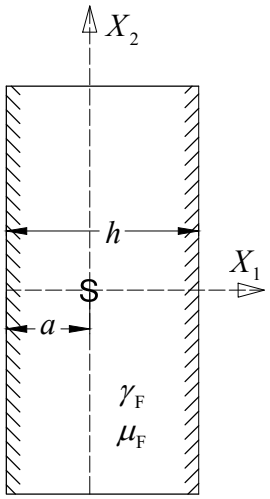

Fig. 8-2- Configuration of the problem of a screw dislocation in an unconfined film

We know that the equation,

$$\nabla^2(1-l_{\mathsf{F}}^2\nabla^2)u_3 = 0, \quad -a \le X_1 \le (h-a), \tag{8.1}$$

governs the anti-plane displacement component u_3. In addition, we separate the displacement field induced by the dislocation in an infinite medium and express the effect of couple stresses and the existence of traction free surfaces to a perturbation term. Formally,

$$u_3^{(\mathsf{F})} = \frac{b}{2\pi}\tan^{-1}\left(\frac{X_2}{X_1}\right) + \hat{u}_3^{(\mathsf{F})}. \tag{8.2},$$

Substituting (8.2) into (8.1) we find,

$$\nabla^2(1-l_{\mathsf{F}}^2\nabla^2)\hat{u}_3 = 0, \quad -a \le X_1 \le (h-a), \tag{8.3}$$

where $l_{\mathsf{F}}^2 = \gamma_{\mathsf{F}} / (2\mu_{\mathsf{F}})$. In this case, the boundary conditions for the two planar free surfaces can be written as

$$\begin{aligned} &\mu_{12}^{(\mathsf{F})}(-a, X_2) = 0, \quad \sigma_{13}^{(\mathsf{F})}(-a, X_2) = 0, \\ &\mu_{12}^{(\mathsf{F})}(h-a, X_2) = 0, \quad \sigma_{13}^{(\mathsf{F})}(h-a, X_2) = 0. \end{aligned} \tag{8.4}$$

Again, we use the Fourier integral transform expressed in (5.25) to convert (8.3) to

$$\left(\frac{\partial^2}{\partial X_1^{\,2}} - s^2\right)\left(\frac{1}{l_{\mathsf{F}}^2} + s^2 - \frac{\partial^2}{\partial X_1^{\,2}}\right)\tilde{U}_3^{(\mathsf{F})}(X_1, s) = 0, \tag{8.5}$$

whose solution can be expressed as

$$\begin{aligned} &\tilde{U}_3^{(\mathsf{F})}(X_1, s) = A(s)e^{-|s|X_1} + B(s)e^{|s|X_1} + C(s)e^{-\beta(s)X_1} + D(s)e^{\beta(s)X_1}, \\ &for \quad -a \le X_1 < h-a, \end{aligned} \tag{8.6}$$

where,

$$\beta = \beta(s) = \sqrt{\frac{1}{l_{\mathsf{F}}^2} + s^2} \tag{8.7}$$

The transformed expressions for the boundary conditions (8.4) are

$$-|s|A(s)e^{a|s|} + |s|B(s)e^{-a|s|} = -\frac{b}{2\sqrt{2\pi}}\left(i\,\mathrm{sgn}(s)e^{-a|s|}\right), \tag{8.8}$$

$$-|s|A(s)e^{-(h-a)|s|}+|s|B(s)e^{(h-a)|s|}=-\frac{b}{2\sqrt{2\pi}}\left(i\,\mathrm{sgn}(s)e^{-(h-a)|s|}\right), \tag{8.9}$$

$$s^2A(s)e^{a|s|}+s^2B(s)e^{-a|s|}+\beta^2C(s)e^{a\beta}+\beta^2D(s)e^{-a\beta}=-\frac{b}{2\sqrt{2\pi}}\left(ise^{-a|s|}\right), \tag{8.10}$$

$$\begin{aligned}s^2A(s)e^{-(h-a)|s|}+s^2B(s)e^{(h-a)|s|}+\beta^2C(s)e^{-(h-a)\beta}+\beta^2D(s)e^{(h-a)\beta}\\ =\frac{b}{2\sqrt{2\pi}}\left(ise^{-(h-a)|s|}\right),\end{aligned} \tag{8.11}$$

The system of algebraic equations (8.8) to (8.11) must be solved for $A(s)$, $B(s)$, $C(s)$ and $D(s)$. In the meantime, to obtain the solution in its normalized form, we adopt the following parameters:

$$\bar{l}_{\mathrm{F}}=\frac{l_{\mathrm{F}}}{a},\quad \bar{h}=\frac{h}{a},\quad \bar{s}=as,\quad \bar{\beta}=a\beta\Rightarrow\bar{\beta}=\sqrt{\bar{s}^2+\frac{1}{\bar{l}_{\mathrm{F}}^2}}, \tag{8.12}$$

and also

$$\begin{aligned}\bar{A}&=\frac{a\sqrt{2\pi}}{b}A=\frac{A^*}{D_1},\quad \bar{B}=\frac{a\sqrt{2\pi}}{b}B=\frac{B^*}{D_1},\\ \bar{C}&=\frac{a\sqrt{2\pi}}{b}C=\frac{C^*}{D_2},\quad \bar{D}=\frac{a\sqrt{2\pi}}{b}D=\frac{D^*}{D_2}.\end{aligned} \tag{8.13}$$

Therefore, by solving the four equations for the four unknowns we obtain

$$D_1=2|\bar{s}|\left(e^{2\bar{h}|\bar{s}|}-1\right), \tag{8.14}$$

$$D_2=2|\bar{s}|\bar{\beta}^2\left(e^{2\bar{h}\bar{\beta}}-1\right)\left(e^{2\bar{h}|\bar{s}|}-1\right), \tag{8.15}$$

$$A^*=i\,\mathrm{sgn}(\bar{s})\left(e^{2(\bar{h}-1)|\bar{s}|}-1\right), \tag{8.16}$$

$$B^*=-i\,\mathrm{sgn}(\bar{s})\left(e^{2|\bar{s}|}-1\right), \tag{8.17}$$

$$C^* = -i\bar{s}e^{(\bar{h}-1)\bar{\beta}-2|\bar{s}|}\Big[\,|\bar{s}|\Big(e^{2\bar{h}|\bar{s}|}-1\Big)\Big(e^{-(\bar{h}-3)|\bar{s}|}+e^{\bar{h}\bar{\beta}+|\bar{s}|}\Big) + \bar{s}\,\mathrm{sgn}(\bar{s})\Big(e^{-(\bar{h}-3)|\bar{s}|}-2e^{(1+\bar{h})|\bar{s}|}+e^{(\bar{h}+3)|\bar{s}|}+e^{\bar{h}\bar{\beta}+|\bar{s}|}-2e^{\bar{h}\bar{\beta}+3|\bar{s}|}+e^{\bar{h}\bar{\beta}+(2\bar{h}+1)|\bar{s}|}\Big)\Big], \tag{8.18}$$

$$D^* = i\bar{s}e^{\bar{\beta}-(\bar{h}+1)|\bar{s}|}\Big[\,|\bar{s}|\Big(e^{2\bar{h}|\bar{s}|}-1\Big)\Big(e^{\bar{h}|\bar{s}|}+e^{\bar{h}\bar{\beta}+2|\bar{s}|}\Big) + \bar{s}\,\mathrm{sgn}(\bar{s})\Big(e^{\bar{h}|\bar{s}|}+e^{3\bar{h}|\bar{s}|}-2e^{(2+\bar{h})|\bar{s}|}-2\,e^{\bar{h}(\bar{\beta}+2|\bar{s}|)}+e^{\bar{h}\bar{\beta}+2|\bar{s}|}+e^{\bar{h}\bar{\beta}+2(\bar{h}+1)|\bar{s}|}\Big)\Big]. \tag{8.19}$$

Then, with reference to (8.12) - (8.19), the non-vanishing component of the displacement field becomes

$$u_3^{(\mathsf{F})} = \frac{b}{2\pi}\Bigg(\tan^{-1}\Big(\frac{x_2}{x_1}\Big) + \int_{-\infty}^{\infty}\Big(\bar{A}(\bar{s})e^{-|\bar{s}|x_1}+\bar{B}(\bar{s})e^{|\bar{s}|x_1}+\bar{C}(\bar{s})e^{-\bar{\beta}(\bar{s})x_1}+\bar{D}(\bar{s})e^{\bar{\beta}(\bar{s})x_1}\Big)e^{i\bar{s}x_2}\,d\bar{s}\Bigg). \tag{8.20}$$

Other aspects of the solution such as stress and couple stress field can be now determined through (5.11) and (5.12). For example, the stress components in integral form become

$$\sigma_{13} = \Big(\frac{\mu_{\mathsf{F}}b}{2\pi a}\Big)\Bigg[\Big(\frac{-x_2}{x_1^2+x_2^2}\Big)+\int_{-\infty}^{\infty}\Big(-|\bar{s}|\,\bar{A}(\bar{s})e^{-|\bar{s}|x_1}+|\bar{s}|\,\bar{B}(\bar{s})e^{|\bar{s}|x_1}\Big)e^{i\bar{s}x_1}\,d\bar{s}\Bigg], \tag{8.21}$$

$$\sigma_{31} = \Big(\frac{\mu_{\mathsf{F}}b}{2\pi a}\Big)\Bigg[\Big(\frac{-x_2}{x_1^2+x_2^2}\Big) + \int_{-\infty}^{\infty}\Big(-|\bar{s}|\,\bar{A}(\bar{s})e^{-|\bar{s}|x_1}+|\bar{s}|\,\bar{B}(\bar{s})e^{|\bar{s}|x_1}-2\bar{\beta}(\bar{s})\bar{C}(\bar{s})e^{-\bar{\beta}(\bar{s})x_1}+2\bar{\beta}(\bar{s})\bar{D}(\bar{s})e^{\bar{\beta}(\bar{s})x_1}\Big)e^{i\bar{s}x_1}\,d\bar{s}\Bigg], \tag{8.22}$$

$$\sigma_{23} = \Big(\frac{\mu_{\mathsf{F}}b}{2\pi a}\Big)\Bigg[\Big(\frac{x_1}{x_1^2+x_2^2}\Big)+\int_{-\infty}^{\infty}i\bar{s}\Big(\bar{A}(\bar{s})e^{-|\bar{s}|x_1}+\bar{B}(\bar{s})e^{|\bar{s}|x_1}\Big)e^{i\bar{s}x_1}\,d\bar{s}\Bigg], \tag{8.23}$$

$$\sigma_{32} = \Big(\frac{\mu_{\mathsf{F}}b}{2\pi a}\Big)\Bigg[\Big(\frac{x_1}{x_1^2+x_2^2}\Big) + \int_{-\infty}^{\infty}i\bar{s}\Big(\bar{A}(\bar{s})e^{-|\bar{s}|x_1}+\bar{B}(\bar{s})e^{|\bar{s}|x_1}+2\bar{C}(\bar{s})e^{-\bar{\beta}(\bar{s})x_1}+2\bar{D}(\bar{s})e^{\bar{\beta}(\bar{s})x_1}\Big)e^{i\bar{s}x_1}\,d\bar{s}\Bigg]. \tag{8.24}$$

Notice that the coefficients $\overline{A}$ and $\overline{B}$, are independent of the characteristic length $\overline{l}_{\mathrm{F}}$, hence the stress components σ_{13} and σ_{23} are independent of $\overline{l}_{\mathrm{F}}$ and equal to their counterparts in classical elasticity. Therefore, only the stress components acting on the surfaces perpendicular to the X_3-axis are affected by the incorporation of couple stress theory. The same conclusion was reached in Section 5.3 for a screw dislocation near a free planar surface. Additionally, the integral terms in (8.21) and (8.23) can be evaluated analytically. Then, we can express the stress components σ_{13} and σ_{23} as

$$\sigma_{13}=\left(\frac{\mu_{\mathrm{F}}b}{2\pi a}\right)\left[\frac{i\pi}{4\overline{h}}\left(\cot\left(\frac{\pi(x_1-ix_2)}{2h}\right)-\cot\left(\frac{\pi(x_1+ix_2)}{2h}\right)\right.\right.$$
$$\left.\left.-\cot\left(\frac{\pi(2+x_1-ix_2)}{2h}\right)+\cot\left(\frac{\pi(2+x_1+ix_2)}{2h}\right)\right)\right], \tag{8.25}$$

$$\sigma_{23}=\left(\frac{\mu_{\mathrm{F}}b}{2\pi a}\right)\left[\frac{\pi}{4\overline{h}}\left(\cot\left(\frac{\pi(x_1-ix_2)}{2h}\right)+\cot\left(\frac{\pi(x_1+ix_2)}{2h}\right)\right.\right.$$
$$\left.\left.-\cot\left(\frac{\pi(2+x_1-ix_2)}{2h}\right)-\cot\left(\frac{\pi(2+x_1+ix_2)}{2h}\right)\right)\right]. \tag{8.26}$$

The foregoing expressions are equivalent to the results reported in Leibfried and Dietze [6] (and restated in Chu [91]) using classical elasticity theory. The stress components σ_{31} and σ_{32}, however, deviate from their classical counterparts as the relative characteristic length of material $\overline{l}_{\mathrm{F}}$ increases. These components are evaluated numerically and shown in Figs. 8-3 and 8-4. From these figures, we can see the change of stress distribution with respect to high relative characteristic lengths.

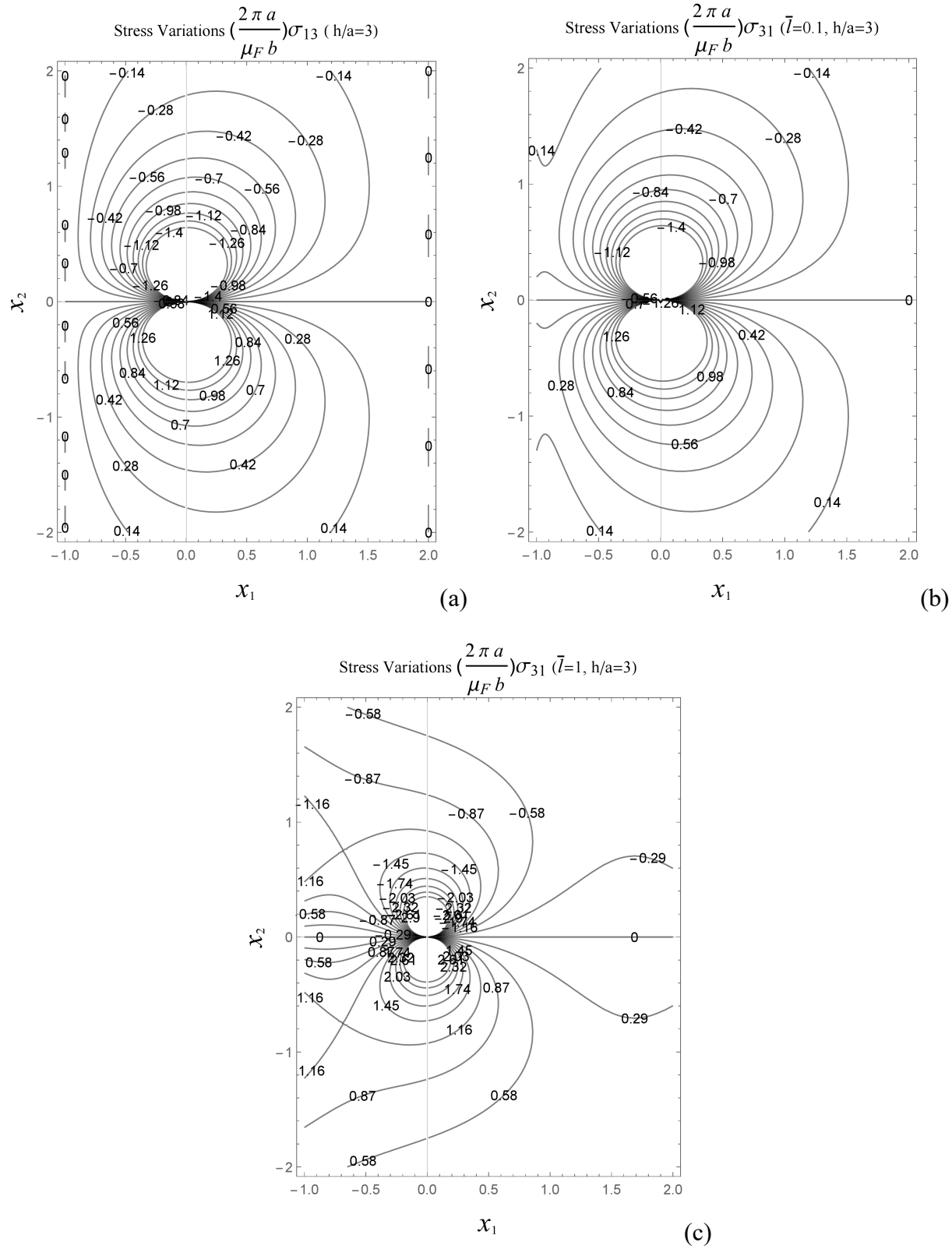

Fig. 8-3-Normalaized distribution of σ_{31} for length of materials $\overline{l_F} = 0.1$ and $\overline{l_F} = 1$.

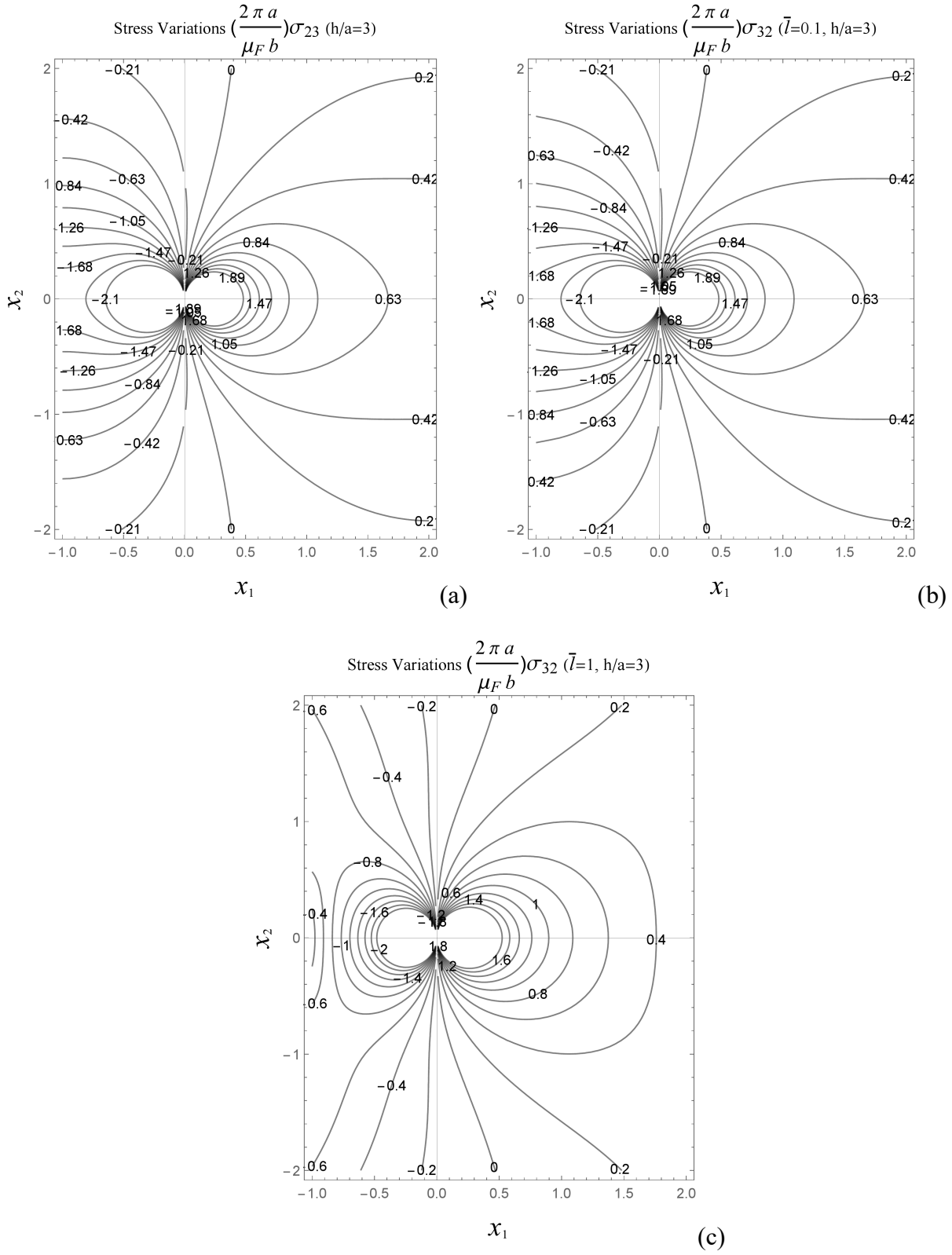

Fig. 8-4-Normalized distribution of σ_{32} for length of materials $\bar{l}_F = 0.1$ and $\bar{l}_F = 1$.

8.1 Force on a screw dislocation in an unconfined film

As in Sections 5.5 and 6.3 after choosing an arbitrary enclosing rectangular path, we use the following J-integral formulation to calculate the force:

$$\frac{F_1}{\left(\frac{\mu_F b^2}{4\pi a}\right)} = \int_{\bar{S}_2}\left(\frac{1}{2\pi}\left(\bar{u}_{3,1}^2+\bar{u}_{3,2}^{\ 2}-2\bar{\sigma}_{13}\bar{u}_{3,1}\right)+\frac{\bar{l}_F^2}{2\pi}\left(\bar{u}_{3,22}^{\ 2}-\bar{u}_{3,11}^{\ 2}\right)\right)dx_2 + \int_{\bar{S}_1}\left(\frac{1}{\pi}\left(\bar{\sigma}_{23}\bar{u}_{3,1}\right)+\frac{\bar{l}_F^2}{\pi}\left(\bar{u}_{3,22}+\bar{u}_{3,11}\right)\bar{u}_{3,12}\right)dx_1, \tag{8.27}$$

where again, $\bar{S}_1$ and $\bar{S}_2$ are the sums of the segments in the x_1 and x_2-directions, and $\bar{u}_3$, $\bar{\sigma}_{13}$ and $\bar{\sigma}_{23}$ are evaluated using (8.20), (8.21), (8.23) in the following forms:

$$\bar{u}_{3,j}^{(F)}=\frac{u_{3,j}^{(F)}}{\left(\frac{b}{2\pi a}\right)},\quad \bar{u}_{3,ij}^{(F)}=\frac{u_{3,ij}^{(F)}}{\left(\frac{b}{2\pi a^2}\right)},\quad \bar{\sigma}_{23}^{(F)}=\frac{\sigma_{23}^{(F)}}{\left(\frac{\mu_F b}{2\pi a}\right)},\quad \bar{\sigma}_{13}^{(F)}=\frac{\sigma_{23}^{(F)}}{\left(\frac{\mu_F b}{2\pi a}\right)}. \tag{8.28}$$

We use the foregoing information to obtain sampling points for evaluating the integral (8.27), numerically. Consequently, the variations of normalized force with h/a are illustrated in Fig. 8-5.

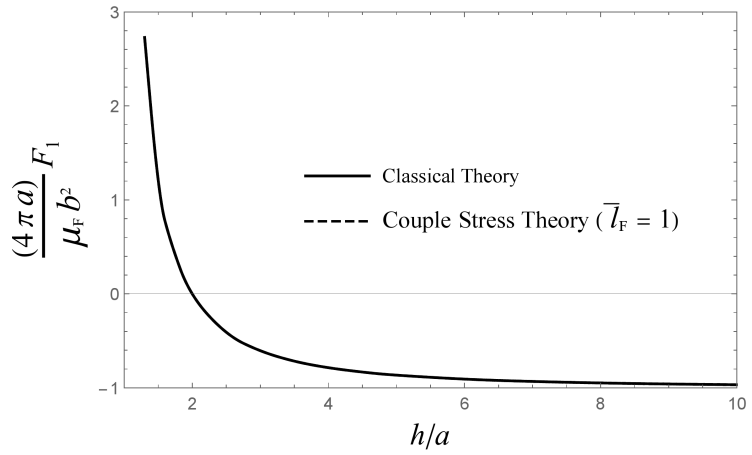

Fig. 8-5-Variations of force with thickness and the location of the dislocation (comparison between classical and couple stress elasticity).

As shown in Fig. 8-5 (which represents evaluated forces), we discover from the numerical analysis that the force is independent of the characteristic length of material and therefore coincides with the classical solution. This statement is consistent with the results obtained for a dislocation near a semi-infinite medium surface treated in Section 5.3, since that case is a special case of an unconfined film as $h/a \to \infty$. Also, as we expect from section 5.3, the normalized force approaches the value -1 as the configuration approaches a semi-infinite medium.

9 Conclusions

Our analysis leads us to the following conclusions regarding the incorporation of couple stress theory in the model of dislocation-interface interaction problem.

- In general, the use of couple stress elasticity as the governing theory to solve the problem of a screw dislocation near interfaces and surfaces leads to intensified responses from the corresponding elastic media. The stress fields and the forces on the dislocation are, in general, of higher magnitudes in couple stress theory. This fact is not surprising since we are practically introducing an extra elastic stiffness namely bending-twisting modulus.
- Almost in every case studied, we encounter a stress concentration on the interface as the characteristic lengths of the materials grow higher and increase the couple stress effects. Additionally, couple stresses create extra discontinuities of the stress field at the interfaces. In fact, when we begin to increase the characteristic length of material from a small amount to acquire couple stress effects, the deviations from classical theory start from interfaces by a small discontinuity and a small stress concentration there. Then, as we continue to increase the couple stress effects, the deviation grows to a global disturbance or even change of signs in the stress field around the dislocation and the interfaces or surfaces.
- Evidently, the tangible changes from the classical model appear when the relative characteristic lengths increase to the values around $0.2 \sim 0.3$ and the changes continue to rise dramatically with increasing characteristic lengths. Therefore, for the use of couple stress theory to be meaningful we must consider the characteristic length of the material relative to the distance of the dislocation from interfaces or surfaces. Below the indicated

values of characteristic length, the size effects on the stress field are negligible except for a narrow region along the interfaces or surfaces (width of the order of the characteristic length).

- In the case of a screw dislocation near a bi-material interface, the interaction force (either attractive or repulsive) is intensified with the increase in the characteristic length of material. The range of change of force with the characteristic length of material is broader when the medium containing the dislocation is made of a softer material and the shear modulus of the dislocation-free medium can approach infinity. This intensified force also explains the higher required loads for the movement of dislocations producing plastic deformation in small scale problems. Hence, it justifies our need to take into account the size dependency in plasticity as well. Therefore, this result is consistent with the fact that on a small scale, the plastic strength of a material is higher.
- We studied the interaction force on a screw dislocation in a substrate near a thin film. In this case, we reach the conclusion that for a certain interaction force to emerge, a smaller thickness of the film is required. Specifically, the couple stress theory predicts a lower thickness of a stiffer thin film to create the state of equilibrium for the dislocation. These results are the consequences of higher intensity of the interaction force in couple stress theory. We also studied the mismatch generated by the difference in couple stress factors only. We showed that the adjoining materials with the same classical elastic moduli but different characteristic lengths induce forces on the nearby dislocations. When this mismatch ratio is zero it means that the film on the substrate is made of a classical material and in this case the force tends to move the dislocation towards the thin film. However, when we increase this mismatch ratio the force reduces to zero. This state of equilibrium occurs at higher mismatch ratios for thinner films. For larger mismatch ratios, the force repels the dislocation from the thin film
- We also studied the interaction force on a dislocation inside a thin film adjoining a substrate. In this case, the use of couple stress theory exacerbates the state of instability of the dislocation by intensifying the force. As for the classical case, the stability of the dislocation is only possible for a certain thickness when the film is stiffer than the substrate. Because of the intensified force, the required thickness for achieving a specific force or stability (zero force) is lower than that for the corresponding classical solutions.

Furthermore, in this case, as well, we studied the mismatch generated only by the difference in couple stress parameters. As a result of the presence of the planar free surface near the dislocation, in this case, the force generated by this kind of mismatch is almost always repulsive from the interface. Only when the thickness is very high (practically an infinite bi-material) the stability of the dislocation is possible. This fact also shows that the mismatch between the lengths of materials (or in other words, bending-twisting modulus) is of secondary importance in causing the force compared to the mismatch between classical elastic moduli (shear moduli) of the materials.

- We have also demonstrated the effects of couple stresses on a half-plane and an unconfined thin film containing a screw dislocation. According to our results, the couple stresses do not change the stress field components on the planes parallel to the dislocation line. On the other planes, however, the stress components start to change from the free surfaces as the characteristic length rises from zero.
- Finally, we conclude from the incorporation of couple stress theory that the force acting on a screw dislocation in a half-plane or an unconfined film remains the same as in the classical theory. In other words, no contribution is made to the force from couple stress effects.

9.1 Future research

- It seems possible to solve the problem in the couple stress theory under different conditions. For instance, we can choose e to be independent instead of equating it to γ. Also, we can deal with the same problem by other non-local or even micropolar theory. In all those cases, we may be encumbered by the mathematical complexities which can be treated only through numerical analyses.
- In the future, we can expand the current problem to the case of imperfect interfaces. The viscoelastic imperfection of the interfaces is one of the attractive subjects that we may combine with the current problem and solve it in couple stress theory.
- It may not be as straightforward as the anti-plane problem presented here, however, we may consider the possibility of solving an edge dislocation problem with the same assumptions made in couple stress theory.

- In the future, we may also expand the problem to the problem of multiple screw dislocations interacting with surfaces or interfaces in couple stress theory.

References

[1] Ewing, J. A., Rosenhain, W., "Bakerian lecture: The crystalline structure of metals," *Philosophical Transactions of the Royal Society A*, vol. 193, pp. 353-375, January 1900.

[2] Volterrra, V., "Sur l'équilibre des corps élastiques multiplement connexes," *Annales scientifiques de l'École Normale Supérieure*, vol. 24, pp. 401-517, 1907.

[3] Love, A. E. H., *A Treatise on the Mathematical Theory of Elasticity*.: Cambridge: At the University Press, 1927.

[4] Taylor, G. I., "The mechanism of plastic deformation of crystals," *Proceedings of the Royal Society of London A*, vol. 145, no. 855, pp. 362-387, July 1934.

[5] Lubliner, J., *Plasticity Theory*.: Dover Publication, 2008.

[6] Leibfried, G. Dietze, H. Z., "Zur theorie der schraubenversetzung," *Zeitschrift für Physik*, vol. 126, no. 10, pp. 790–808., 1949.

[7] Peierls, R., "The size of a dislocation," *Proceedings of the Physical Society B*, vol. 52, no. 1, pp. 34-37, 1940.

[8] Nabarro, F. R. N., "Dislocations in a simple cubic lattice," *Proceedings of the Physical Society*, vol. 59, no. 2, pp. 256-272, 1947.

[9] Read, W. T., *Dislocations in Crystals*. New York: McGrow-Hill, 1953.

[10] Head, A. K., "The interaction of dislocations with boundaries and surface films," *Australian Journal of Physics*, vol. 13, p. 278, 1960.

[11] Head, A. K., "Edge dislocations in inhomogeneous media," *Proceedings of the Physical Society B*, vol. 66, no. 9, pp. 793-801, 1953.

[12] Head, A. K., "The interaction of dislocations and boundaries," *The London, Edinburgh, and Dublin Philosophical Magazine and Journal of Science*, vol. 44, no. 348, pp. 92-94, 1953.

[13] Smith, E., "The interaction between dislocations and inhomogeneities-I," *International Journal of Engineering Science*, vol. 6, no. 3, pp. 129-143, June 1968.

[14] Smith, E., "The interaction between dislocations and inhomogeneities-II: A screw dislocation pile-up in an infinite body containing an elliptically cylindrical rigid inhomogeneity," *International Journal of Engineering Science*, vol. 6, no. 3, pp. 145-152, June 1968.

[15] Dundurs, J., "Elastic interaction of dislocations with inhomogeneities," *In: Mathematical Theory of Dislocations*, pp. 70-115, 1969.

[16] Kröner, E., "On the physical reality of torque stresses in continuum mechanics," *International Journal of Engineering Science*, vol. 1, pp. 261-278, 1963.

[17] Kaloni, P. N., Ariman, T., "Stress concentration effects in micropolar elasticity," *Journal of Applied Mathematics and Physics*, vol. 18, no. 1, pp. 136-141, January 1967.

[18] Mindlin, R. D., "Influence of couple-stresses on stress concentrations," *Experimental Mechanics*, vol. 3, pp. 573–579, 1963.

[19] Schijve, J., "Note on couple stresses," *Journal of the Mechanics and Physics of Solids*, vol. 14, no. 2, pp. 113-120, March 1966.

[20] Cowin, S. C., "An incorrect inequality in micropolar elasticity," *Journal of Applied Mathematics and Physics*, vol. 21, no. 3, pp. 494–497, May 1970.

[21] Cosserat, E., Cosserat, F., *Théorie de Corps Déformables*. Paris, 1909.

[22] Eringen, A. C., "Linear Theory of Micropolar Elasticity," Office of Naval Research, Lafayette, Indiana, Technical Report 29, 1965.

[23] Eringen, A. C., "Theory of Micropolar Elasticity," Office of Naval Research, Princton, Technical Report 1, 1967.

[24] Eringen, A. C., Suhubi, E. S., "Nonlinear theory of simple microelastic solids," *International Journal of Engineering Science*, vol. 2, pp. 189-203, 1964.

[25] Nowacki, W., Olszak, W., "Micropolar Elasticity," International Centre for Mechanical Sciences, Courses and Lectures 151, 1974.

[26] Toupin, R. A., "Elastic materials with couple-stresses," *Archive for Rational Mechanics and Analysis*, vol. 11, no. 1, pp. 385-414, January 1962.

[27] Mindlin, R. D., "Micro-structure in linear elasticity," *Archive for Rational Mechanics and Analysis*, vol. 16, no. 1, pp. 51-78, January 1964.

[28] Mindlin, R. D., Eshel, N. N., "On first strain gradient theories in linear elasticity," *International Journal of Solids and Structures*, vol. 4, pp. 109-124, 1968.

[29] Eringen, A. C., Edelen, D. G. B., "On nonlocal elasticity," *International Journal of Engineering Science*, vol. 10, no. 3, pp. 233-248, March 1972.

[30] Tiffen, R., Stevenson, A. C., "Elastic isotropy with body force and couple," *Quarterly Journal of Mechanics and Applied Mathematics*, vol. 9, p. 306, 1956.

[31] Truesdell, C., Toupin, R., *The Classical Field Theories*. Berlin Heidelberg: Springer, 1960.

[32] Grioli, G., "Elasticità asimmetrica," *Annali di Matematica Pura ed Applicata*, vol. 50, pp. 389-417, 1960.

[33] Koiter, W. T., "Couple-stresses in the theory of elasticity: I and II," *Proceedings of the Koninklijke Nederlandse Akademie van Wetenschappen, Series B*, vol. 67, no. 1, pp. 17-44,

1964.

[34] Toupin, R., "Theories of elasticity with couple-stress," *Archive for Rational Mechanics and Analysis*, vol. 17, no. 2, pp. 85-112, 1964.

[35] Mindlin, R. D., Tiersten, H. F., "Effects of couple-stresses in linear elasticity," *Archive for Rational Mechanics and Analysis*, vol. 11, no. 1, pp. 415-448, 1962.

[36] Fleck, N. A., Muller, M. G., Ashby, M. F., Hutchinson, J. W., "Strain gradient placticity: theory and experiment," *Acta Metallurgica et Materialia*, vol. 42, no. 2, pp. 475-487, February 1994.

[37] Joshi, R. B., Bayoumi, A. E., Zbib, H. M., "Evaluation of macroscopic shear banding using a digital image processing technique," *Scripta Metallurgica et Materialia*, vol. 24, no. 9, pp. 1747-1752, September 1990.

[38] Zbib, H. M., Aifantis, E. C., "On the gradient-dependent theory of plasticity and shear banding ," *Acta Mechanica*, vol. 92, pp. 209-225, March 1992.

[39] Ma, Q., Clarke, D. R., "Size dependent hardness of silver single crystals," *Journal of Materials Research*, vol. 10, no. 4, pp. 853-863, April 1995.

[40] Nix, W. D., "Mechanical properties of thin films," *Metallurgical Transactions A*, vol. 20, pp. 2217-2245, November 1989.

[41] Stelmashenko, N. A., Walls, M. G., Brown, L. M., Milman, Y. V., "Microindentations on W and Mo oriented single crystals: an STM study," *Acta Metallurgica et Materialia*, vol. 41, no. 10, pp. 2855-2865, October 1993.

[42] Drugan, W. J., Willis, J. R., "A micromechanics-based nonlocal constitutive equation and estimates of representative volume element size for elastic composites," *Journal of the Mechanics and Physics of Solids*, vol. 44, no. 4, pp. 497-524, April 1996.

[43] Fleck, N. A., Hutchinson, J. W., "A phenomenological theory for strain gradient effects in plasticity," *Journal of the Mechanics and Physics of Solids*, vol. 41, no. 12, pp. 1825-1857,

1993.

[44] Fleck, N. A., Hutchinson, J. W., "Strain gradient plasticity," *Advances in Applied Mechanics*, vol. 33, pp. 295–361, 1997.

[45] Kenway, P. R., "Calculated structures and energies of grain boundaries in a-Al2O3," *Journal of the American Ceramic Society*, vol. 77, no. 2, pp. 349–355, February 1994.

[46] Watson, G. W., Kelsey, E. T., De Leeuw, N. H., Harris, D. J., Parker, S. C., "Atomistic simulation of dislocations, surfaces and interfaces in MgO," *Journal of the Chemical Society, Faraday Transactions*, vol. 92, pp. 433-438, 1996.

[47] Devincre, B., Kubin, L. P., "Mesoscopic simulations of dislocations and plasticity," *Materials Science and Engineering: A*, vol. 234–236, pp. 8-14, August 1997.

[48] Verdier, M., Fivel, M., Groma, I., "Mesoscopic scale simulation of dislocation dynamics in fcc metals: principles and applications," *Modelling and Simulation in Materials Science and Engineering*, vol. 6, pp. 755-770, 1998.

[49] Blanckenhagen, B., Arzt, E., Gumbsch, P., "Discrete dislocation simulation of plastic deformation in metal thin films," *Acta Materialia*, vol. 52, no. 3, pp. 773–784, February 2004.

[50] Espinosa, H. D., Panico, M., Berbenna, S., Schwarz, K. W., "Discrete dislocation dynamics simulations to interpret plasticity size and surface effects in freestanding FCC thin films," *International Journal of Plasticity*, vol. 22, no. 11, pp. 2091–2117, 2006.

[51] Espinosa, H.D., Prorok, B.C., Peng, B., "Plasticity size effects in free-standing submicron polycrystalline FCC films subjected to pure tension," *Journal of Mechanics and Physics of Solids*, vol. 52, no. 3, pp. 667–689, March 2004.

[52] Wang, Z. Q., Beyerlein, I. J., "An atomistically-informed dislocation dynamics model for the plastic anisotropy and tension–compression asymmetry of BCC metals," *International Journal of Plasticity*, vol. 27, no. 10, pp. 1471–1484, October 2011.

[53] Shin, I., Carter, E. A., "Simulations of dislocation mobility in magnesium from first principles," *International Journal of Plasticity*, vol. 60, pp. 58–70, September 2014.

[54] Wen, M., Ngan, A. H. W., "Atomistic simulation of kink-pairs of screw dislocations in body-centred cubic iron," *Acta Materialia*, vol. 48, no. 17, pp. 4255–4265, November 2000.

[55] Cohen, H., "Dislocations in couple stress elasticity," *Journal of Mathematics and Physics*, vol. 45, pp. 35-44, 1966.

[56] Eringen, A. C., "Edge dislocation in nonlocal elasticity," *International Journal of Engineering Science*, vol. 15, no. 3, pp. 177-183, 1977.

[57] Eringen, A. C., "Screw dislocation in non-local elasticity," *Journal of Physics D: Applied Physics*, vol. 10, no. 5, pp. 671-678, 1977.

[58] Eringen, A. C., "On differential equations of nonlocal elasticity and solutions of screw dislocation and surface waves," *Journal of Applied Physics*, vol. 54, pp. 4703-4710, 1983.

[59] Eringen, A. C., *Continuum Physics (vol. IV: Polar and Nonlocal Field Theories)*. New York, San Francisco, London: Academinc Press, 1976.

[60] Lazar, M., Maugin, G. A., Aifantis, E. C., "On dislocations in a special class of generalized elasticity," *Physica Status Solidi (B)*, vol. 242, no. 12, pp. 2365–2390, October 2005.

[61] Lazar, M., Maugin, G. A., Aifantis, E. C., "Dislocations in second strain gradient elasticity," *International Journal of Solids and Structures*, vol. 43, no. 6, pp. 1787–1817, 2006.

[62] Eringen, A. C., "Vistas of nonlocal continuum physics," *International Journal of Engineering Science*, vol. 30, no. 10, pp. 1551-1565, October 1992.

[63] Lazar, M., Maugin, G. A., "Defects in gradient micropolar elasticity-I: screw dislocation," *Journal of the Mechanics and Physics of Solids*, vol. 52, no. 10, pp. 2263–2284, October 2004.

[64] Lazar, M., Maugin, G. A., "Defects in gradient micropolar elasticity-II: edge dislocation and wedge disclination," *Journal of the Mechanics and Physics of Solids*, vol. 52, no. 10, pp.

2285–2307, October 2004.

[65] Lardner, R. W., "Dislocations in materials with couple stress," *Journal of the Institute of Mathematics and its Applications*, vol. 7, pp. 126-137, 1971.

[66] Knésl, Z., Semela, F., "The influence of couple-stresses on the elastic properties of an edge dislocation," *International Journal of Engineering Science*, vol. 10, no. 1, pp. 83-91, January 1972.

[67] Lubarda, V. A., "The effects of couple stresses on dislocation strain energy," *International Journal of Solids and Structures*, vol. 40, pp. 3807-3826, 2003.

[68] Shankar, M. R., Chandrasekar, S., Farris, T. N., "Interaction between dislocations in a couple stress medium," *Journal of Applied Mechanics*, vol. 71, no. 4, pp. 546-550, September 2004.

[69] Gourgiotis, P. A., Georgiadis, H. G., "Distributed dislocation approach for cracks in couple-stress," *Defect and Material Mechanics*, pp. 83-102, 2007.

[70] Gourgiotis, P. A., Georgiadis, H. G., "An approach based on distributed dislocations and disclinations for crack problems in couple-stress elasticity," *International Journal of Solids and Structures*, vol. 45, no. 21, pp. 5521–5539, October 2008.

[71] Voigt, W., *Theoretische Studien über die Elasticitätsverhältnisse der Krystalle*.: Göttingen : in der Dieterichschen Buchhandlung, 1887.

[72] Ogden, R. W., *Non-linear Elastic Deformations*.: Courier Corporation, 1997.

[73] Hirth, J. P., Lothe, J., *Theory of Dislocations*, 2nd ed.: John Wiley & Sons, 1982.

[74] Eshelby, J. D., "The force on an elastic singularity," *Philosophical Transactions of Royal Society of London, A, Mathematical and Physical Sciences*, vol. 244, pp. 87-112, 1951.

[75] Eshelby, J. D., "The continuum theory of lattice defects," *Solid State Physics*, vol. 3, pp. 79–144, 1956.

[76] Eshelby, J. D., "Energy relations and the energy-momentum tensor in continuum mechanics," in *Fundamental Contributions to the Continuum Theory of Evolving Phase Interfaces in Solids*, J. M., Kinderlehrer, D., Podio-Guidugli, P., Slemrod, M., Ball, Ed.: Springer, 1999, pp. 82-119.

[77] Eshelby, J. D., "The energy-momentum tensor of complex continua," *Proceedings of the Third Symposium on Continuum Models of Discrete Systems*, pp. 651-665, 1980.

[78] Peach, M., Koehler, J. S., "The forces exerted on dislocations and the stress fields produced by them," *Physical Review*, vol. 80, pp. 436-439, November 1950.

[79] Ma, C. C., Lu, H. T., "Theoretical analysis of screw dislocations and image forces in anisotropic multilayered media," *Physical Review B*, vol. 73, no. 14, April 2006.

[80] Kröner, E., "Elasticity theory of materials with long range cohesive forces," *International Journal of Solids and Structures*, vol. 3, no. 5, pp. 731-742, September 1967.

[81] Rice, J. R., "A path independent integral and the approximate analysis of strain concentration by notches and cracks," *Journal of Applied Mechanics*, vol. 35, no. 2, pp. 379-386, June 1968.

[82] Budiansky, B., Rice, J. R., "Conservation laws and energy-release rates," *Journal of Applied Mechanics*, vol. 40, no. 1, pp. 201-203, Mars 1973.

[83] Wu, K. C., "Line inclusions at anisotropic bimaterial interface," *Mechanics of Materials*, vol. 10, no. 3, pp. 173-182, December 1990.

[84] Markenscoff, X., "Driving forces on phase boundaries: “The Eshelby principle for an interface”," *International Journal of Fracture*, vol. 165, no. 2, pp. 223–227, October 2010.

[85] Lubarda, V. A., "Determination of interaction forces between parallel dislocations by the evaluation of J integrals of plane elasticity," *Continuum Mechanics and Thermodynamics*, vol. 28, no. 1, pp. 391–405, March 2016.

[86] Atkinson, C., Leppington, F.G., "Some calculations of the energy-release rate G for cracks

in micropolar and couple-stress elastic media," *International Journal of Fracture*, vol. 10, no. 4, pp. 599–602, December 1974.

[87] Atkinson, C., Leppington, F. G., "The effect of couple stresses on the tip of a crack," *International Journal of Solids and Structures*.

[88] Lubarda, V. A., Markenscoff, X., "Conservation integrals in couple stress elasticity," *Journal of the Mechanics and Physics of Solids*, vol. 48, no. 3, pp. 553–564, March 2000.

[89] Herrmann, G., Kienzle, R., *Configurational Mechanics of Materials*, R., Maugin, G. A., Kienzler, Ed. New York: Springer-Verlag Wien GmbH, 2001.

[90] Yang, J. F. C., Lakes, R. S., "Experimental study of micropolar and couple stress elasticity in compact bone in bending," *Journal of Biomechanics*, vol. 15, no. 2, pp. 91-98, 1982.

[91] Chu, S. N. G., "Screw dislocation in a two-phase isotropic thin film," *Journal of Applied Physics*, vol. 53, no. 4, pp. 3019-3023, 1982.